International
Progress Report

IPR-01-56

Äspö Hard Rock Laboratory

TRUE Block Scale project

Preliminary results of selective pressure build-up tests in borehole KI0025F02

Joel Adams
Solexperts AG

Peter Andersson
GEOSIGMA AB

Peter Meier
ANDRA

November 1999

Svensk Kärnbränslehantering AB
Swedish Nuclear Fuel
and Waste Management Co
Box 5864
SE-102 40 Stockholm Sweden
Tel +46 8 459 84 00
Fax +46 8 661 57 19

Äspö Hard Rock
Laboratory

Report no.
IPR-01-56

No.
F56K

Author
Adams, Andersson, Meier

Date
99-11-01

Checked by

Date

Approved
Christer Svemar

Date
02-08-23

Äspö Hard Rock Laboratory

TRUE Block Scale project

Preliminary results of selective pressure build-up tests in borehole KI0025F02

Joel Adams
Solexperts AG

Peter Andersson
GEOSIGMA AB

Peter Meier
ANDRA

November 1999

Keywords: KI0025F02, pressure build-up tests, preliminary results

Abstract

Selective flow and pressure build-up tests were conducted as part of the characterisation of borehole KI0025F02 in the TRUE Block Scale array. In all, 31 test intervals were characterised using the SKB UHT Equipment. In addition, a series of tracer dilution tests were performed to study flow responses. The description of the Selective Flow and Pressure Build-up Tests includes analysis and interpretation of the hydraulic responses recorded during the cross-hole, single-hole and tracer-dilution tests, as well as comparison of results with POSIVA flow logging.

Sammanfattning

Som en del av karakteriseringen av borrhål KI0025F02 i TRUE Block Scale-området utfördes selektiva flödes- och tryckuppbyggnadstester. Med SKB UHT-utrustningen karakteriserades 31 testintervaller. Dessutom utfördes en serie av utspädningsmätningar med spårämnesteknik för att studera flödesresponser. Beskrivningen av de selektiva flödes-och tryckuppbyggnadstesterna inkluderar analys och tolkning av hydrauliska responser dokumenterade under de olika testerna: mellanhålsmätningar, enhålsmätningar och utspädningsmätningar, och även en jämförelse med POSIVAs flödesloggning.

Contents

List of Figures

List of Tables

1 Introduction

During 1996, characterisation work for the TRUE Block Scale Project commenced at Äspö with drilling of borehole KA2563A from the spiral tunnel. Characterisation data from this borehole and data from boreholes KA2511A, KA3510A, KI0025F, and KI0023B have been used to update the structural model of the south-western part of the Äspö HRL (HERMANSON, in prep). On the basis of this updated model and the identified centre of gravity for further investigations, an additional borehole, KI0025F02, has been completed, which is located in the ”I-tunnel”.

Borehole KI0025F02 has been characterised with acoustic flow logging (UCM), borehole radar (RAMAC), borehole TV (RAAX-BIPS), and POSIVA Flow logging.

This report documents the methods and preliminary results of the "Selective Flow and Pressure Build-up Tests" performed in Borehole KI0025F02 from September 22 – October 4, 1998.

1.1 Scope

The general objective of the selective flow and pressure build-up tests is to provide detailed information regarding the hydraulic characteristics of features within Borehole KI0025F02 which may be regarded as boundaries to, or target features of, future block-scale hydraulic and transport experiments.

1.1.1 Objectives

In past testing campaigns (e.g. those conducted in Boreholes KI0023B and KI0025F), emphasis was placed on characterising discrete features using single-well testing techniques. An increased density of observation points and a better definition of the structural model afforded a greater emphasis on inter-borehole reactions for the testing campaign in KI0025F02. This approach provides critical information for configuring the multi-packer system (possibly decreasing the need to re-configure the system after initial installation) and maximises the information collected during the testing campaign (potentially reducing the number of interference tests that must be conducted once the multi-packer system is in place). The specific objectives of the test campaign were:

1. Characterise discrete fractures.

2. Compare results of hydraulic testing with POSIVA flow-logging results.

3. Provide information for refining the structural model.

4. Evaluate connectivity within the block by observing interference responses within the existing monitoring network.

5. Provide information for configuring the multi-packer system for KI0025F02.

6. Assess the effects of turbulence on flow from discrete fractures.

1.1.2 Strategy

The test program conducted in KI0025F02 comprised three main parts:

- **Cross-hole Tests**: Short-term constant-pressure flow and build-up tests were performed in 9 intervals within the principal zone of interest in the borehole (between 30 – 140 m), including detailed observation of interference responses within the existing observation network. These tests were conducted using a 4-meter-long packer straddle in an attempt to isolate complete structural features, which in some cases consist of a number of discrete fractures. Analyses are presented for both the producing intervals and selected observation intervals.

- **Single-hole Tests**: Short-term constant-pressure flow and build-up tests were performed in 10 intervals outside of the principal zone of interest. These tests, which were conducted using a 1-meter-long straddle, focused on the properties of discrete features and can also be used to verify the accuracy of the POSIVA flow logging results.

- **Step-drawdown test**: A step-drawdown test was conducted in a selected interval to evaluate the effects of turbulence on flow from a discrete fracture

- **Tracer-dilution Tests**: Based on the results of the cross-hole tests, tracer-dilution tests were performed in conjunction with longer-term constant-pressure and build-up tests in 2 intervals to document the feasibility of performing tracer tests within the existing monitoring network.

2 Methods

2.1 Test Interval Selection

Test interval selection was a co-operative effort between ANDRA (P. Meier), SKB (A. Winberg), and Solexperts (J. Adams). Selection was based primarily on correlation of the drilling data, detailed POSIVA flow logging data, and the BIPS imaging data. Thirty-one potential test intervals were selected. Each interval was assigned a priority value of 1, 2 or 3, based on its geometric and potential hydraulic significance (Table 2-1). Priority 1 intervals were to be tested in any case; Priority 2 intervals were to be cancelled only in the case of extreme time restrictions; and Priority 3 Intervals were to be tested only if time allowed.

Following completion of the short-term cross-hole tests, it was decided that longer-term flow tests would be conducted in Intervals 4 and 5 for the purpose of performing tracer-dilution tests in selected observation intervals (dilution tests 1 and 2). Due to time restrictions, all intervals having priority designations of 2 and 3 were cancelled in order to accomplish the additional tests.

Table 2-1: Proposed Intervals for Selective Flow and Pressure Build-up Tests in Borehole K10025F02

Int. No.	Interval (Borehole m)	Interval Length (m)	Test Type	Priority	Comments
1	38.0 – 42.0	4	X-H	1	Major Single Open Fracture at 39.77 metres (5mm)
					Single Open Fracture at 40.75 metres
2	51.0 – 55.0	4	X-H	1	Moderate Open Fracture at 52.2 metres
					Minor Open Fracture 53.3 metres
					Single Open Fracture at 54.4 metres
3	58.0 - 62.0	4	X-H	1	Moderate Open Frac. 59.1 metres
					Minor Open Fracture at 60.4 metres
					Major Open Frac 61.0 metres
					Normal Minor Fractures 61.2 & 61.4 metres
4	64.2 – 68.2	4	X-H	1	Minor Open Fracture at 65.0 metres
					Multiple Parallel and Complex Fractures 66.4 – 66.8 metres (Major)
					Moderate Parallel Open Fractures at 67.1 & 67.3 metres
5	73.3 - 77.3	4	X-H	1	Moderate Single Open Fracture at 74.1 metres
					Moderate Single Open Fracture at 74.6 metres
					Possible Single Open Fracture at 76.5 metres
6	91.0 – 95.0	4	X-H	1	Possible Complex Fractures 94.1 – 94.3 metres
7	96.0 – 100.0	4	X-H	1	Moderate Single Open Fracture at 96.9 metres
					Moderate Single Open Fracture at 97.2 metres
					Major Open Fracture at 97.85 metres
					Possible Open Low angle fracture 98.3 – 99.1 metres (Posiva flow anomaly at 98.8 metres)

Int. No.	Interval (Borehole m)	Interval Length (m)	Test Type	Priority	Comments
8	130.0 – 134.0	4	X-H	1	Minor Open Fracture at 130.8 metres
					Complex Fracture Zone from 131.1 to 131.9 metres with major fracture at 131.65 metres
					Complex Fracture Zone from 132.5 to 133.3 metres with major fracture at 132.95 metres
9	136.0 – 140.0	4	X-H	1	Minor Open Fracture at 138.5 metres
					Possible Minor Open Fracture at 138.7 metres
10	29.5 – 30.5	1	S-H	2	Possible Single Open Fracture at 30.0 metres
11	33.2 – 34.2	1	S-H	1	Minor Single Open Fracture at 33.8 metres
12	34.3 – 35.3	1	S-H	1	Minor Single Open Fracture at 34.8 metres
13	43.8 – 44.8	1	S-H	1	Minor Parallel Open Fractures at 44.3 & 44.31 metres
14	143.35 – 144.35	1	S-H	2	Low Angle Fracture 143.3 – 144.4 metres
15	144.7 – 145.7	1	S-H	3	Possible Minor Open Fracture at 145.2 metres
16	162.3 – 163.3	1	S-H	3	Possible Open Fracture 162.8 metres
17	162.6 – 163.6	1	S-H	3	(No fracture seen) Posiva Anomaly at 63.1 metres
18	163.8 – 164.8	1	S-H	1	Moderate Single Open Fracture at 164.6 metres
19	167.2 – 168.2	1	S-H	1	Parallel Moderate Open fractures at 167.7 & 167.8 metres
20	172.7 – 173.7	1	S-H	1	Minor Single open fracture at 172.9 metres
					Parallel Moderate Open fractures at 173.3 & 173.5 metres
21	174.4 – 175.4	1	S-H	3	Low Angle Fracture 174.7 – 175.0 metres
22	177.5 – 178.5	1	S-H	3	Possible Open Fracture (healed fracture) at 178 metres
23	180.2 – 181.2	1	S-H	1	Minor Single open fracture at 180.5 metres
					Minor Single Open Fracture at 180.9 metres
24	181.5 – 182.5	1	S-H	2	Minor Single Open Fracture at 182 metres
25	183.3 – 184.3	1	S-H	2	Moderate Single open fracture 183.65 metres
26	184.7 – 185.7	1	S-H	1	Moderate Single open fracture 184.9 metres
					Moderate Single open fracture 185.4 metres
27	188.75 – 189.75	1	S-H	1	Complex Fracture Zone from 188.9 to 189.6 metres with major fracture at 189.1 metres
28	191.7 – 192.7	1	S-H	3	Minor Fracture Zone from 191.9 to 192.4 metres
29	193.8 – 194.8	1	S-H	2	Moderate Single open fracture 194.25 metres
30	198.5 – 199.5	1	S-H	3	No feature seen on BIPS, (Posiva anomaly at 199) metres
31	199.6 – 200.6	1	S-H	1	Major Single Fracture at 200.1 metres
4a	64.2 – 68.2	4	T-D	1	See Interval 4
5a	73.0 – 77.0	4	T-D	1	See Interval 5

Legend:

X-H	Cross-hole Test
S-H	Single-hole Test
T-D	Dilution Test

2.2 Equipment

2.2.1 Hydraulic Tests

The underground hydraulic test system (UHT-1) developed by SKB was used for performing the tests in KI0025F02. The UHT is documented in detail in Adams (1998). The UHT-1 is constructed for underground hydraulic testing in 56 mm and 76 mm diameter boreholes. Maximum borehole length is 300 m and the maximum working depth is 500 metres below sea level. In general, the testing system consists of three main components:

- **Down-hole System**: including packer system (double or single) for isolating the target test interval, down-hole shut-in valve, central tubing, and control lines for packer inflation and pressure measurement.
- **Hoisting Rig**: for installing and removing the packer system.
- **Surface System**: including data acquisition, flow and pressure control and measurement equipment.

The down-hole system includes a flow bypass that interconnects the guard intervals below the lower packer and above the upper packer (i.e. the entire borehole except the test interval). The by-pass was sealed during the testing to minimise cross-flow between deep and shallow producing zones during the testing campaign. A consequence of this action is that no pressure measurement is registered for the zone below the lower packer.

During the tests designated as “Cross-Hole Tests”, the HMS Data Acquisition System was used for collection of data in the observation intervals.

In general, the equipment functioned well. However, some tests were disturbed because the system depressurised the interval to a pressure far below the target pressure when initiating the test. This had a particularly great impact on tests in low-permeable intervals because the time required to recover from the depressurisation is dependent on the inflow rate from the interval. In addition, the shut-in valve malfunctioned during the cross-hole tests.

2.2.2 Tracer Dilution Tests

The equipment for tracer dilution tests was originally constructed for the TRUE-1 project (Figure 2-1). The basic idea is to create an internal circulation of the borehole fluid in the borehole section. The circulation makes it possible to obtain homogeneous tracer concentration inside the borehole and to sample the tracer concentration outside the borehole in order to monitor the dilution of the tracer with time.

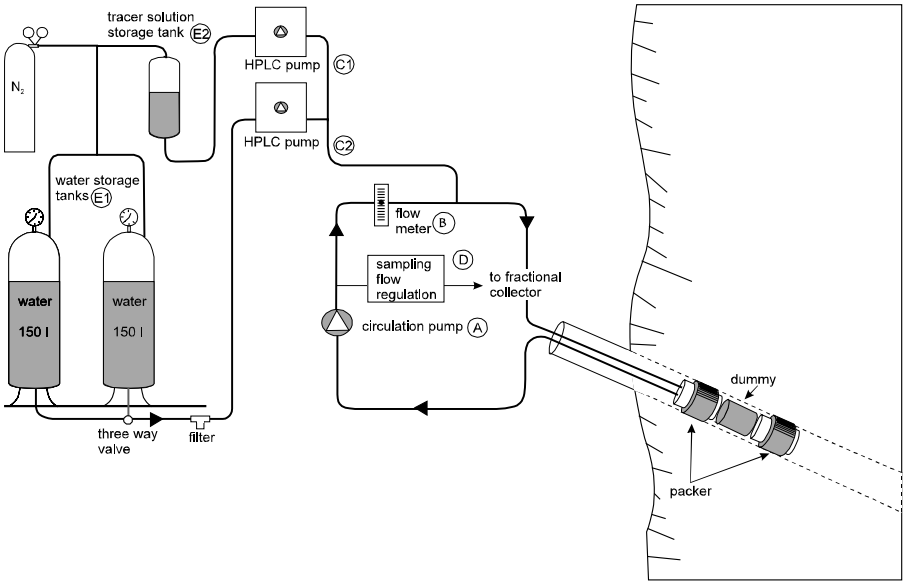

Figure 2-1 *Schematic drawing of the injection/sampling system for the tracer dilution tests.*

Circulation is controlled by a pump with variable speed (A) and measured by a flow meter (B). Tracer injections with Uranine are made directly into the circulating loop with a HPLC plunger pump (C1). The tracer concentration in the circulation loop is measured by sampling and subsequent analysis. The sampling is done by continuously extracting a small volume of water from the system through a flow controller (constant leak) to a fractional sampler (D). The equipment also allows injection of water (C2) and storage of water and tracer solution (E1 and E2). The latter options were not used for the tracer dilution tests.

The three packer-isolated borehole sections used for the tracer dilution tests were equipped with three lines, one for pressure measurements (Äspö HMS system) and two for tracer circulation.

2.3 Test Performance

2.3.1 Hydraulic Tests

The test sequence planned for each interval consisted of a compliance period (packer inflation), a constant-pressure withdrawal test (HW), followed by a pressure recovery period (HWS). The length of each period was approximately 30 min.

The test sequence conducted in Interval 13 is an exception to the above-described testing approach because no measurable flow was observed during an attempted HW. The shut-in valve was closed after a short period and the ensuing recovery was treated as a pulse test.

The HW events were conducted by decreasing the ambient pressure in the test section by between 500 and 2000 kPa (50 to 200 m water column). For the cross-hole tests, a 2000 kPa pressure drop (dP) was applied in order to maximise the signal at the observation points. For single-hole tests, the dP was designed based on the POSIVA flow logging results to strike a balance between minimising flow losses at the well in high-T zones and maximising flow rates from low-T zones. Intervals that flowed >500 ml/min during flow logging were tested with a dP of 500 kPa. For flows between 50 and 500 ml/min, a dP of 1000 kPa was applied. A dP of 2000 was applied for flows less than 50 ml/min.

The data collection rate of the HMS data acquisition was increased for the TRUE Block Scale observation intervals during the cross-hole tests.

2.3.2 Tracer Dilution Tests

The flow rates in the selected sections were determined by tracer dilution tests in three selected borehole sections during two different pumping tests in borehole KI0025F02 (intervals 4 and 5, cf. Table 2-1). The dilution tests were performed both under natural gradient (before start of pumping) and under stressed conditions (pumping in KI0025F02). Thus, it is possible to simultaneously account both for flow and pressure changes due to the pumping. The three sections used for tracer dilution tests and the test schedule are listed in Table 2-2. The collected samples were analysed for dye tracer content at the GEOSIGMA laboratory, Uppsala, using a Jasco FP777 Spectro-fluorometer.

Table 2-2: Test schedule and section used for the dilution tests performed during selective pumping of borehole KI0025F02.

Day #	Activity	Borehole section(s)
1	Preparation for dilution tests	KA2563A:R5,KI0025F:R4, KI0023B:P6
1	Installation of double packer system in KFI0025F02,	73.3-77.3 m
2	Start dilution tests #1-3, no pumping	KA2563A:R5,KI0025F:R4, KI0023B:P6
3	Start pumping	KI0025F02, 73.3-77.3 m
4	Stop pumping, change pumping section in KFI0025F02	64.2-68.2 m
4	Start dilution tests #4-6	KA2563A:R5,KI0025F:R4, KI0023B:P6
5	Start pumping	KI0025F02, 64.2-68.2 m
6	Stop pumping, stop dilution test	
6	Demobilization of pumping and dilution test equipment	

2.4 Analysis Methods for Single-Hole Hydraulic Test Responses

The preliminary test interpretation is conducted using standard analytical models to produce hydraulic coefficients for the test intervals.

Objectives of the preliminary interpretation are the following:

- Flow-model identification (if possible)
- Evaluation of hydraulic parameters (T) and wellbore effects (wellbore storage, skin)

Flow-model identification is conducted using diagnostic plots. Once the various parts of the well response have been identified (i.e. inner boundary, basic flow model, and outer boundary), the appropriate analytical method is applied.

2.4.1 Constant-pressure Analysis

Transient analysis of constant-pressure tests is conducted using the straight-line method described by Jacob & Lohman, 1952. Straight-line analysis is performed by plotting 1/q versus the log of time. If an infinite-acting radial-flow period is identified on the diagnostic plot, a straight-line is fit to the data and transmissivity (T) is calculated using the following formula:

$$T = \frac{2.3}{4\pi \Delta hm} \qquad 2.1$$

where:

Δh = constant change in pressure expressed as head [m]
m = slope of straight line [(s/m^3)/log cycle]

The skin factor (s) are estimated using the following formulas:

$$s = -\ln\left(\frac{\sqrt{2.25Tt_0/S_{est}}}{r_w}\right) \qquad 2.2$$

where:

r = radius of well, radial to observation point
t_o = zero intercept
S_{est} = estimated storativity

A steady-state approximation of transmissivity is calculated for each flow period using the following formula presented by Zeigler, (1976). The formula can be applied to both constant pressure and constant rate data.

$$T = \left[\frac{Q_p}{2\pi\Delta h}\right] \ln\left[\frac{r_i}{r_w}\right] \qquad 2.3$$

where:

T	=	transmissivity	[m^2/s]
Q_p	=	flow at the end of the flow phase	[m^3/s]
Δh	=	pressure drop in the test section expressed in meters of water	[m]
L	=	interval length	[m]
r_i	=	radius of influence (estimated)	[m]
r_w	=	borehole radius	[m]

An initial value of 1 m is assumed for the radius of influence, r_i. T and r_I are then calculated iteratively using the above equation for T and the following equation for r_i:

$$r_i = \sqrt{\frac{2.25Tt}{S}} \qquad 2.4$$

where:

t	=	time at which steady-state conditions are reached	[s]
S	=	storativity	[-]

If steady-state conditions have not been achieved by the end of the pumping period, then t is taken as the total pumping time. In addition, a storativity value is required to solve the above equation. Because a reliable estimate of storativity cannot be made from single-well tests in a heterogeneous medium (Meier, 1998), a value must be assumed. S-values ranging from $1x10^{-8}$ to $2x10^{-5}$ have been reported for the flow system at Äspö (Uchida et al, 1994, and Winberg, 1996). Uchida et al (1994), report an empirical relationship where:

$$S = .001\sqrt{T} \qquad 2.5$$

The above approach yields S-values ranging from $1.1x10^{-8}$ to $8.8x10^{-7}$ for tests conducted in the TRUE-1 Experiment. This range is consistent with values presented in Rutqvist et al. (1998). A constant S-value of $5x10^{-7}$ is assumed for the steady-state and skin-factor analyses reported in this document.

2.4.2 Pressure Build-up Analysis

The pressure recovery period following a constant pressure test is treated as a constant rate period. For a constant rate test, a straight line is fit to the indicated data set on a semi-log graph of Δp vs. log time. Transmissivity is estimated using the following equation (Cooper & Jacob, 1946):

$$T = \frac{2.3q}{4\pi m} \qquad 2.6$$

where:

q	=	flow rate	[m^3/s]
m	=	slope of a straight line	[m/log cycle]

The pressure build-up period following a constant-pressure test can be analysed in a manner comparable to a constant rate test. A log-log diagnostic plot is prepared according to Agarwal (1980), who presented a relationship that plots the recovery pressure change versus an equivalent time instead of elapsed time. The equivalent time function essentially converts the pressure recovery event to an equivalent constant rate test response that can be analysed using the straight-line analysis method presented above. Equivalent time is calculated using the following formula:

$$\Delta t_e = \frac{t_p \Delta t}{t_p + \Delta t} \qquad 2.7$$

where:

Δt_e	=	equivalent time	[s]
tp	=	duration of preceding flow period	[s]
Δt	=	elapsed recovery time	[s]

2.4.3 Pulse Analysis

A pulse test is performed by subjecting a test interval to an instantaneous change in pressure and observing the transient pressure response as the system recovers toward its static pressure. The recovery response is related to the diffusivity of the formation and the geometry of the borehole. Pulse test analysis is conducted as described in Bredehoeft & Papadopulos (1980). The type-curve matching technique is not described in detail here because it is widely available in the literature. A brief description of the calculation of T and S from pulse test responses is presented below.

A type-curve match yields three parameters, α, β, and the time match, t (Cooper et al., 1967). The dimensionless storage coefficient, α, defines the shape of the type curve and, for pulse tests, is attained by:

$$\alpha = \frac{r_w^2 S}{r_e^2} \qquad 2.8$$

where:

α	=	dimensionless storage parameter	[-]
r_w	=	radius of the well	[m]
r_e	=	effective radius of the well (Black,1985)	[m]

Transmissivity is calculated from the type-curve match:

$$T = \frac{\beta r_e^2}{t} \qquad 2.9$$

where:

β = dimensionless time parameter [-]
t = match time [s]

If the isolated wellbore storage coefficient, C, is known, r_e can be calculated according to the following equation:

$$r_e = \sqrt{\frac{C\rho g}{\pi}} \qquad 2.10$$

where:

r_e = effective radius [m]

The C value can be obtained during a pulse test by observing the change in volume of water in the tubing caused by exposing the interval to a known pressure change. Assuming that no flow into or out of the test formation occurred during the short time the pressure was applied, C can be calculated by dividing the volume change, ΔV, by the applied pressure change, Δp.

2.5 Analysis Methods for Interference Test Responses

Cross-hole tests provide important information about the connectivity between the pumping well and the observation points. This information is crucial for building a hydro-structural model in fractured rocks. An adequate analysis of the drawdown responses at the observation points can also provide parameter estimates on the transmissivity and the storativity of the tested system. These parameters are important for forward numerical modelling and can be used as prior information for inverse modelling. Measures of connectivity and the estimation of T and S from interference test responses are discussed in the following sections.

2.5.1 Measures of Connectivity

Two measures of connectivity are normally applied within the TRUE experiments (Andersson et al., 1998):

- s_p/Q is the normalised drawdown at the end of a pumping tests (s_p is the drawdown at an observation point and Q is the flow rate)

- t_R/R^2 is the ratio of the response time t_R (defined as the elapsed time when a drawdown of 1 kPa (0.1 m) is observed) and the squared distance R in space between the midpoint of the source section and the midpoint of an observation section.

From the plots of s_p/Q versus t_R/R^2 for each test, sections with anomalous fast response times and large drawdowns can be identified. Such sections are well connected with the pumping well and are interconnected via conducting fractures. These measures are useful for building the hydro-structural model.

In general, s_p/Q measurements are more reliable than t_R/R^2 because (1) the exact determination of t_r is difficult in relatively tight sections which frequently show long-term pressure recovery trends and (2) the physical meaning of the division by R^2 is not clear in heterogeneous 3-D fractured systems. Because of the latter, it suffices to use t_r instead of t_r/R^2. On the other hand, s_p/Q values are influenced by boundary effects, which causes difficulties for comparing s_p/Q values from different pumping tests.

Besides the sp/Q and t_R/R^2 measures, storativity estimates obtained from analysing cross-hole tests with conventional methods can be used as a qualitative measure of connectivity. Meier et al. (1998) review some cross-hole pumping test data in fractured rock from the Grimsel test site (Switzerland) and the El Cabril site (Spain). They find that transmissivity estimates obtained from applying Jacob's method (Cooper and Jacob, 1946) to the drawdown data at the observation points are fairly constant whereas the storativity estimates vary within several orders of magnitude. A numerical study in heterogeneous two-dimensional T fields shows that the T estimates agree well with the effective transmissivity for parallel flow conditions. The numerical study shows also that the storativity estimates are a measure of the connectivity between the pumping well and the observation point. A high S estimate indicates a low connectivity between the pumping and the observation well and vice versa for a low S estimate. The numerical work of Meier et al. (1998) was confirmed by an analytical study of Sanchez-Vila et al. (1999).

2.5.2 Estimation of Transmissivity and Storativity from Interference Tests

Previous analyses of interference tests for the TRUE Block Scale project (Andersson et al., 1998) have shown that different analytical interpretation methods (Hantush, Theis, Jacob) yield similar T estimates. As discussed in the previous section, T estimates obtained from conventional analysis techniques can provide representative values for the effective T of heterogeneous media in 2-D flow systems (Meier et al., 1998). On the other hand, storativity estimates are in general not representative of the formation storativity because they are strongly influenced by the heterogeneity (especially by the connectivity between the pumping and observation wells). The validity of these findings has not been proven for 3-D fractured systems. The objective of our analyses is an assessment of the use of Jacob's method for the interpretation of interference responses at the TRUE Block Scale experiment.

2.6 Analysis Methods for Tracer Dilution Tests

The groundwater flow rates were calculated from the decay of tracer concentration versus time obtained through dilution with natural (non-labelled) groundwater. The dilution of tracer with time in the injection sections was determined by analysing the samples withdrawn from the sections. The so-called "dilution curves" were plotted as the natural logarithm of concentration versus time. Theoretically, a straight-line relationship exists between the natural logarithm of the relative tracer concentration (c/c_0) and time (t):

$$Q_{bh} = -V \cdot \Delta \ln (c/c_0) / \Delta t \qquad 2.11$$

where Q_{bh} (m^3/s) is the groundwater flow rate through the borehole section and V is the volume of the borehole section (m^3). The flow Q_{bh} may be translated into a Darcy velocity by taking into account the distortion of the flow caused by the borehole and the angle between borehole and flow direction, c.f. Rhén *et al*. (1991). The relation between the flow in the rock, the Darcy velocity, q_w (m/s), and the measured flow through the borehole with a dilution test, Q_{bh} (m^3) can be expressed as:

$$Q_{bh} = q_w \cdot L_{bh}^2 \left[r_d \cdot \alpha \cdot \sin\beta + \pi \cdot \cos\beta \left(\frac{a_{D1}}{2} + \frac{a_{D2}}{4} + \frac{a_{D3}}{6} \right) \right] \qquad 2.12$$

$$r_d = \frac{2r_w}{L_{bh}} \qquad 2.13$$

Assuming a 90° angle between borehole and flow direction, the relationship between Q_{bh} and q_w may be estimated from:

$$Q_{bh} = q_w \cdot L_{bh} \cdot 2r_w \cdot \alpha \qquad 2.14$$

where L_{bh} is the length of the borehole section (m), r_w is the borehole radius (m) and α is the factor accounting for the distortion of flow caused by the borehole. The factor α was given the value 2 in the calculations, which is the theoretical value for a homogeneous porous media.

3 Results

The test results are presented in the following two categories:

- **Selective Flow and Pressure Build-up Tests:** This includes analysis and interpretation of the hydraulic responses recorded during the Cross-hole, Single-hole and Tracer-dilution tests, as well as a comparison of results with the POSIVA Flow Logging.

- **Tracer-dilution Tests:** This includes analysis and interpretation of the dilution responses.

3.1 Selective Flow and Pressure Build-up Tests

Analysis and interpretation of the hydraulic test sequences conducted during the cross-hole, single-hole and tracer-dilution tests yield information regarding the flow models that control the test responses, the transmissivity of the intervals, and the pressure distribution along the borehole. The interference responses provide additional information regarding the connectivity of particular structures, and help to further define the structural model for the experimental block. The analyses of the individual intervals are presented in Appendices A, B and C. Results of the analyses are summarised in Table 3-1 and described in the following sections.

3.1.1 Flow Model Identification

The majority of the producing-well responses indicate a short infinite-acting radial flow period that is followed by a constant-head boundary response. Unambiguous identification of an IARF period is not always possible because:

1. the "1.5 Log Cycle Rule" as described by Horne, (1995) (i.e. on a log-log diagnostic plot, the IARF period should start approximately 1.5 log cycles after the pressure derivative deviates from the unit slope of a wellbore storage period) is not always satisfied.

2. the straight-line portion of the pressure derivative is poorly defined in some cases.

Intervals 6, 9 and 23 are not affected by a constant-pressure boundary, whilst Intervals 12 and 26 can be interpreted as composite systems. There appears to be no correlation between transmissivity and flow models, as was reported for KI0023B.

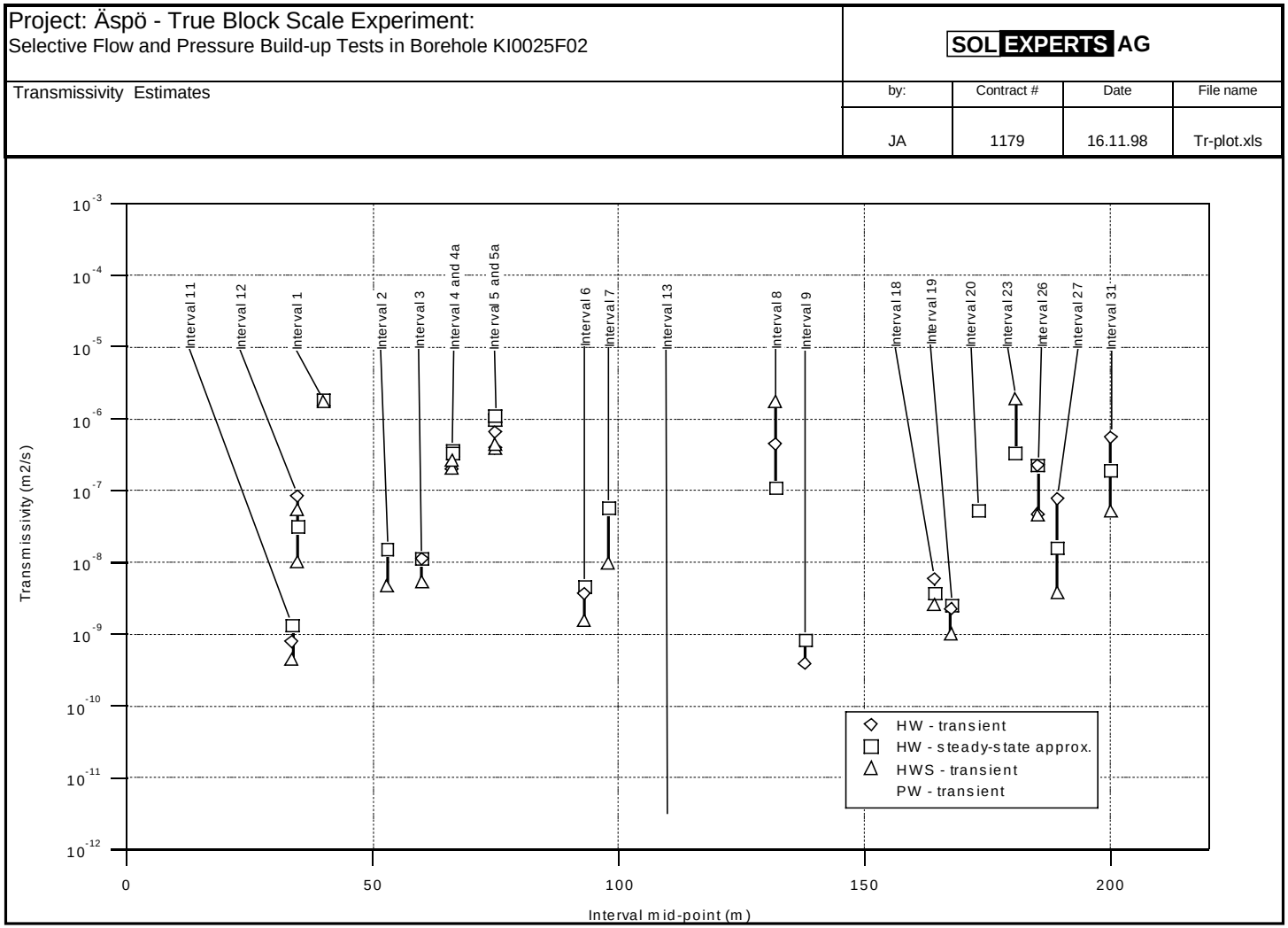

Figure 3-1 *Summary of Transmissivity Estimates for the Intervals Tested in KI0025F02*

3.1.2 Transmissivity

Interpretation of the single-hole responses yield T-values ranging from $2x10^{-12}$ to $2x10^{-6}$ m^2/s (Figure 3-1). The majority of the intervals tested exhibited transmissivity values between 10^{-9} and 10^{-6} m^2/s. The degree of confidence that can be assigned to any particular value is highly variable. The "scatter" of T-values for certain intervals were as great as an order of magnitude.

3.1.3 Pressure Distribution

The pressures measured in the test intervals during the test campaign are affected by a complex borehole history, which includes flowing at atmospheric pressure (during flow logging and installation of the packer system), and extensive short circuiting when the borehole was shut in at the wellhead. The pressures measured during the relatively short pressure recovery phases do not represent "static" formation pressures. Considering the fact that long-term monitoring following the selective flow and build-up testing will yield the static pressures, a detailed analysis is not warranted at this stage.

A qualitative interpretation of the pressure data indicates that a pressure difference of approximately 40 bar exists between the tunnel wall and Interval 11 (33 m depth). From Interval 11 to Interval 31 (200 m depth), the pressure gradient is markedly less, increasing approximately 2.5 bar over 167 m.

3.2 Interference Test Responses

The analyses of the interference test responses focus on (1) a comparison of connectivity measures, (2) the hydro-structural model and (3) the problems associated with the analysis of the interference responses with conventional evaluation methods.

3.2.1 Comparison of connectivity measures

The four connectivity measures s_p/Q, t_R/R^2 , t_R and S_{est} (storativity estimates) are plotted against each other in Figs. D-1 to D-8 for dilution tests 1 and 2 in order to compare their content of information on connectivity.

The relatively good correlation between S_{est} and t_R/R^2 (Figs. D-1 and D-6) and between S_{est} and t_R (Figs. D-2 and D-7) show that these three measures contain similar information, in contrast to s_p/Q which seems to contain different information. Plotting s_p/Q versus t_R/R^2, t_R or S_{est} (Figs. D-3,D-4,D-5,D-8,D-9,D-10) allows separation of the responses into two main groups of strong and weak responses (s_p/Q values > 100000 and s_p/Q < 50000). Note that only the positions within the main groups change when plotting s_p/Q versus t_R/R^2, t_R or S_{est}.
It is difficult to decide whether t_R/R^2, t_R or S_{est} are more appropriate to use due to the uncertainty associated with the physical meaning of R^2. For a clarification of this

question we show in Figs. D-11 and D-12 the drawdown curves obtained at observation points within structures #20 and #13. These structures are known with a high precision. Figs. D-11 and D-12 show that responses within a certain structure are very similar to each other (with the exception of the response in KI0025F:R4 during Dilution Test 1). This implies that also the values of s_p/Q and t_R should be very similar to each other for a specific structure. The deviation from this conjecture in Figs. D-4 and D-9 stems from the difficulty in defining t_R accurately because of the combination of fast responses for the defined pressure response threshold and the relatively slow data scan rates.

It seems that the most robust measure is s_p/Q, if only responses from one pumping test are compared. The disadvantage of the s_p/Q measure for comparing s_p/Q values from different pumping tests is that the s_p/Q values can be strongly influenced by boundary effects, which can be different for each pumping test.

The cluster of values for structures #13 and #20 in Figs. D-5 and D-10 indicate that the S_{est} values are also robust measures for connectivity although their meaning in 3-D heterogeneous media is not clearly defined from a theoretical point of view. The advantage of the S_{est} measure is that it is, in principle, influenced neither by boundary effects nor by the accuracy of the response time.

In summary, the s_p/Q measure seems to be of greatest use because of its robustness and simplicity (at least until the theoretical uncertainties of S_{est} as a connectivity measure in 3-D fractured media are clarified). However, the S_{est} measures are preferable for 2-D heterogeneous media, because their physical meaning is well understood (Meier et al., 1998).

3.2.2 Information for the Hydro-structural Model

Pressure responses were monitored in all sections of boreholes KI0023B, KI0025F, KA2511A, KA2563A, KG0048A, KG0021A, KA2598A, KA3548A, KA3600A, KA3573A and KA3510A. The drawdown at the end of the tests and the s_p/Q measures are presented in Tables 3-4 and 3-5 for the cross-hole tests 1 through 8 and in Table 3-6 for the dilution tests. The most dominant responses within one borehole are indicated in bold. Only negligible responses were observed in boreholes KG0048A, KG0021A, KA2598A, KA3548A, KA3600A, KA3573A and KA3510A during all cross-hole tests with the exception of dilution test 1. Furthermore, only negligible cross-hole pressure responses were observed during cross-hole tests 6 and 9.

Table 3-3 shows that the response pattern of cross-hole test 1 is significantly different from the response pattern of the other tests. The responses in bold may reveal structure #7. This structure can therefore clearly be defined in a hydraulic sense.

The s_p/Q measures for cross-hole tests 2 and 3 indicate that these test intervals are well connected to structure #20, although the tested features produce only 0.2 and 0.1 l/min, respectively, for a drawdown of 20 bar. Both tests show generally the same pattern. The test intervals of cross-hole tests 4 (dilution test 2) and 5 (dilution test 1) lie within important features which are well interconnected. Test interval 4 probably lies within

structure #6 and test interval 5 within structure #20. The drawdown responses during dilution tests 1 and 2 will be discussed separately in the following section.

Cross-hole test 7 resulted in comparatively small responses indicating that this test interval is not strongly connected to the remainder of the system. The responses during test 8 suggest that structure #19 is tested and that structure #19 is not well connected to the structures responding during tests 4 and 5.

3.2.3 Analysis of Interference Test Responses with Conventional Methods

This section focuses on the problems associated with the analysis of the interference responses with conventional evaluation methods. To this end, a detailed discussion of the evaluation of the single-hole and cross-hole pressure responses during dilution tests 1 and 2 is included.

3.2.3.1 Dilution test 1: pumping in interval 5a (73.0-77.0 m)

The normalized flow rates and the plots for the pressure recovery phases are shown in Figure C-4. The plots show that a transition from a possible infinite acting radial flow (IARF) regime towards flow controlled by a constant head boundary may start at about 500 to 1000 seconds and the effects of a constant head boundary dominate the normalized flow rates during the pumping phase and the pressure recovery after 10000 seconds. Transient analysis of the assumed IARF period of the single-hole data yield T estimates of about $4x10^{-7}$ m^2/s, and a steady-state analysis yields a T estimate which is about two times higher.

The cross-hole pressure responses in the observation boreholes during dilution test 1 are shown in semi-log plots (Figs. D-3 – D-6). Strong pressure responses are observed in KI0023B (P3, P4, P5, P6), in KI0025B (only in P4, but the strongest response of all boreholes), and in KA2563A (P1, P4, P5, P6; note that the fast response of interval KA2563A :R1 may be due to an equipment-related artifact). Only weak responses were observed in KA2511, but all intervals react similarly. Only weak responses were observed in the other boreholes (not shown). All fast pressure responses clearly show the effects of constant head type boundaries between 1000 and 10000 seconds.

Analyses with Jacob's method of the possible IARF periods provide T estimates within a narrow range from $6x10^{-7}$ to $8x10^{-7}$ m^2/s. These values are up to two times higher than the T estimates from the single-hole analysis, and are only slightly lower than the estimates obtained for structure #20 from the interference test of the preliminary characterization stage (Andersson et al., 1998). This corroborates the conjecture that structure #20 was tested. An analysis with a leaky aquifer model (Hantush) yields estimates which are slightly smaller than the estimates obtained from Jacob's method.

3.2.3.2 Dilution test 2: pumping in interval 4a (64.2-68.2 m)

The normalized flow rates and the plots for the recovery phases are shown in Fig. C-2. The behavior of the normalized flow rates and the pressures is similar as for dilution test 1. However, the transition phase may start at about 200 to 300 seconds and the constant head type boundary already dominates the responses after 800 seconds. Transient analyses of the assumed IARF period of the single-hole responses yield T estimates of about $2x10^{-7}$ m^2/s and a steady-state analysis yields a T estimate which is slightly higher.

The cross-hole pressure responses are similar to those of dilution test 1 (Figs. D-17 – D-20). As an example, the pressure responses in KI0023 are shown in Fig. 7. The analyses with Jacob's method and with the Hantush model yield T estimates of about $2x10^{-6}$ m^2/s. This is in contrast to the value obtained from the single-hole test analysis and also in contrast to a steady-state cross-hole analysis, which yields T estimates of about $3x10^{-7}$ m^2/s. The high estimates resulting from the transient analysis are most probably due to a fast and direct transition from the start of the test into a flow regime, which is completely dominated by constant head boundaries. Therefore, the slopes of the straight-lines in Figs. D-17 –D20 are too small and the transmissivity will be overestimated applying transient evaluation methods, which do not explicitly account for the constant head boundaries. Note that an analysis with a leaky aquifer model (Hantush) yields estimates which are slightly smaller than the estimates obtained from Jacob's method.

3.2.3.3 Reciprocity

The principal of reciprocity states that drawdown curves are identical for constant rate pumping tests in heterogeneous media when pumping well and observation well are interchanged (Earlougher, 1977). After the instrumentation of borehole KI0025F02 with a Solexperts multipacker system, a third dilution test was performed by pumping in KI0023B:P6 and monitoring pressure responses and dilution rates in KI0025F02. Drawdown data, normalised with the pumping rates, from dilution tests 1, 2 and 3 are presented in Figures D-21 and D-22. The figures show that the principle of reciprocity is only fulfilled for intervals KI0025F02:P5 – KI0023B:P6 (the small deviations are probably due to different flow rate histories at the pumping wells). The reasons for the violation of the principle of reciprocity for intervals KI0025F05:P6 – KI0023B:P6 are not clear. Possible reasons are (1) equipment-related problems during dilution test 1 and (2) a change in the flow system. Equipment-related problems can be ruled out, because no such problems were evident during testing and because two tests with almost identical results were performed in KI0025F05:P6. A change in the flow system is more probable since a transmissivity reduction of the fracture in dilution test interval KI0025F05:P6 due to depressurisation and/or the effects of turbulent flow are possible scenarios, which were observed for step drawdown testing in interval 12 (Fig. B-5). Both effects would lead to the smaller drawdown observed in KI0023:P6.

3.2.3.4 Discussion

The constant head boundaries evident in both tests may be (1) the product of a connection to a higher conducting fracture or (2) due to flow becoming 3-dimensional in a well-connected fracture network away from the borehole. It is almost impossible to favor one or the other interpretation, because 1) it is clear from the pressure responses at the observation points that we tested a network of fractures, and 2) most of the dominant fractures can be viewed as planar features at the scale of 50 m or more. The fast transition into steady-state conditions during testing a fracture of lower conductivity (dilution test #2), in contrast to the comparatively slow transition within the more conductive fracture (structure #20, during dilution test #1), may indicate that interpretation (1) is more appropriate.

The transmissivity estimates for dilution tests 1 and 2 demonstrate the problems associated with using conventional analysis techniques for the interpretation of cross-hole pressure responses if boundary effects are dominant or if the conceptual flow model is not well understood. In principle, the cross-hole data analysis of both dilution tests should yield very similar T estimates because basically the same flow system is tested (same observation points and good connectivity between both pumping wells). However, the T estimates from transient analyses of the cross-hole test responses from dilution test 2 are three times larger than the T estimates for dilution test 1. This fact indicates that the transient analyses may not be reliable because of the constant head type boundary effect. This conjecture is supported by the fast transition into steady-state conditions of the single-hole flow and pressure responses, especially for dilution test 2.

Because of the uncertainties associated with the use of conventional analysis techniques, these T values should be considered rough estimates which should be refined by calibrating numerical models with cross-hole interference data.

3.3 Comparison with POSIVA Flow Logging

POSIVA Flow Logging was conducted as part of the characterisation work carried out in KI0025F02 (Rouhianen & Heikkinen, 1998). As this was the first application of the method in the TRUE Block Scale Experiment, the results of the flow logging are compared to the results of the Selective Flow and Pressure Build-up tests. The objectives of the exercise are:

- to compare the flow rates derived from discrete features during flow logging to the rates observed during selective flow and pressure build-up tests.

- to evaluate the head-dependent variation in specific capacity due to either pressure-dependent storativity or turbulence.

To compare the flow rates derived from the Flow logging and hydraulic testing, it is necessary to calculate the specific capacity (C_s) for each event (Table 3-2). In calculating C_s for the flow logging, it was assumed that the borehole was open and a constant dH of 400 m was exerted on the flowing intervals. The error introduced by this assumption is expected to be a maximum of 10%.

With only one exception, C_s for the hydraulic testing is greater than that estimated for the flow logging. In 14 of the 18 cases, the ratio, $C_{s\text{-}PBU}$ /$C_{s\text{-}POSIVA}$,, ranges from 1.1 to 2.1. The most extreme case occurs in Interval 23, where the ratio is 4.6 (higher ratios were calculated for Intervals 1 and 5; however, in these cases the measured flow during flow logging was affected by a flow limiter).

The dependency of specific capacity on the dH applied is best illustrated in Interval 12, in which a step drawdown analysis was conducted. The $C_{s\text{-}PBU}$ /$C_{s\text{-}POSIVA}$ ranges from 1.3 to 1.9 for the various steps. The physics of this variation in specific capacity requires further investigation.

In general, the specific capacities for discrete features tend to be underestimated using the open-hole flow-logging technique. Consequently, transmissivity values estimated based on the open-hole flow logging will also most likely be underestimated.

3.4 Tracer Dilution Test Responses

The dilution tests were performed between September 29th and October 3rd in three borehole sections associated with structures #9 and #20 (KFI0025F:R4, KFI0023B:P6 and KA2563A:R5). The analysis and interpretation were performed according to the procedure described in Chapter 2.6. The results are summarised in Table 3-6.

Borehole section KA2563A:R5 shows a very marked influence from the pumping, especially the pumping in section 73.3-77.3 m, (Figure 3-2), where the flow increased from about 15 ml/min to 90 ml/min, i.e. a factor of 6. The pumping in section 64.2-68.2 m also resulted in an increase, although not marked, from about 10 ml/min to 20 ml/min (Figure 3-2).

The borehole section KI0023B:P6 shows an influence from the pumping in section 73.3-77.3 m (Figure 3-3) with an increase in flow from about 3 ml/h to 11 ml/h, i.e. a factor of 4. There is no influence from the pumping in section 64.2-68.2 m. The flow rate is 2.5-3 ml/h both before and during pumping (Figure 3-3).

The data for borehole section KI0025F:R4 are quite scattered and it is difficult to see a clear effect on the flow due to pumping in any of the sections, (Figure 3-4). A possible interpretation is that section 73.3-77.3 m reacts to pumping whereas section 64.2-68.2 m is more uncertain.

A preliminary conclusion based on the outcome of the tracer dilution tests is that section 73.3-77.3 m in KI0025F02 is associated with structure #20 whereas section 64.2-68.2 is more uncertain.

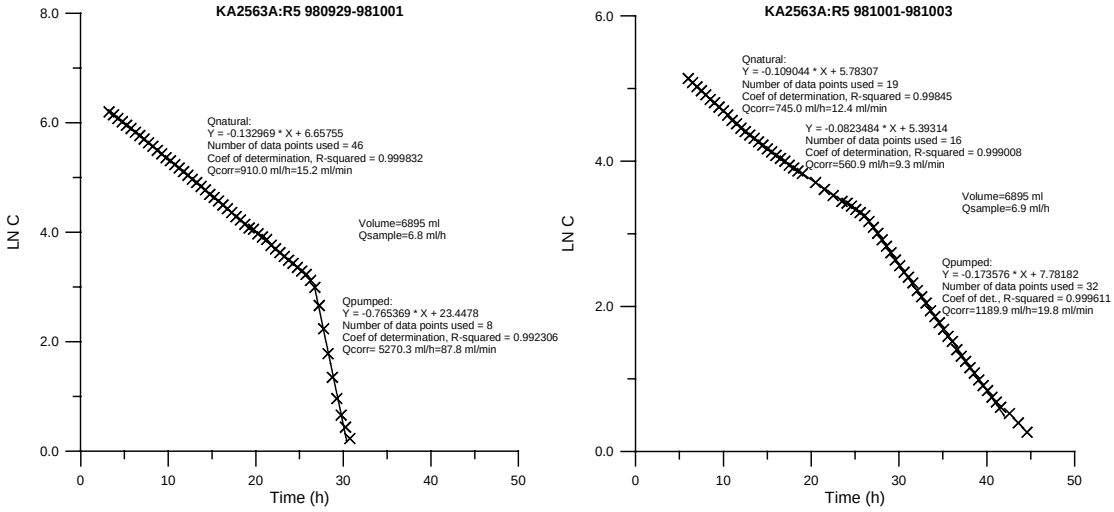

Figure 3-2 *Tracer dilution curve for borehole section KA2563A:R5 before and during pumping in KFI0025F02 section 73.3-77.3m (left) and 64.2.3-68.2m (right).*

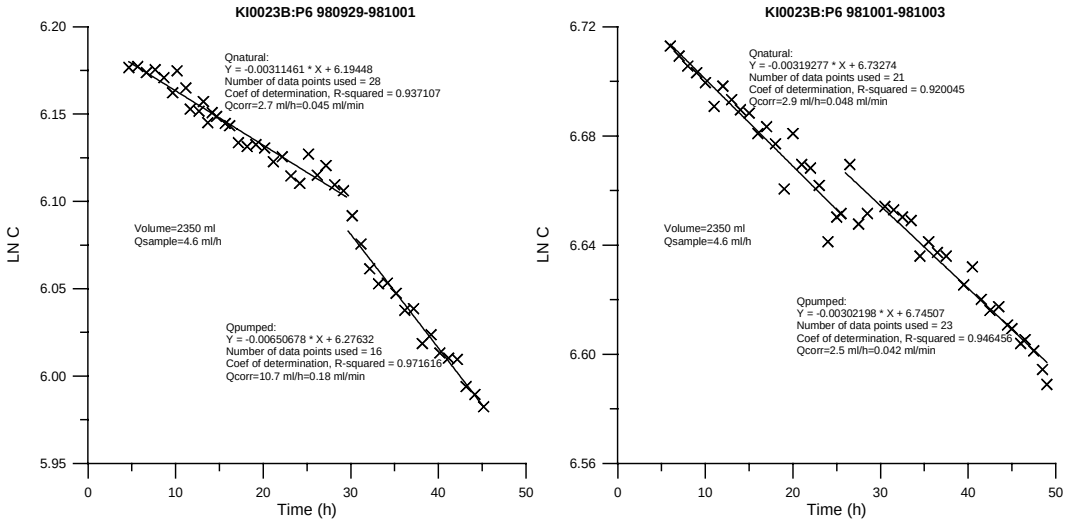

Figure 3-3 *Tracer dilution curve for borehole section KI0023B:P6 before and during pumping in KFI0025F02 section 73.3-77.3m (left) and 64.2.3-68.2m (right).*

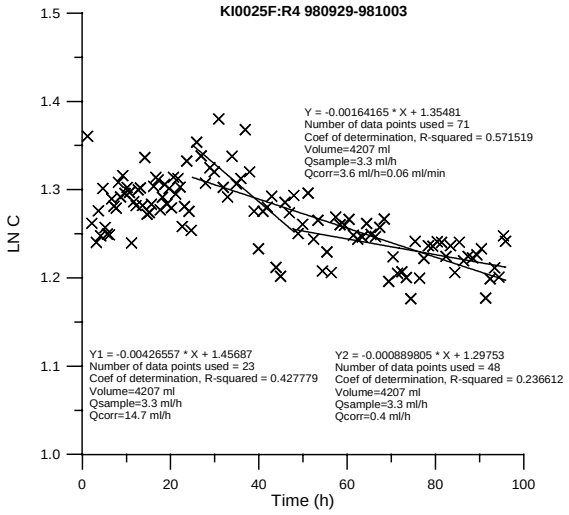

Figure 3-4 *Tracer dilution curve for borehole section KI0025F:R4 before (0-24 h) and during pumping in sections 73.3-77.3m (24-48 h) and 64.2.3-68.2m (72-96 h) in KFI0025F02.*

Table 3-1: Summary of Results of Selective Flow and Pressure Build-up Tests in Borehole KI0025F02.

Interval No.	Position [m]	Length (m)	Tests	Flow Model	T [m^2/s]	C_s [m^2/s]	Comments
1	**38.0 – 42.0**	4	INF				No squeeze
			HW		$1.8x10^{-6}$	$1.4x10^{-6}$	Steady state approx.
			HWS	W-s-2-p	$1.7x10^{-6}$		
2	**51.0 – 55.0**	4	INF				No squeeze
			HW		$1.5x10^{-8}$	$1.6x10^{-8}$	Steady state approx.
			HWS	W-s-2-p	($4.7x10^{-9}$)		<1.5 Log Cycles
3	**58.0 – 62.0**	4	INF				Slight squeeze
			HW	s-2	($1.1x10^{-8}$) $1.1x10^{-8}$	$1.2x10^{-8}$	Transient (large data scatter) Steady state approx.
			HWS	W-s-2-p	$5.3x10^{-9}$		
4	**64.2 – 68.2**	4	INF				No squeeze
			HW		$3.3x10^{-7}$	$2.8x10^{-7}$	Steady-state approx.
			HWS	W-s-2-p	$2.6x10^{-7}$		
5	**73.0 – 77.0**	4	INF				No squeeze
			HW	s-2	$6.5x10^{-7}$ $1.1x10^{-6}$	$8.7x10^{-7}$	Transient Steady-state approx.
			HWS	W-s-2-p	($4.4x10^{-7}$)		IARF not clearly defined
6	**91.0 – 95.0**	4	INF				Shut-in at surface
			HW	s-2	$3.6x10^{-9}$ $4.6x10^{-9}$	$5.7x10^{-9}$	Transient Steady-state approx.
			HWS	W-s-2	$1.5x10^{-9}$		
7	**96.0 – 100.0**	4	INF				Shut-in at surface
			HW		$5.0x10^{-8}$	$5.0x10^{-8}$	Steady-state approx.
			HWS	W-s-2-p	($9.6x10^{-9}$)		<1.5 Log Cycles
8	**130.0 – 134.0**	4	INF				Shut-in at surface
			HW	s-2	$4.4x10^{-7}$ $1.1x10^{-7}$	$1.3x10^{-7}$	Transient Steady state approx.
			HWS	W-s-2	$1.7x10^{-6}$		
9	**136.0 – 140.0**	4	INF				Shut-in at surface
			HW	s-2	$3.8x10^{-10}$ $8.3x10^{-10}$	$1.2x10^{-9}$	Transient Steady-state approx.
			HWS	W			
11	**33.2 – 34.2**	1	INF				Moderate squeeze
			HW	s-2-p	($7.8x10^{-10}$) $1.3x10^{-9}$	$1.8x10^{-9}$	large data scatter Steady-state approx.
			HWS	W-s-2-p	($4.4x10^{-10}$)		IARF not clearly defined
12	**34.3 – 35.3**	1	INF				Slight squeeze
			HW	s-2	$8.3x10^{-8}$ $3.1x10^{-8}$	$3.2x10^{-8}$	Transient Steady-state approx.
			HWS	W-s-2-C	($1.0x10^{-8}$) $5.3x10^{-8}$		Early-time (<1.5 Log Cycles) Late time
13	**109.5 - 110.5**	1	INF				Big Squeeze
			PW	s-2	$2.4x10^{-12}$	-	Transient
18	**163.8 – 164.8**	1	INF				Moderate squeeze
			HW	s-2-n	$5.8x10^{-9}$ $3.7x10^{-9}$	$4.6x10^{-9}$	Transient (no flow boundary) Steady-state approx.
			HWS	W-s-2-?	$2.5x10^{-9}$		<1.5 Log Cycles
19	**167.2 – 168.2**	1	INF				Moderate squeeze
			HW	s-2	$2.2x10^{-9}$ $2.5x10^{-9}$	$3.3x10^{-9}$	Transient Steady state approx.
			HWS	W-s-2-p	($1.0x10^{-9}$)		IARF not clearly defined

Interval No.	Position [m]	Length (m)	Tests	Flow Model	T [m^2/s]	C_s [m^2/s]	Comments
20	**172.7 – 173.7**	1	INF				
			HW	s-2	$5.3x10^{-8}$	$5.3x10^{-8}$	Steady-state approx.
			HWS	W-s-p			No analysis
23	**180.2 – 181.2**	1	INF				Moderate squeeze
			HW		$3.3x10^{-7}$	$2.9x10^{-7}$	Steady-state approx.
			HWS	W-s-2	$1.9x10^{-6}$		
26	**184.7 – 185.7**	1	INF				No squeeze
			HW	s-2-C	$4.6x10^{-8}$ $2.2x10^{-7}$ $2.2x10^{-7}$	 $2.0x10^{-7}$	Transient: Early-time Transient: Later-time Steady state approx.
			HWS	W-s-2-p	($4.5x10^{-8}$)		IARF not clearly defined
27	**188.75 – 189.75**	1	INF				No squeeze
			HW	s-2	$7.6x10^{-8}$ $1.6x10^{-8}$	 $1.8x10^{-8}$	Transient Steady state approx.
			HWS	W-s-2-p	($3.7x10^{-9}$)		<1.5 Log Cycles
31	**199.6 – 200.6**	1	INF				Slight squeeze
			HW	s-2	$5.5x10^{-7}$ $1.9x10^{-7}$	 $1.8x10^{-7}$	Transient Steady state approx.
			HWS	W-s-2-p	$5.1x10^{-8}$		<1.5 Log Cycles
4a	**64.2 – 68.2**	4	INF				No squeeze
			HW	s-2-p	$2.0x10^{-7}$ $3.6\ x10^{-7}$	 $2.4\ x10^{-7}$	Transient Steady state approx.
			HWS	W-s-2-p	$2.0x10^{-7}$		
5a	**73.0 – 77.0**	4	INF				No squeeze
			HW	s-2-p	$3.9x10^{-7}$ $9.5x10^{-7}$	 $6.3x10^{-7}$	Transient Steady-state approx.
			HWS	W-s-2-p	($3.9x10^{-7}$)		IARF not clearly defined

Test Legend:

INF	Inflation Period
HW	Constant Pressure (Head) Withdrawal Test
HWS	Pressure Build-up after Constant Pressure (Head) Withdrawal Test
PW	Pulse Withdrawal Test

Flow Model Legend:

W	Wellbore Storage	Skin	
2	Flow Dimension of 2	p	Positive-acting Boundary
n	Negative-acting Boundary	C	Composite

Comment Legend:

IARF: Infinite-acting Radial Flow (flow dimension of 2)
<1.5 Log Cycle: Identified IARF-period does not meet the "1.5 Log Cycle-rule"
Transmissivity values in parenthesis () are presented with a low degree of confidence

Table 3-2: Comparison of Results between POSIVA Flow Logging and Selective Flow and Pressure Build-up Tests in Borehole KI0025F02.

Selective Flow and Pressure Build-up Tests					POSIVA Flow Logging					
Int. No.	**Interval Location** [m]	**DH** [m]	**Flow Rate** [ml/mn]	**C_s** [m^2/s]	**Flow Pick** [m]	**Flow Rate** [ml/mn]	**dH** [m]	**C_s** [m^2/s]	**Sum C_s** [m^2/s]	**Ratio $C_{s\text{-}PBU}$ / $C_{s\text{-}POSIVA}$**
1	38.0 – 42.0	200	17'350	1.4E-06	38.3	76	400	3.2E-09	1.7E-07	8.2 [1)]
					39.9	4000	400	1.7E-07		
					40.9	17	400	7.1E-10		
2	51.0 – 55.0	200	200	1.6E-08	52.4	280	400	1.2E-08	1.2E-08	1.3
					54.5	12.5	400	5.2E-10		
3	58.0 – 62.0	200	150	1.2E-08	59.25	134	400	5.6E-09	5.8E-09	2.1
					60.05	4	400	1.7E-10		
					61.5	2	400	8.3E-11		
4	64.2 – 68.2	201	3'500	2.8E-07	65.15	680	400	2.8E-08	1.7E-07	1.6 [1)]
					66.9	2500	400	1.0E-07		
					67.2	900	400	3.8E-08		
					67.45	95	400	4.0E-09		
5	73.0 – 77.0	200	10'700	8.7E-07	74.2	130	400	5.4E-09	1.3E-07	6.7 [1)]
					74.7	3000	400	1.3E-07		
					76.6	6	400	2.5E-10		
6	91.0 – 95.0	199	70	5.7E-09	94	97	400	4.0E-09	4.0E-09	1.4
7	96.0 – 100.0	200	610	5.0E-08	97	5	400	2.1E-10	3.0E-08	1.7
					97.3	10	400	4.2E-10		
					97.95	700	400	2.9E-08		
					98.8	2.5	400	1.0E-10		
8	130.0 – 134.0	200	1'620	1.3E-07	130.5	70	400	2.9E-09	1.6E-07	0.8
					131.65	1550	400	6.5E-08		
					131.85	1200	400	5.0E-08		
					133	900	400	3.8E-08		
					133.2	50	400	2.1E-09		
9	136.0 – 140.0	199	20	1.2E-09	138.55	20	400	8.3E-10	8.3E-10	1.4
11	33.2 – 34.2	200	20	1.8E-09	33.9	26	400	1.1E-09	1.1E-09	1.7
12	34.3 – 35.3	382	610	2.6E-08	34.9	490	400	2.0E-08	2.0E-08	1.3
		302	520	2.8E-08						1.4
		199	390	3.2E-08						1.6
		102	210	3.4E-08						1.7
		52	120	3.8E-08						1.9
18	163.8 – 164.8	200	60	4.6E-09	164.55	60	400	2.5E-09	2.5E-09	1.8
19	167.2 – 168.2	200	40	3.3E-09	167.7	55	400	2.3E-09	2.3E-09	1.4
20	172.7 – 173.7	100	320	5.3E-08	173.3	800	400	3.3E-08	3.3E-08	1.6
					173.5	2	400	8.3E-11		
23	180.2 – 181.2	50	900	2.9E-07	180.55	900	400	3.8E-08	6.3E-08	4.6
					180.85	600	400	2.5E-08		
26	184.7 – 185.7	50	610	2.0E-07	184.8	20	400	8.3E-10	1.4E-07	1.4 [1)]
					185.15	3400	400	1.4E-07		
27	188.75 – 189.75	100	110	1.8E-08	189.1	380	400	1.6E-08	1.6E-08	1.1
31	199.6 – 200.6	50	540	1.8E-07	200.05	2300	400	9.6E-08	9.6E-08	1.9 [1)]

[1)] Reported flow rate is in excess of the 2 l/min flow limiter that was installed for the measurements

Table 3-3: Drawdown at the end of the cross-hole tests.

Obs. Point	Test 1 Q=17.4 [kPa]	Test 2 Q=0.22 [kPa]	Test 3 Q=0.1 [kPa]	Test 4 Q=3.5 [kPa]	Test 5 Q=10.0 [kPa]	Test 7 Q=0.6 [kPa]	Test 8 Q=1.7 [kPa]
KI0023B:1	-	-	-	9	2	-	-
KI0023B:2	-	-	-	5	4	-	35
KI0023B:3	-	-	-	11	100	-	3
KI0023B:4	-	-	-	29	205	-	-
KI0023B:5	5	8	0.7	60	540	0.6	-
KI0023B:6	7	9	1.0	75	650	1.0	-
KI0023B:7	13	8	1.5	70	630	1.0	-
KI0023B:8	96	-	0.5	-	10	-	-
KI0023B:9	10	-	-	-	3	-	-
KI0025F:1	-	-	-	-	-	-	1
KI0025F:2	-	-	-	-	-	-	3
KI0025F:3	-	-	-	4	40	-	2.5
KI0025F:4	2	4	0.7	73	870	0.8	-
KI0025F:5	400	-	?	-	27	0.6	-
KI0025F:6	23	-	0.5	-	22	-	-
KA2563A:1	5	4	0.8	60	440	0.8	-
KA2563A:2	-	-	Other act	-	7	-	1.5
KA2563A:3	2	-	Other act	-	15	-	-
KA2563A:4	-	-	-	23	160	-	-
KA2563A:5	6	6	0.8	75	650	1.0	-
KA2563A:6	20	3	1.0	25	160	-	-
KA2563A:7	9	-	0.7	-	-	-	-
KA2511A:1	4	-	-	-	-	-	-
KA2511A:2	-	-	-	3	-	-	-
KA2511A:3	3	-	-	-	-	-	-
KA2511A:4	5	-	0.3	-	-	-	-
KA2511A:5	12	-	-	-	3	0.3	-

Q : Flow rates in ml/min due to an imposed drawdown of 2000 kPa at the pumping interval (constant head test)

other act: Pressure response might be influenced by other activities

Table 3-4: s_p/Q index for cross-hole tests 1 - 8.

Obs. Point	Test 1 Q=17.4 [s/m^2]	Test 2 Q=0.22 [s/m^2]	Test 3 Q=0.10 [s/m^2]	Test 4 Q=3.5 [s/m^2]	Test 5 Q=10.0 [s/m^2]	Test 7 Q=0.6 [s/m^2]	Test 8 Q=1.7 [s/m^2]
KI0023B:1	-	-	-	15430	1200	-	-
KI0023B:2	-	-	-	7700	2400	-	**124000**
KI0023B:3	-	-	-	18900	60000	-	10600
KI0023B:4	-	-	-	49700	123000	-	-
KI0023B:5	1730	223000	42000	103000	324000	6000	-
KI0023B:6	2244	**250000**	60000	**130000**	**390000**	**10000**	-
KI0023B:7	4300	223000	**90000**	120000	378000	**10000**	-
KI0023B:8	**33100**	-	30000	-	6000	-	-
KI0023B:9	3500	-	-	-	1800	-	-
KI0025F:1	-	-	-	-	-	-	3500
KI0025F:2	-	-	-	-	-	-	**10600**
KI0025F:3	-	-	-	6000	24000	-	8800
KI0025F:4	700	**111600**	**42000**	**125000**	**522000**	**8000**	-
KI0025F:5	**138000**	-	?	-	16200	6000	-
KI0025F:6	7900	-	30000	-	13200	-	-
KA2563A:1	1700	111600	48000	103000	264000	8000	-
KA2563A:2	-	-	Other act	-	4200	-	**5300**
KA2563A:3	690	-	Other act	-	9000	-	-
KA2563A:4	-	-	-	39000	95800	-	-
KA2563A:5	2100	**167400**	48000	**130000**	**390000**	**10000**	-
KA2563A:6	**6900**	83700	**60000**	43000	95800	-	-
KA2563A:7	3100	-	42000	-	-	-	-
KA2511A:1	1400	-	-	-	-	-	-
KA2511A:2	-	-	-	**5100**	-	-	-
KA2511A:3	1000	-	-	-	-	-	-
KA2511A:4	1700	-	-	-	-	-	-
KA2511A:5	**4100**	-	**18000**	-	**1800**	**3000**	-

Q : Flow rates in ml/min due to an imposed drawdown of 2000 kPa at the pumping interval (constant head test)

other act: Pressure response might be influenced by other activities

bold numbers indicate the maximum value for each borehole

Table 3-5: Drawdown (s) at the end of the dilution tests and sp/Q index.

Interval	Dilution Test 1 s [kPa]	Dilution Test 1 s_p/Q [s/m^2]	Dilution Test 2 s [kPa]	Dilution Test 2 s_p/Q [s/m^2]
KI0023B:1	-	-	16	22171
KI0023B:2	-	-	13	18013
KI0023B:3	574	299739	59	81755
KI0023B:4	785	409921	82	113626
KI0023B:5	961	501828	103	142725
KI0023B:6	998	**521149**	106	**146882**
KI0023B:7	960	501305	103	142725
KI0023B:8	-	-	-	-
KI0023B:9	-	-	-	-
KI0025F:1	-	-	6	8314
KI0025F:2	-	-	5	6928
KI0025F:3	91	47520	11	15242
KI0025F:4	1269	**662663**	114	**157968**
KI0025F:5	55	28720	10	13857
KI0025F:6	47	24543	13	18014
KA2563A:1	655	**342036**	86	**119169**
KA2563A:2	29	15143	5	6928
KA2563A:3	?	-	?	?
KA2563A:4	747	390078	78	108038
KA2563A:5	991	**517493**	107	**148268**
KA2563A:6	340	177545	37	51270
KA2563A:7	-	-	-	-
KA2511A:1	12	6266	11	15242
KA2511A:2	12	6266	10	13857
KA2511A:3	15	7833	14	19400
KA2511A:4	15	7833	15	20785
KA2511A:5	17	**8877**	16	**22171**
KG0048A01	24	12533	-	-
KG0021A	-	-	-	-
KA2598A	-	-	-	-
KA3548A:1	20	10443	-	-
KA3548A:2	23	**12010**	-	-
KA3600A:1	13	6789	-	-
KA3600A:2	14	**7311**	-	-
KA3573A:1	20	10443	-	-
KA3573A:2	20	10443	-	-
KA3510A:1	14	7311	-	-

The values in bold indicate the most dominant responses in each of the boreholes.

Table 3-6: Summary of tracer dilution test results.

Dilution test interval	Pump interval	Natural flow (ml/h)	Induced flow (ml/h)
KA2563A:5	4a	900	5300
	5a	750	1200
KI0023B:6	4a	3	11
	5a	5	3
KI0025F:4	4a	<1	(15)
	5a	<1	<1

4 Conclusions and Recommendations

a) The combination of single-well double packer testing with immediate qualitative on-site analysis of pressure responses at the observation points allowed optimisation of the multi-packer system configuration with respect to the hydro-structural model.

b) The cross-hole responses allow clear identification of structures #7, #20 and #19. Structures #7 and #19 are only weakly connected to #20 and could be considered to form the limits for the area of the planned tracer tests. Structure #20 is the dominant feature within this area. All features within this area respond quickly to pressure changes within structure #20.

c) In most structures, steady-state conditions were attained in the pumping well within a few minutes, which may be the result of a connection to a more conductive fracture or due to flow becoming 3-dimensional. The T values of the single-well tests range from $1x10^{-12}$ to $2x10^{-6}$ m^2/s.

d) Most cross-hole pressure responses showed the influence of some type of constant head boundary, which is in agreement with the steady-state conditions observed in many pumping wells. The boundary effects might lead to an overestimation of T using conventional analysis techniques (Jacob's method, Theis, Hantush). The T estimates should be considered rough estimates, which should be refined by calibrating numerical models with cross-hole interference data.

e) All connectivity measures provide important qualitative information for the hydro-structural model. The flow rate normalised drawdown at the end of a pumping test s_p/Q seems to be the most robust connectivity index in 3-D fractured flow systems. Storativity estimates from conventional analysis (Jacob's method) of cross-hole pressure responses also contain valuable information on the connectivity between pumping and observation wells. The use of storativity estimates seems to be more appropriate in 2-D heterogeneous media because of the existing scientific basis.

f) The principle of reciprocity is fulfilled for one of the dilution tests. Changing fracture near-well transmissivity due to depressurisation and/or the effects of turbulent flow are possible reasons for the deviation from the principle of reciprocity in the second dilution test.

g) The step drawdown test indicates a pressure-dependent near-well transmissivity due to fracture aperture variation or the effects of turbulent flow. It is recommended that this point be investigated with Pac-ex measurements. Such measurements could also provide important information for the correct interpretation of PRG-OY/POSIVA high-precision flow meter measurements, as well as information about the fracture storativity, a parameter which cannot be estimated by hydraulic testing in heterogeneous media.

h) A comparison of the PRG-OY/POSIVA high-precision flow meter and double-packer measurements indicates a good agreement between the two techniques. The specific capacity values obtained from the PRG-OY/POSIVA flow logging lie in general below the values from the double-packer tests by less than a factor of two. The systematically lower values could be a result of the effects of pressure-dependent fracture aperture and/or effects of turbulent flow.

i) The tracer dilution tests performed under both natural and pumped conditions clearly indicates that section 73.0-77.0 m in KI0025F02 is structure #20, whereas the pumping in section 64.2-68.2 m shows either no, or much less, increase in the three observation sections. However, the significant flow increase in section KA2563A-5 indicates that section 64.2-68.2 is also, at least indirectly, associated with structure #20.

5 References

Agarwal, R.G. (1980): A New Method to Account for Producing Time Effects When Drawdown Type Curves Are Used to Analyze Pressure Build-up and Other Test Data. - Soc. of Petroleum Engineers, SPE Paper 9289, presented at SPE-AIME Meeting, Dallas, Texas, September 21-24, 1980.

Andersson, P., Ludvigsson J.-E. & Wass E. (1998): TRUE Block Scale Project, preliminary characterization stage, Combined interference tests and tracer tests, Performance and preliminary evaluation. – Äspö Hard Rock Laboratory, International Progress Report IPR-01-44.

Black, J.H. (1985): The Interpretation of Slug Tests in Fissured Rocks. - Q. Jour. Eng. Geology, Vol. 18, pp. 161-171.

Cooper, H.H. Jr. & Jacob, C.E. (1946): A Generalized Graphical Method for Evaluating Formation Constants and Summarizing Well-Field History. - Am. Geophys. Union Trans., Vol. 27, No. 4, pp. 526-534.

Earlougher, R.C. Jr. (1977): Advances in Well Test Analysis. - Soc. of Petroleum Engineers, Monograph Volume 5 of the Henry L. Doherty Series, 264 p.

Jacob, C.E. & Lohman, S.W. (1952): Non-steady Flow to a Well of Constant Drawdown in an Extensive Aquifer. - Transactions, American Geophysical Union, Volume 33, No. 4, pp. 559-569.

Hermanson, Jan, (1997): October 1997 Structural Model; Update using Characterization Data from KA2511A and KI0025F. Äspö Hard Rock Laboratory, International Progress Report IPR-01-41.

Horne, Roland N., (1995): Modern Well Test Analysis, A Computer-Aided Approach. Petroway, Inc. Palo Alto California.

Meier, P., Carrera, J., and Sanchez-Vila, X. (1998): An evaluation of Jacob's method for the interpretation of pumping tests in heterogeneous formations. Water Resources Research, Vol. 34, No. 5, Pp 1011 – 1025.

Rouhianen & Heikkinen, (1998): Difference Flow Measurements in Borehole KI0025F02 at the Äspö Hard Rock Laboratory International Progress Report IPR-01-46.

Rutqvist, J., Noorishad, J., Tsang, C-F., and Stephansson, O., (1998): Determination of fracture storativity in hard rocks using high-perssure injection testing. Water Resources Research, Vol. 34, No. 10, Pp 2551 – 2560.

Sánchez-Vila, X., P.M. Meier and J. Carrera, (1999): Pumping tests in heterogeneous aquifers: an analytical study of what can be really obtained from their interpretation using Jacob's method, Water Resour. Res., in press. 1999.

Uchida, M., Doe, T., Dershowitz, W., Thomas, A., Wallmann, P., & Sawada, A. (1994): Discrete-fracture network modelling of the Aspo LPT-2, large-scale pumping and tracer test. SKB. Äspö Hard Rock Lab. ICR 95-05.

Winberg, A. ed. (1996): First TRUE Stage - Tracer Retention Understanding Experiments. Descriptive structural-hydraulic models on block and detailed scales of the TRUE-1 Site. SKB ICR 96-04.

Zeigler, T.W. (1976): Determination of Rock Mass Permeability, U.S. Army Engineering Waterways Experiment Station, Technical Report S-76-2, Vicksburg, Mississippi

APPENDIX A

Single-hole Analyses

During Cross-hole Tests

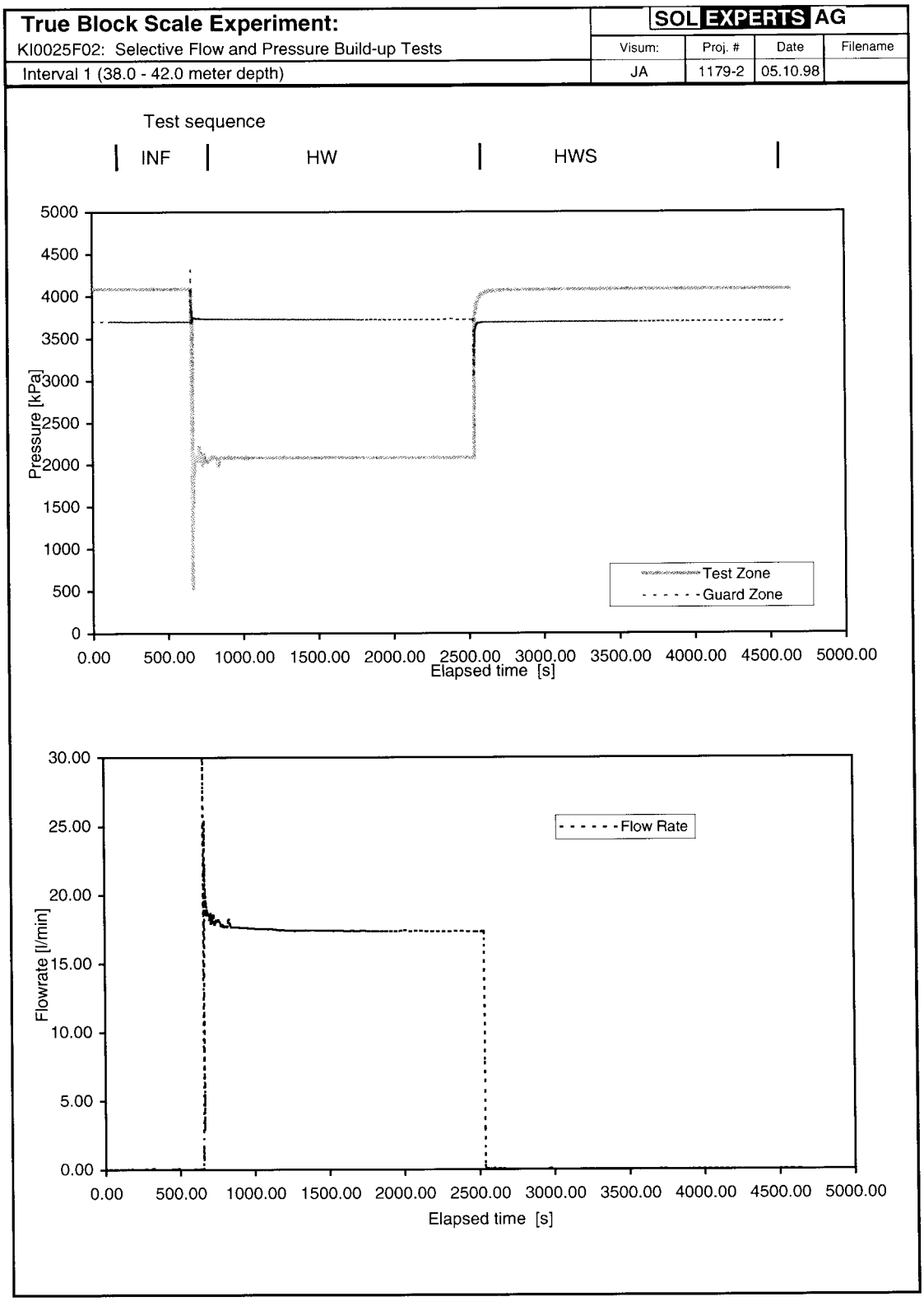

Figure A-1 *Interval 1: Cartesian plots of Interval Pressure, Guard-zone Pressure and Flow Rate –vs- Time*

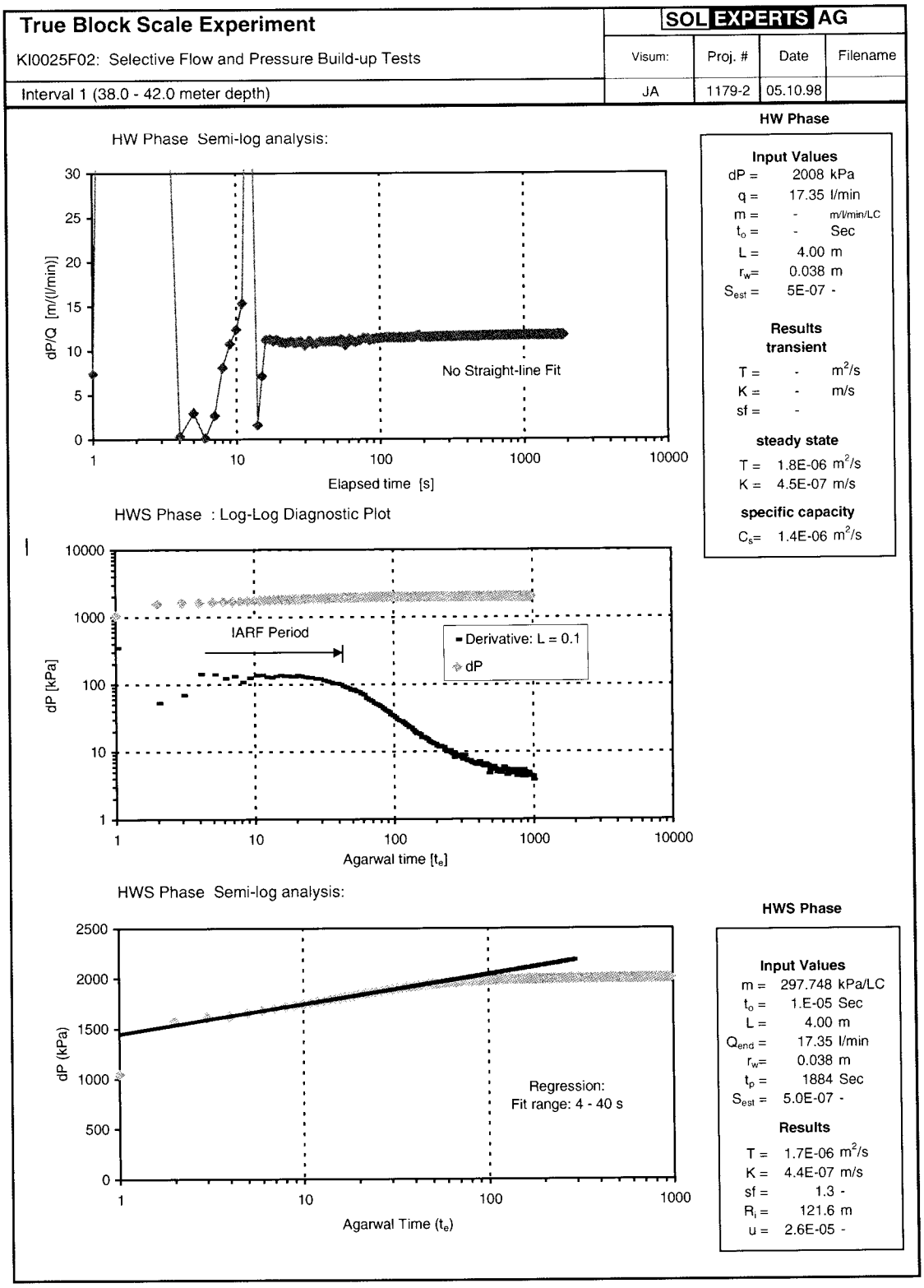

Figure A-2 Interval 1: Analysis Plots

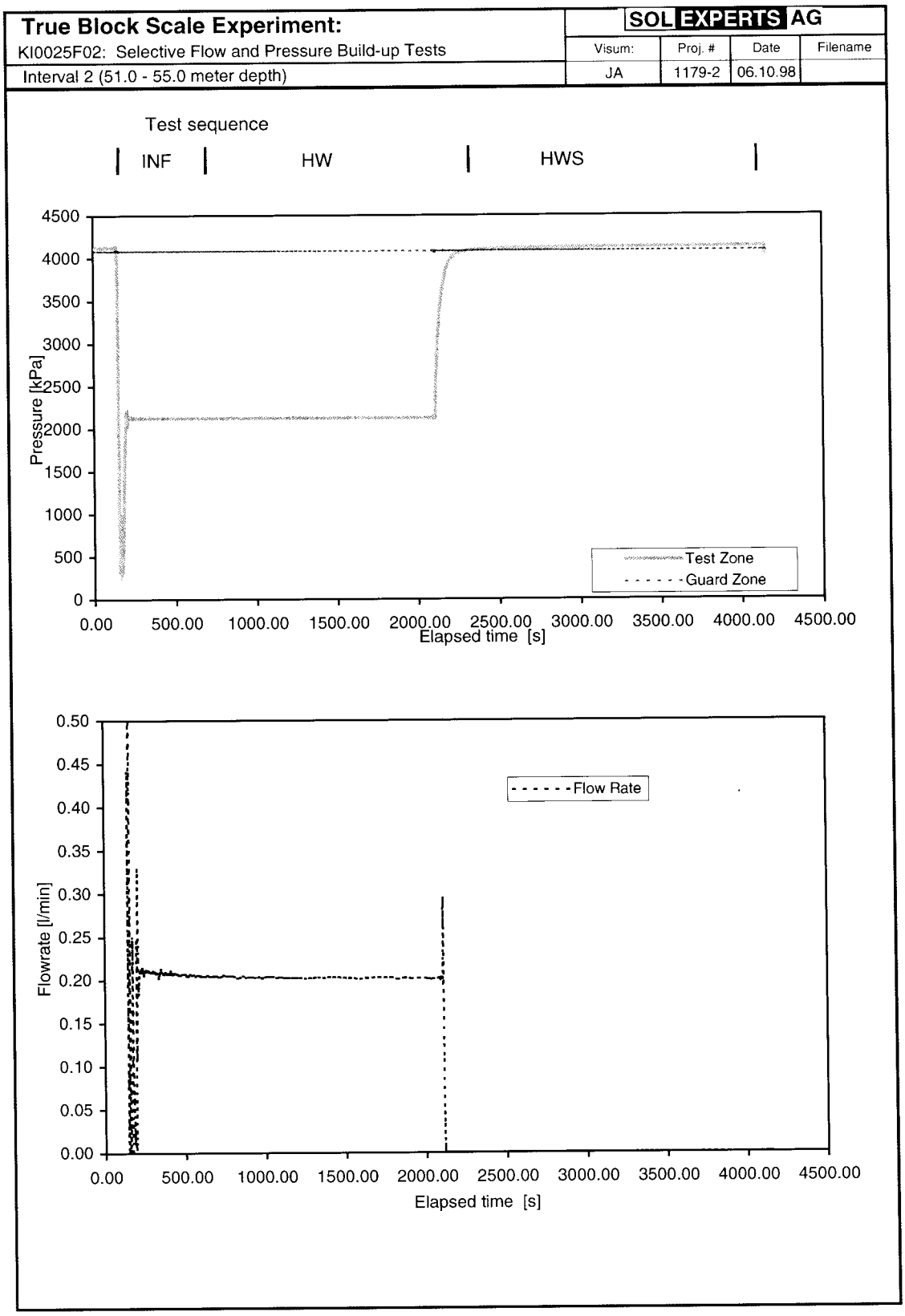

Figure A-3 *Interval 2: Cartesian plots of Interval Pressure, Guard-zone Pressure and Flow Rate –vs- Time*

True Block Scale Experiment — SOL EXPERTS AG

KI0025F02: Selective Flow and Pressure Build-up Tests

Interval 2 (51.0 - 55.0 meter depth)

Visum:	Proj. #	Date	Filename
JA	1179-2	06.10.98	

HW Phase Semi-log analysis:

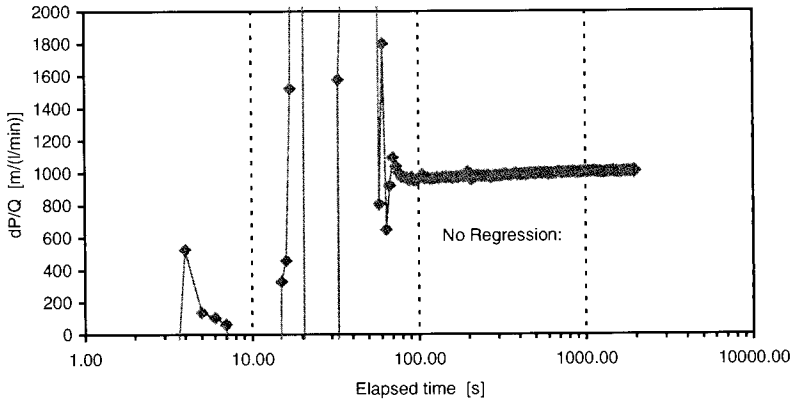

HW Phase

Input Values

dP =	2006	kPa
q_{end} =	0.20	l/min
m =	-	m/(l/min)/LC
t_o =	-	Sec
L =	4.00	m
r_w=	0.038	m
S_{est} =	5.0E-07	-

Results

transient

T =	-	m^2/s
K =	-	m/s
sf =	-	

steady state

T =	1.5E-08	m^2/s
K =	3.7E-09	m/s

specific capacity

C_s=	1.6E-08	m^2/s

HWS Phase : Log-Log Diagnostic Plot

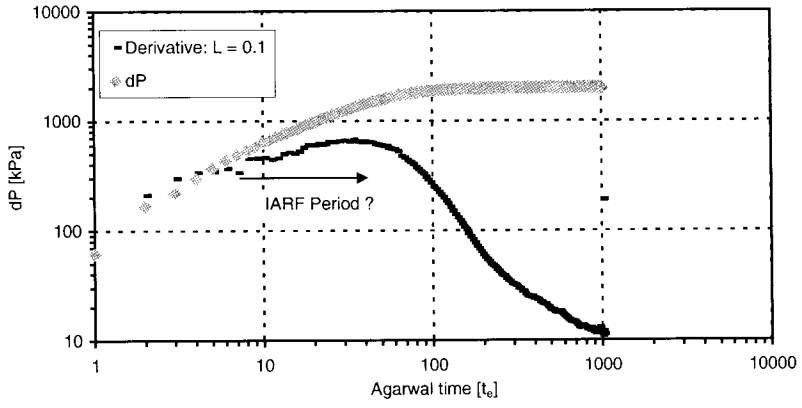

HWS Phase Semi-log analysis:

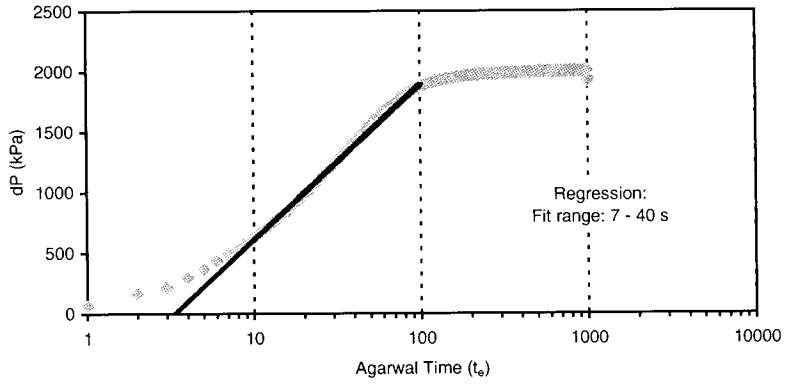

HWS Phase

Input Values

m =	1284.26	kPa/LC
t_o =	3.E+00	Sec
L =	4.00	m
Q_{end} =	0.20	l/min
r_w=	0.038	m
t_p =	1966	Sec
S_{est} =	1.0E-07	-

Results

T =	4.7E-09	m^2/s
K =	1.2E-09	m/s
sf =	-2.8	-
R_i =	14.4	m
u =	1.1E-03	-

Figure A-4 Interval 2: Analysis Plots

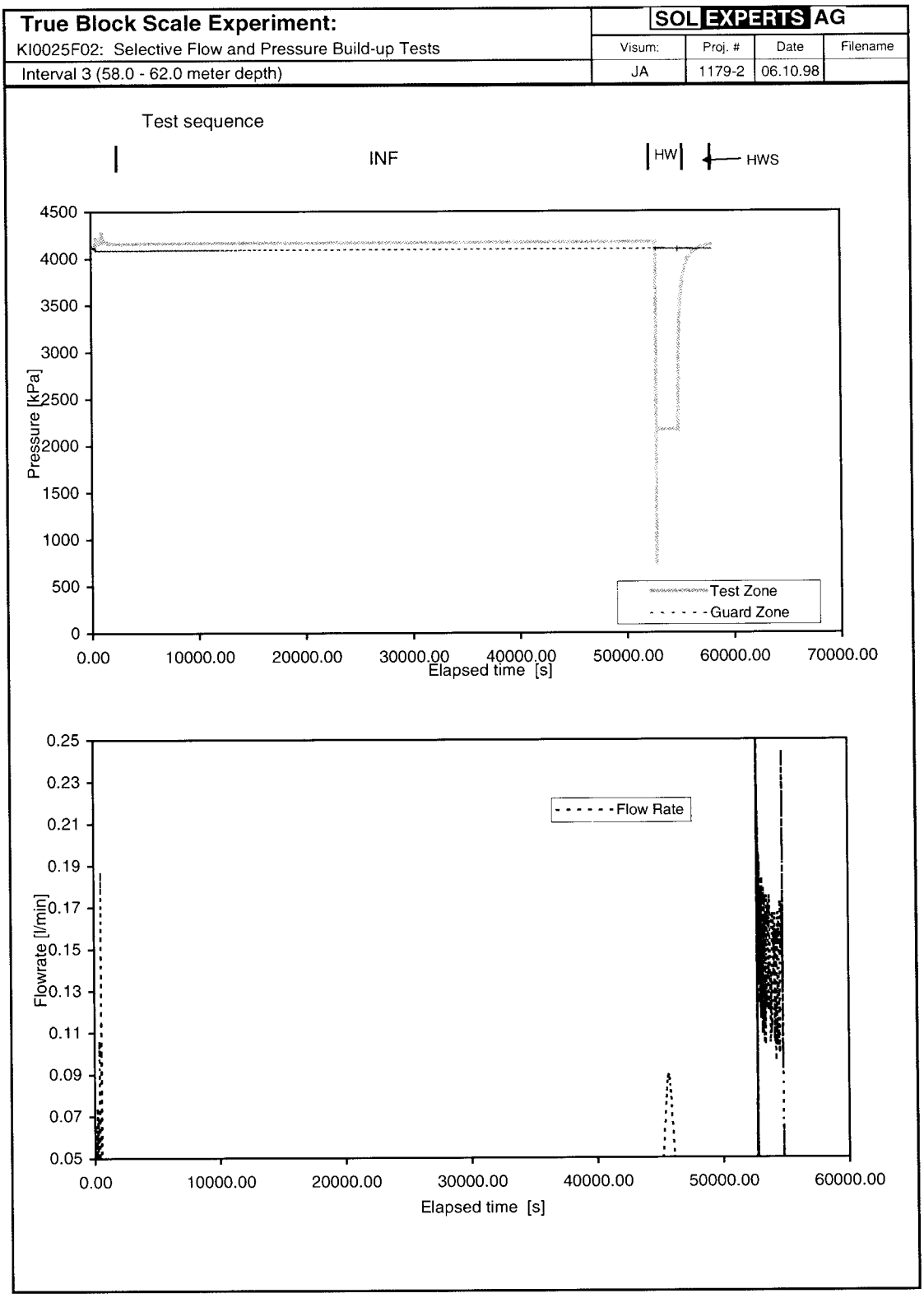

Figure A-5 *Interval 3: Cartesian plots of Interval Pressure, Guard-zone Pressure and Flow Rate –vs- Time*

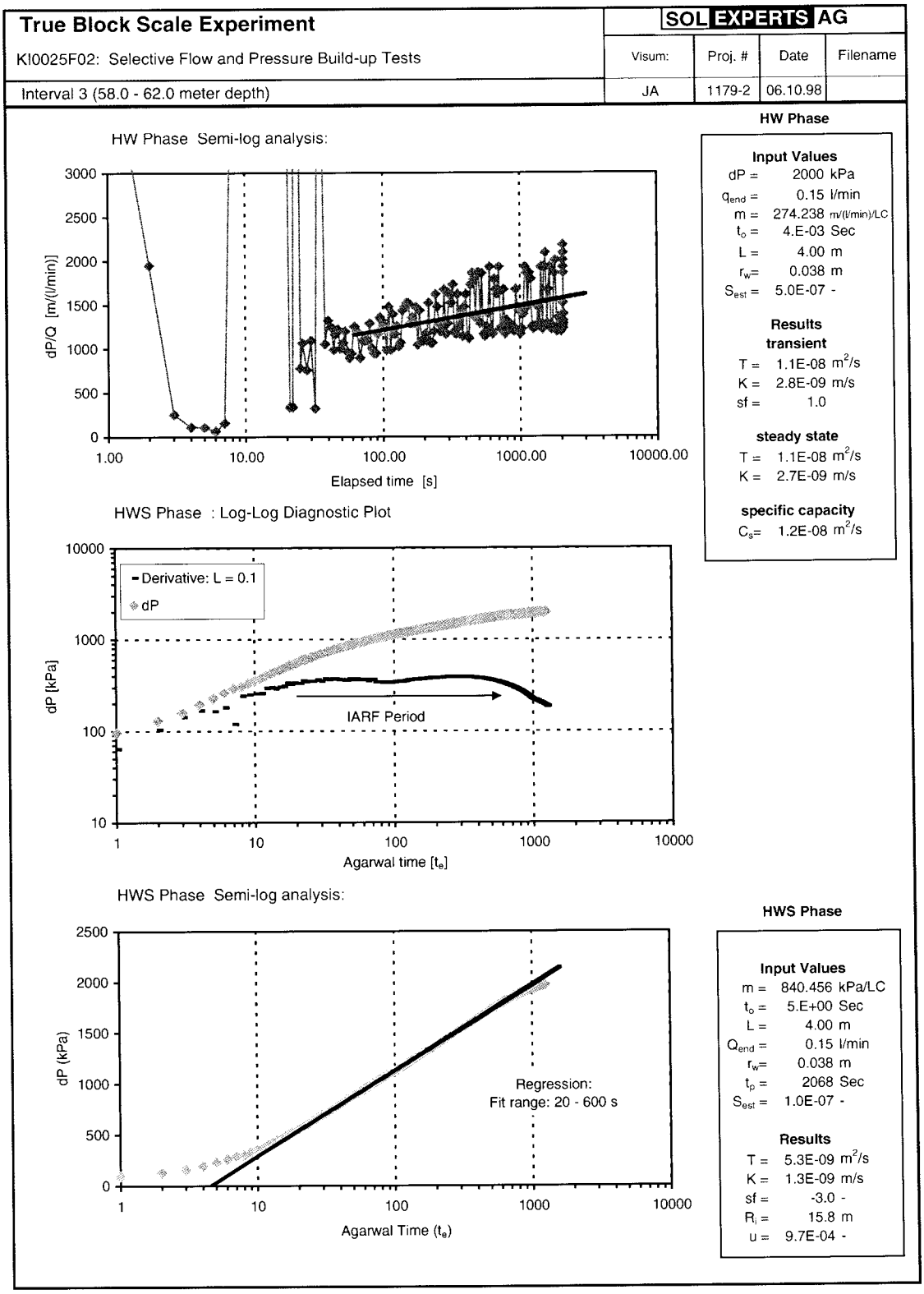

Figure A-6 Interval 3: Analysis Plots

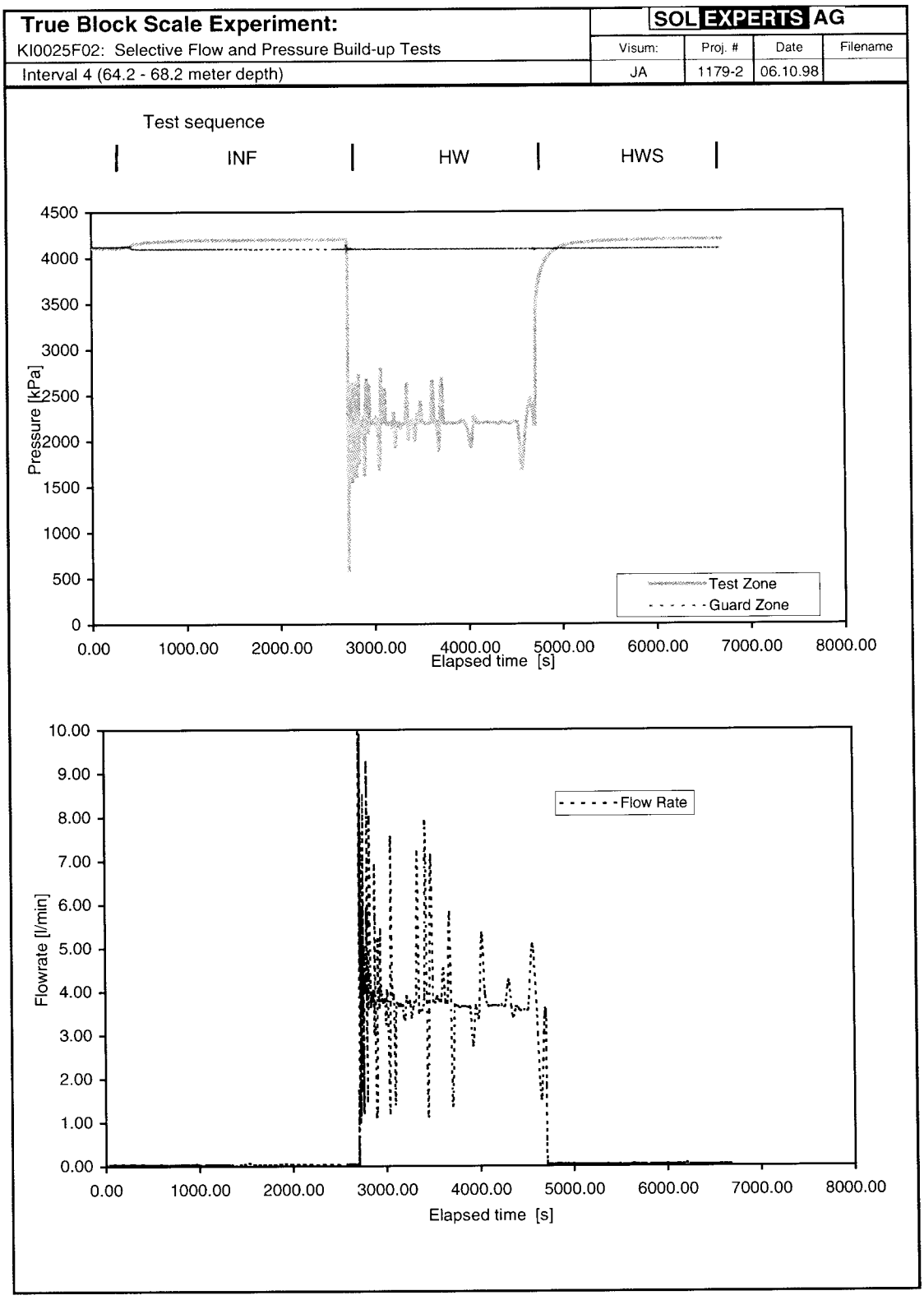

Figure A-7 *Interval 4: Cartesian plots of Interval Pressure, Guard-zone Pressure and Flow Rate –vs- Time*

True Block Scale Experiment

KI0025F02: Selective Flow and Pressure Build-up Tests

Interval 4 (64.2 - 68.2 meter depth)

SOL EXPERTS AG

Visum:	Proj. #	Date	Filename
JA	1179-2	06.10.98	

HW Phase Semi-log analysis:

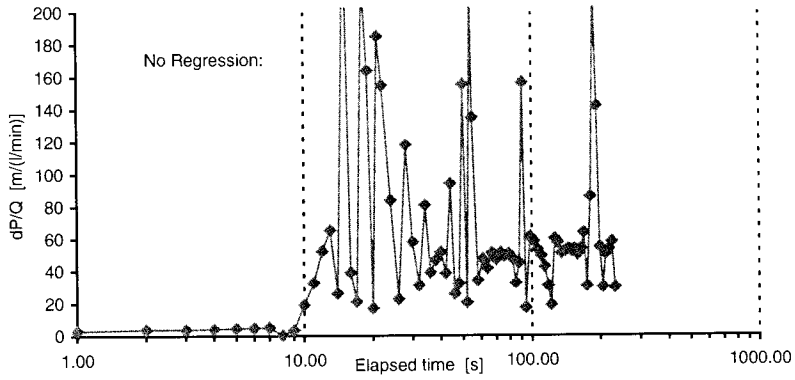

HW Phase

Input Values

dP =	2012	kPa
q_{end} =	3.50	l/min
m =	-	m/(l/min)/LC
t_o =	-	Sec
L =	4.00	m
r_w =	0.038	m
S_{est} =	5.0E-07	-

Results

transient

T =	-	m^2/s
K =	-	m/s
sf =	-	

steady state

T =	3.3E-07	m^2/s
K =	8.2E-08	m/s

specific capacity

C_s = 2.8E-07 m^2/s

HWS Phase : Log-Log Diagnostic Plot

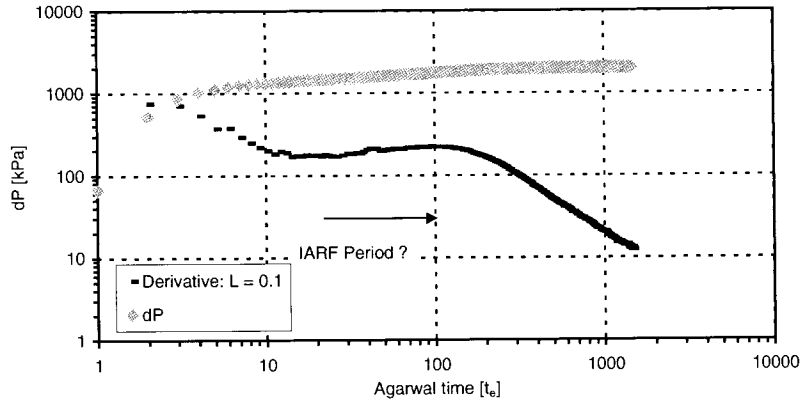

HWS Phase Semi-log analysis:

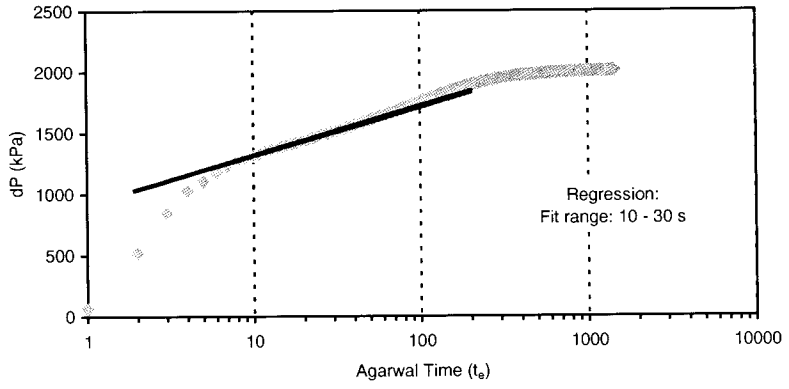

HWS Phase

Input Values

m =	399.949	kPa/LC
t_o =	5.E-03	Sec
L =	4.00	m
Q_{end} =	3.50	l/min
r_w =	0.038	m
t_p =	2000	Sec
S_{est} =	1.0E-07	-

Results

T =	2.6E-07	m^2/s
K =	6.5E-08	m/s
sf =	-1.5	-
R_i =	108.5	m
u =	2.0E-05	-

Figure A-8 Interval 4: Analysis Plots

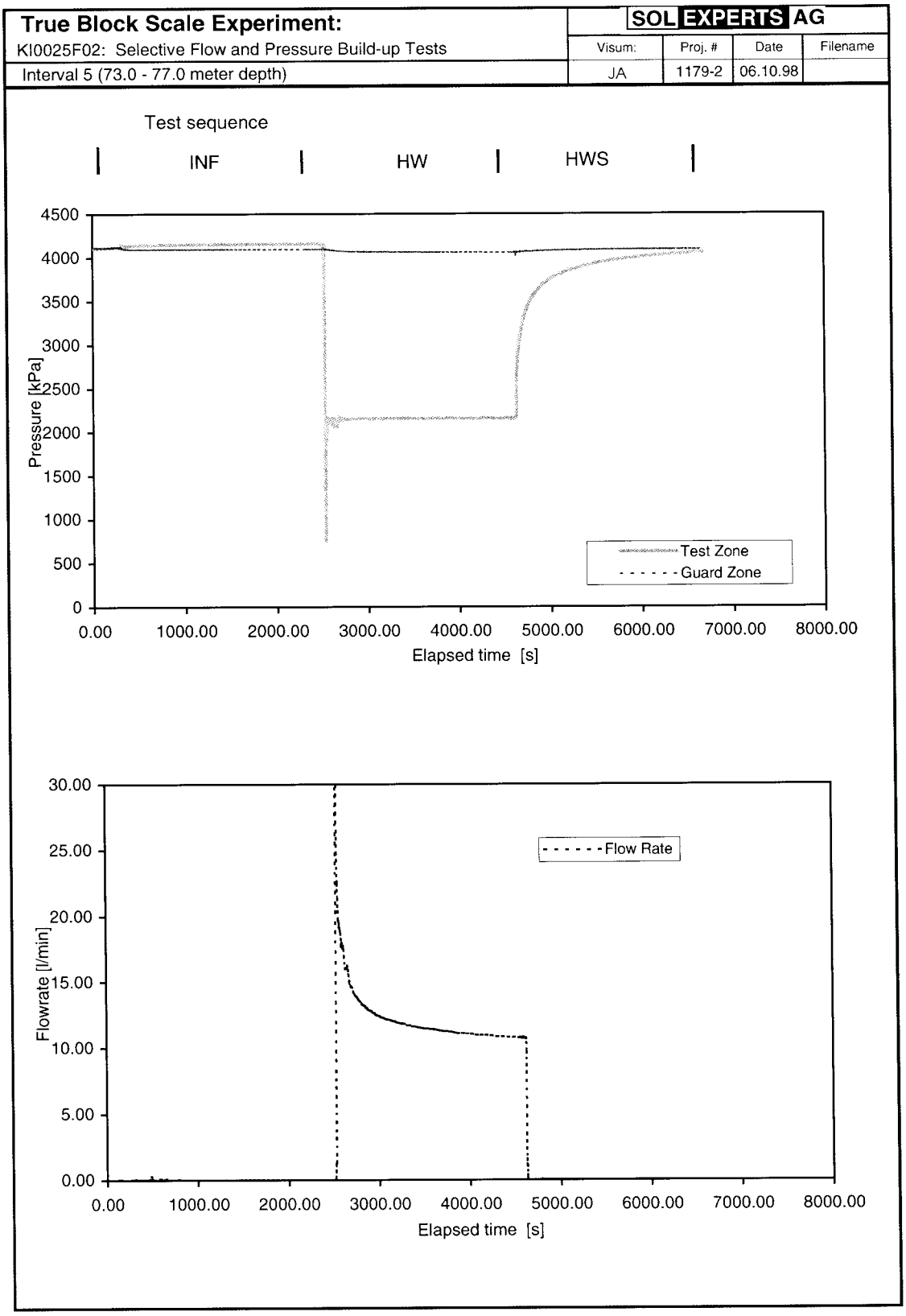

Figure A-9 *Interval 5: Cartesian plots of Interval Pressure, Guard-zone Pressure and Flow Rate –vs- Time*

True Block Scale Experiment

KI0025F02: Selective Flow and Pressure Build-up Tests

Interval 5 (73.0 - 77.0 meter depth)

SOL EXPERTS AG

Visum:	Proj. #	Date	Filename
JA	1179-2	06.10.98	

HW Phase Semi-log analysis:

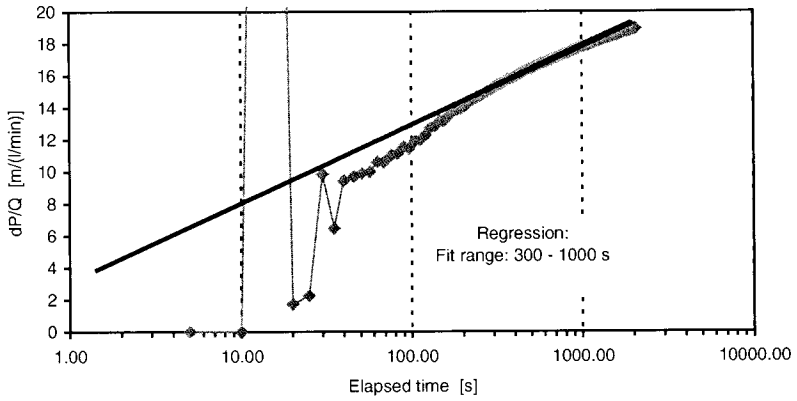

HW Phase

Input Values

dP =	2000	kPa
q_{end} =	10.70	l/min
m =	4.70437	m/(l/min)/LC
t_o =	2.E-01	Sec
L =	4.00	m
r_w =	0.038	m
S_{est} =	5.0E-07	-

Results

transient

T =	6.5E-07	m^2/s
K =	1.6E-07	m/s
sf =	-2.9	

steady state

T =	1.1E-06	m^2/s
K =	2.7E-07	m/s

specific capacity

C_s =	8.7E-07	m^2/s

HWS Phase : Log-Log Diagnostic Plot

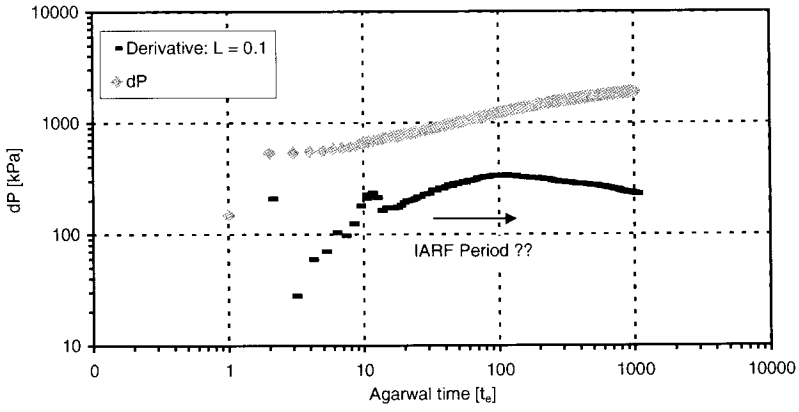

HWS Phase Semi-log analysis:

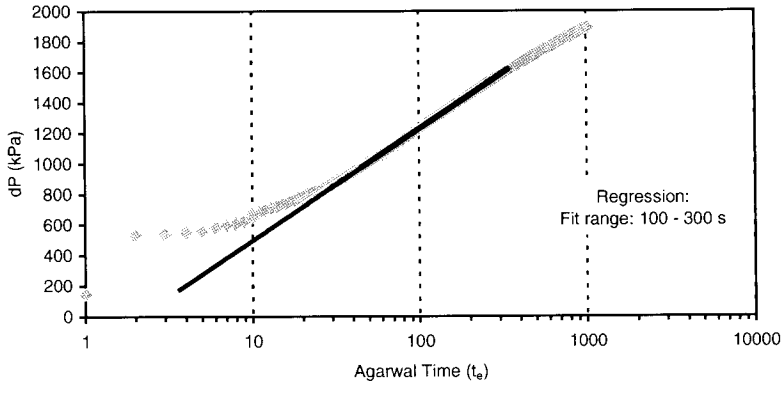

HWS Phase

Input Values

m =	727.409	kPa/LC
t_o =	5.E-01	Sec
L =	4.00	m
Q_{end} =	10.70	l/min
r_w =	0.038	m
t_p =	2120	Sec
S_{est} =	5.0E-07	-

Results

T =	4.4E-07	m^2/s
K =	1.1E-07	m/s
sf =	-3.3	-
R_i =	64.8	m
u =	4.1E-06	-

Figure A-10 Interval 5: Analysis Plots

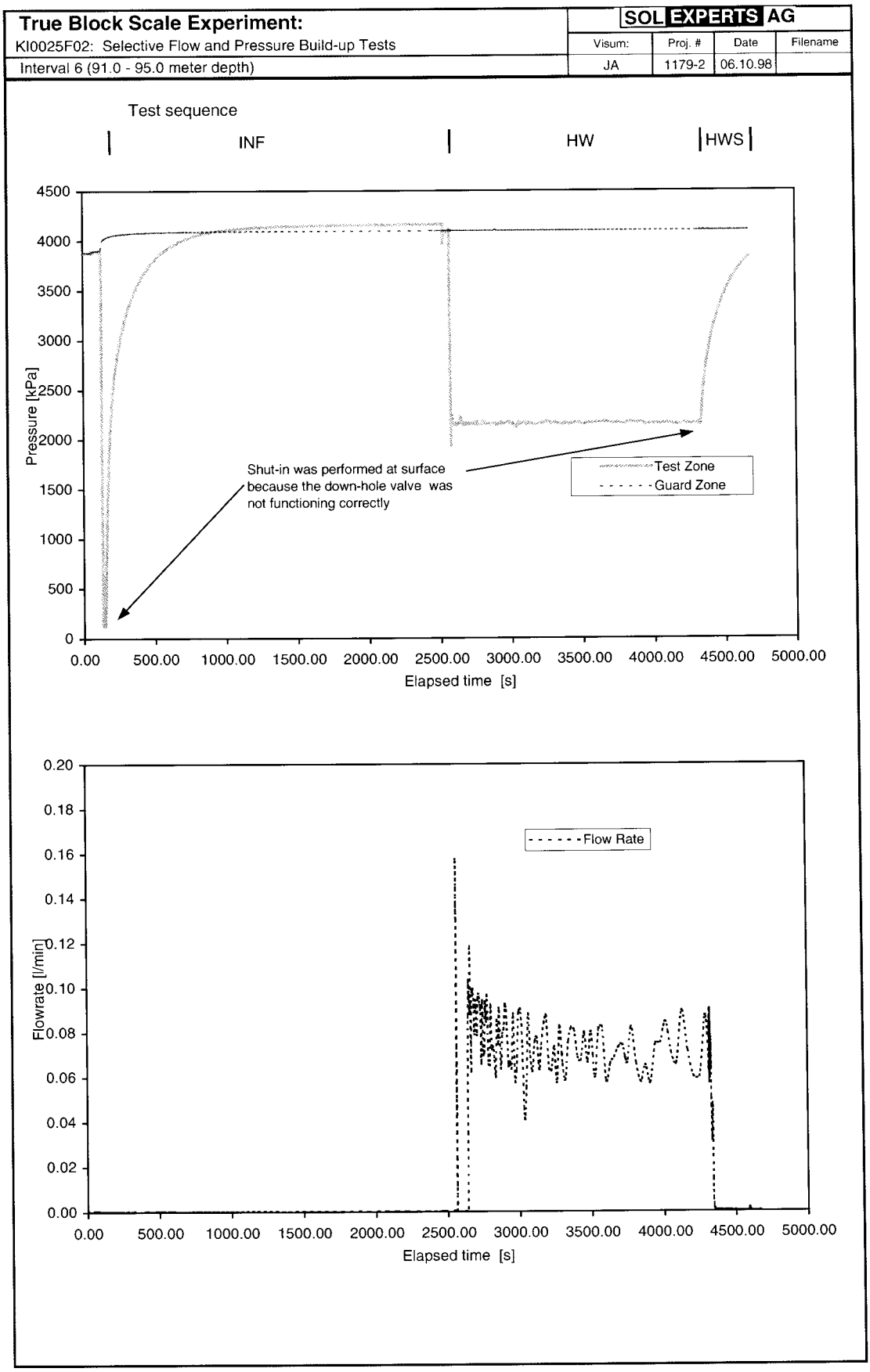

Figure A-11 Interval 6: Cartesian plots of Interval Pressure, Guard-zone Pressure and Flow Rate –vs- Time

True Block Scale Experiment

KI0025F02: Selective Flow and Pressure Build-up Tests

Interval 6 (91.0 - 95.0 meter depth)

SOL EXPERTS AG

Visum:	Proj. #	Date	Filename
JA	1179-2	06.10.98	

HW Phase Semi-log analysis:

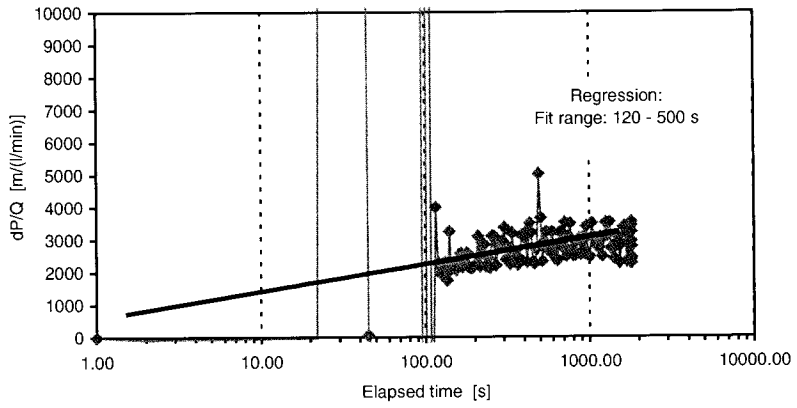

HW Phase

Input Values

dP =	1995	kPa
q_{end} =	0.07	l/min
m =	840.782	m/(l/min)/LC
t_o =	2.E-01	Sec
L =	4.00	m
r_w=	0.038	m
S_{est} =	5.0E-07	-

Results

transient

T =	3.6E-09	m^2/s
K =	9.1E-10	m/s
sf =	-0.5	

steady state

T =	4.6E-09	m^2/s
K =	1.2E-09	m/s

specific capacity

C_s=	5.7E-09	m^2/s

HWS Phase : Log-Log Diagnostic Plot

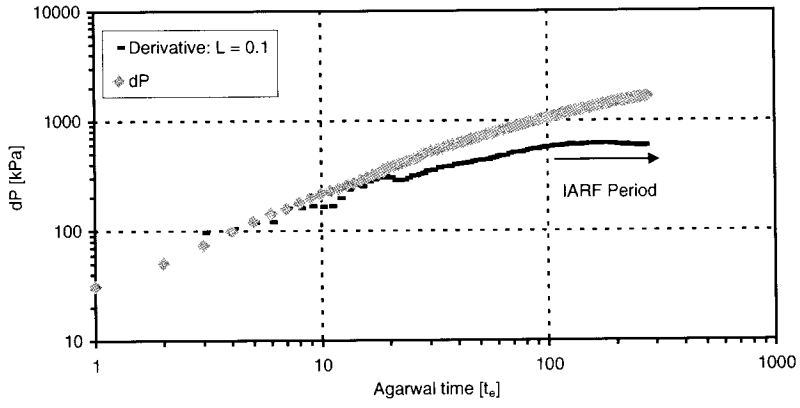

HWS Phase Semi-log analysis:

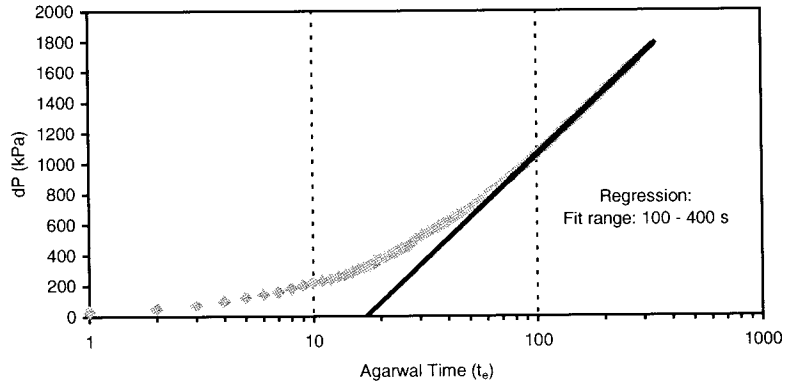

HWS Phase

Input Values

m =	1391.12	kPa/LC
t_o =	2.E+01	Sec
L =	4.00	m
Q_{end} =	0.07	l/min
r_w=	0.038	m
t_p =	1809	Sec
S_{est} =	5.0E-07	-

Results

T =	1.5E-09	m^2/s
K =	3.8E-10	m/s
sf =	-2.2	-
R_i =	3.5	m
u =	1.2E-03	-

Figure A-12 Interval 6: Analysis Plots

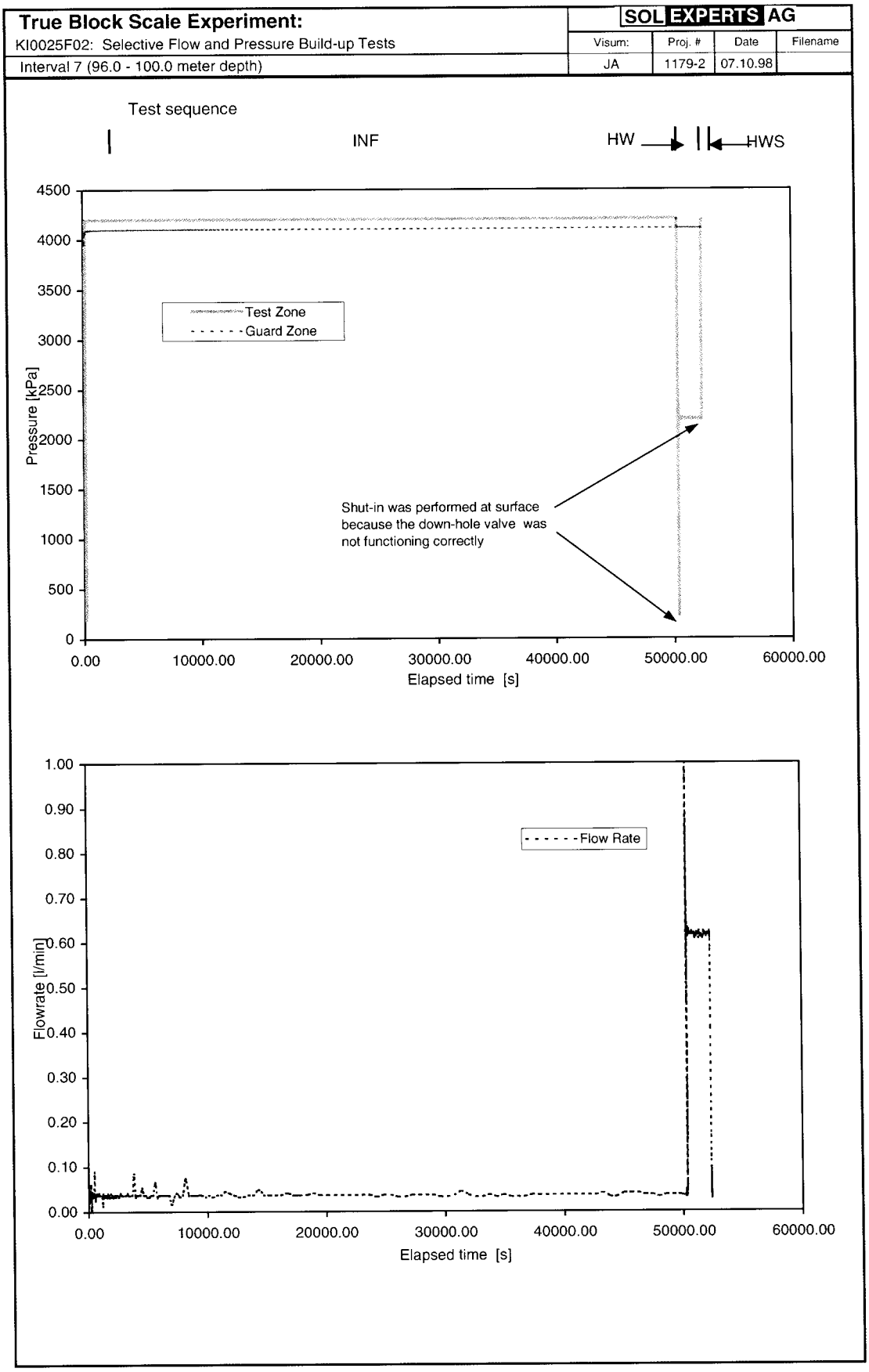

Figure A-13 Interval 7: Cartesian plots of Interval Pressure, Guard-zone Pressure and Flow Rate –vs- Time

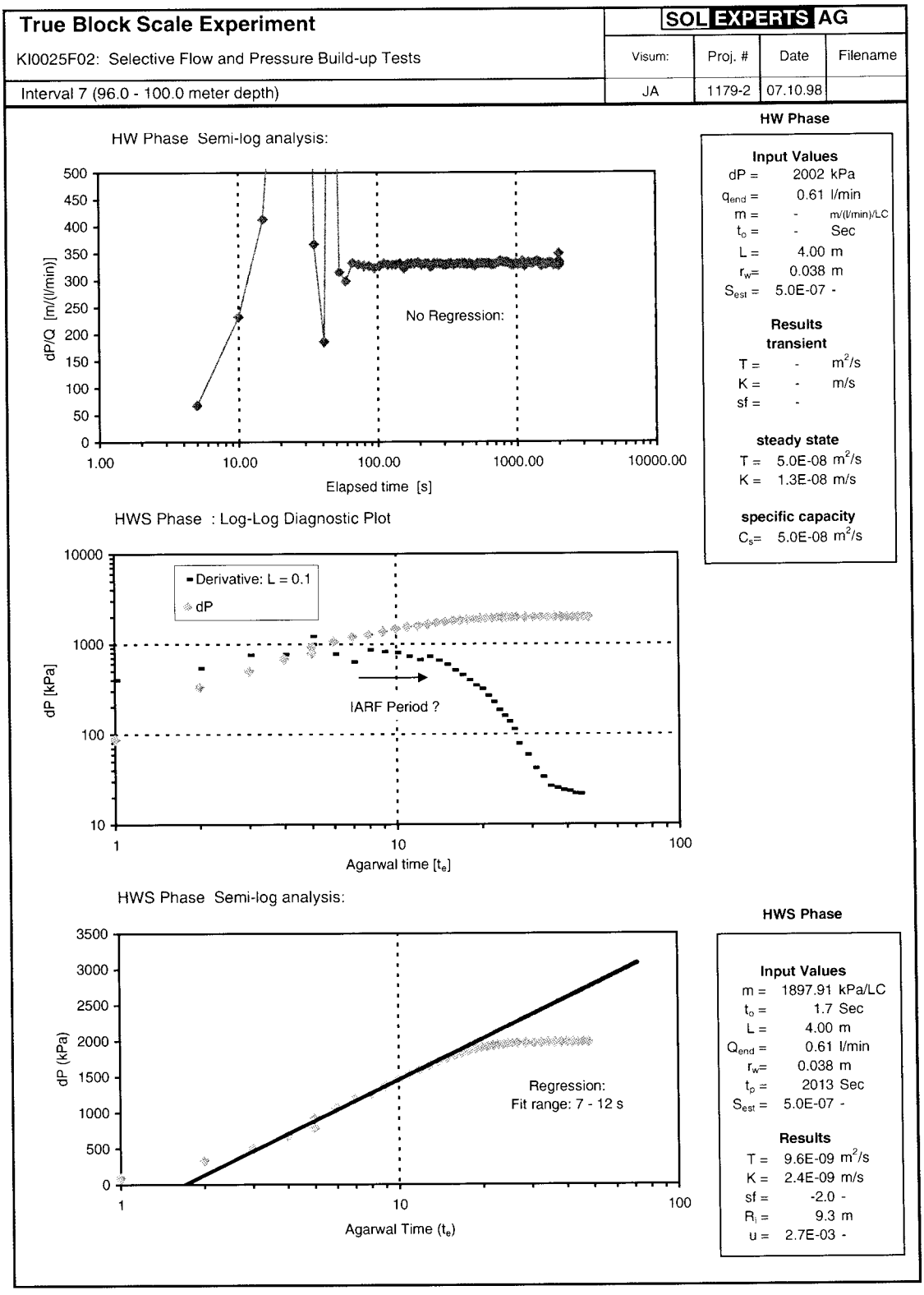

Figure A-14 Interval 7: Analysis Plots

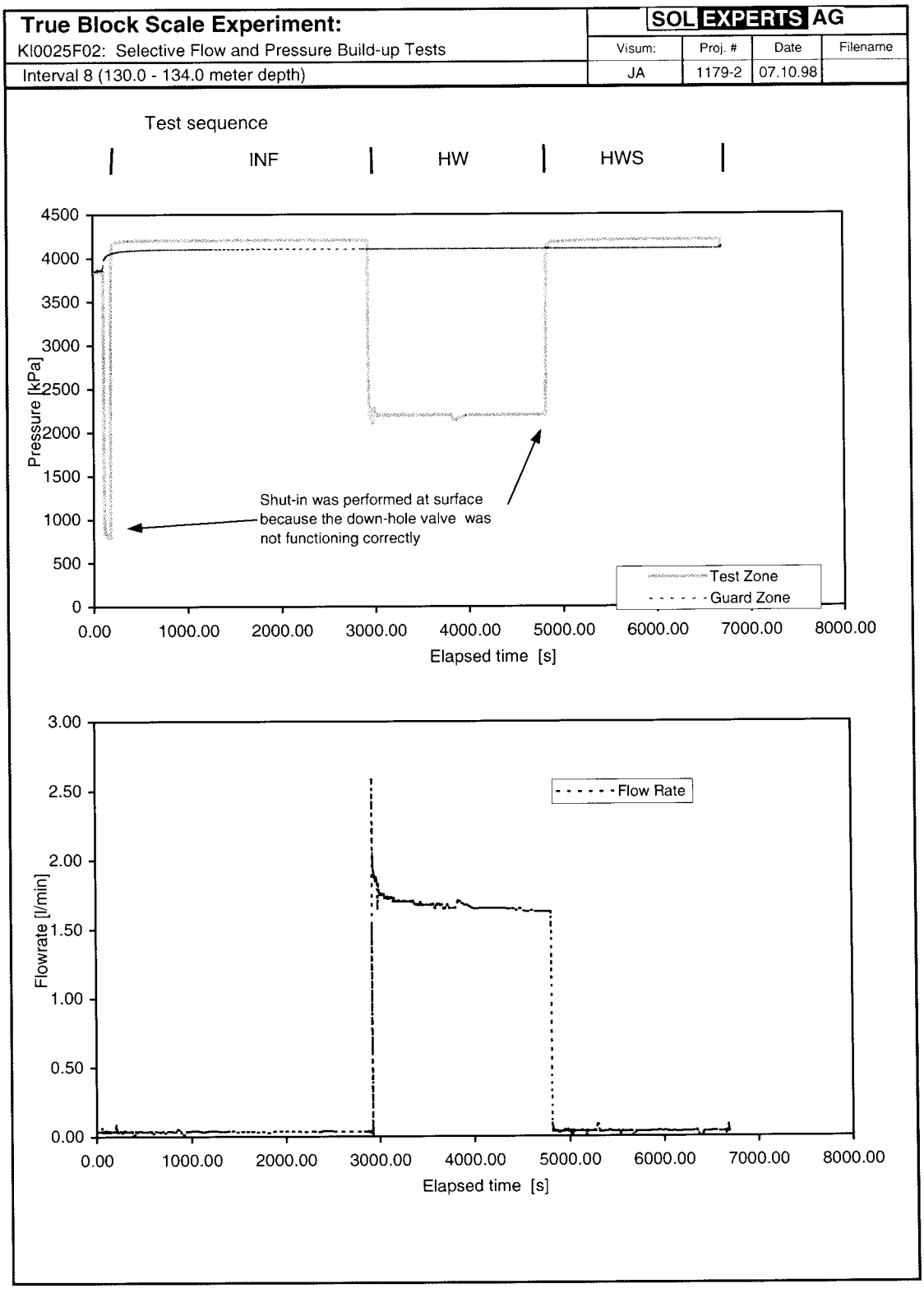

Figure A-15 Interval 8: Cartesian plots of Interval Pressure, Guard-zone Pressure and Flow Rate –vs- Time

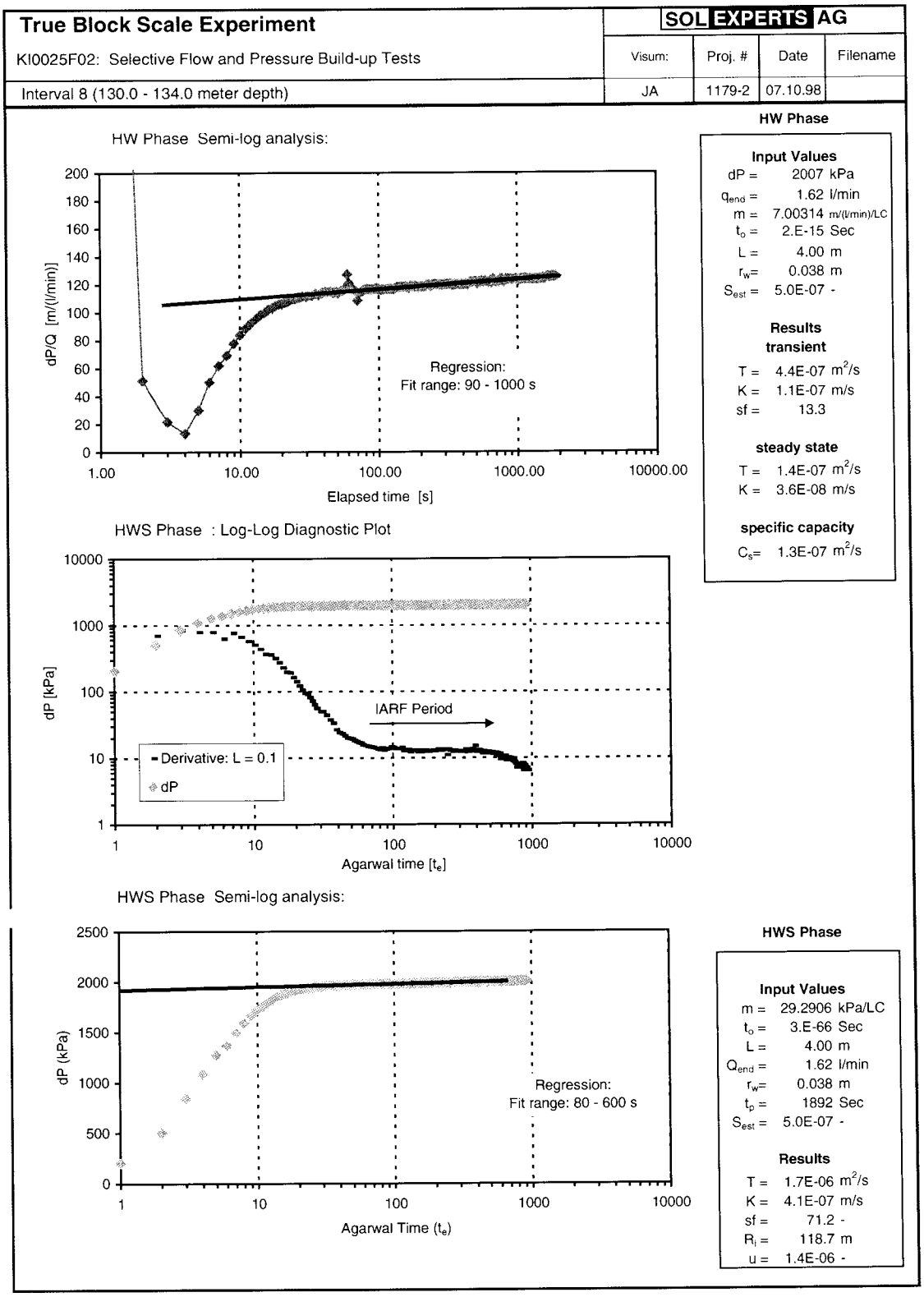

Figure A-16 Interval 8: Analysis Plots

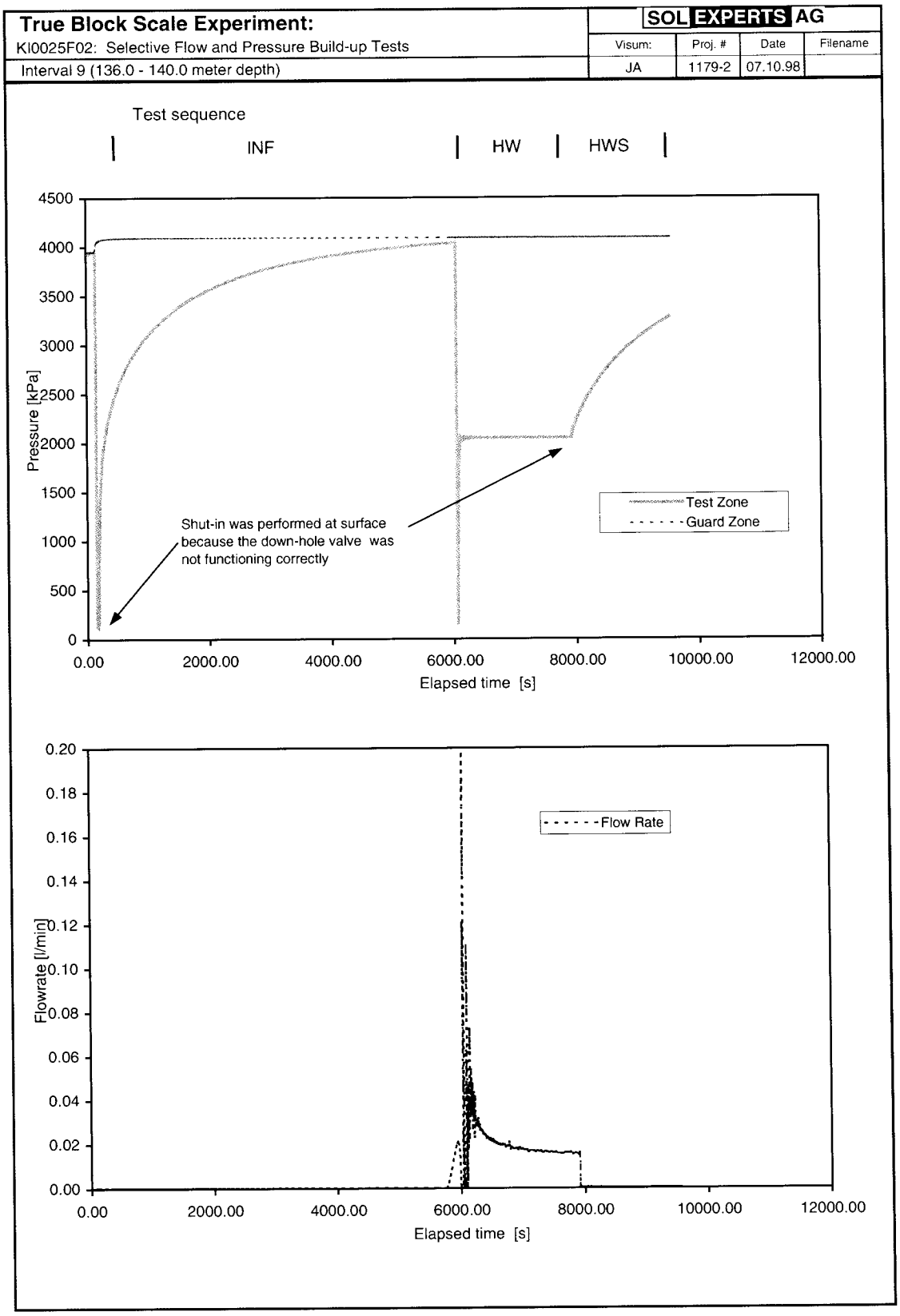

Figure A-17 Interval 9: Cartesian plots of Interval Pressure, Guard-zone Pressure and Flow Rate –vs- Time

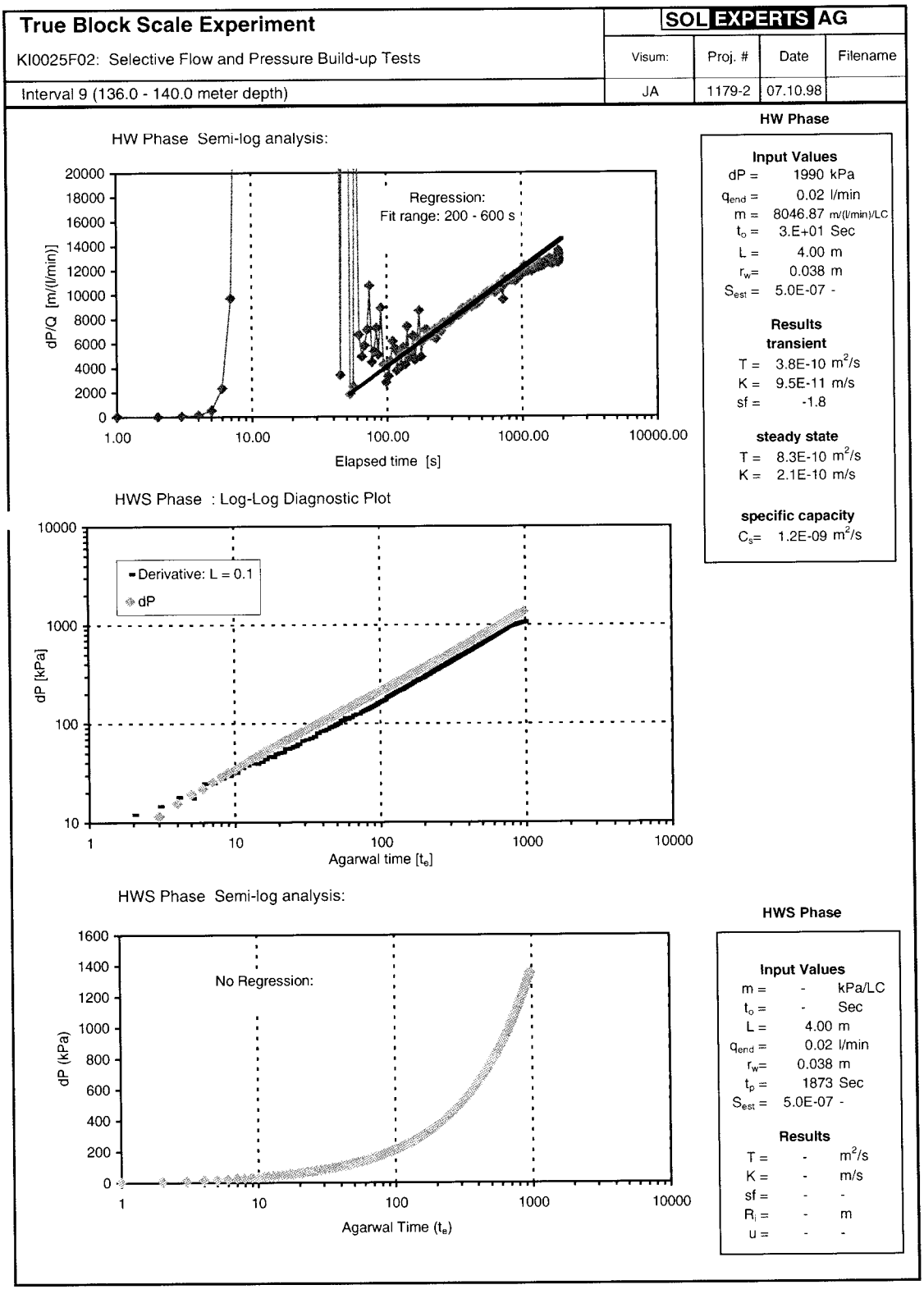

Figure A-18 Interval 9: Analysis Plots

APPENDIX B

Analyses for Single-hole Tests

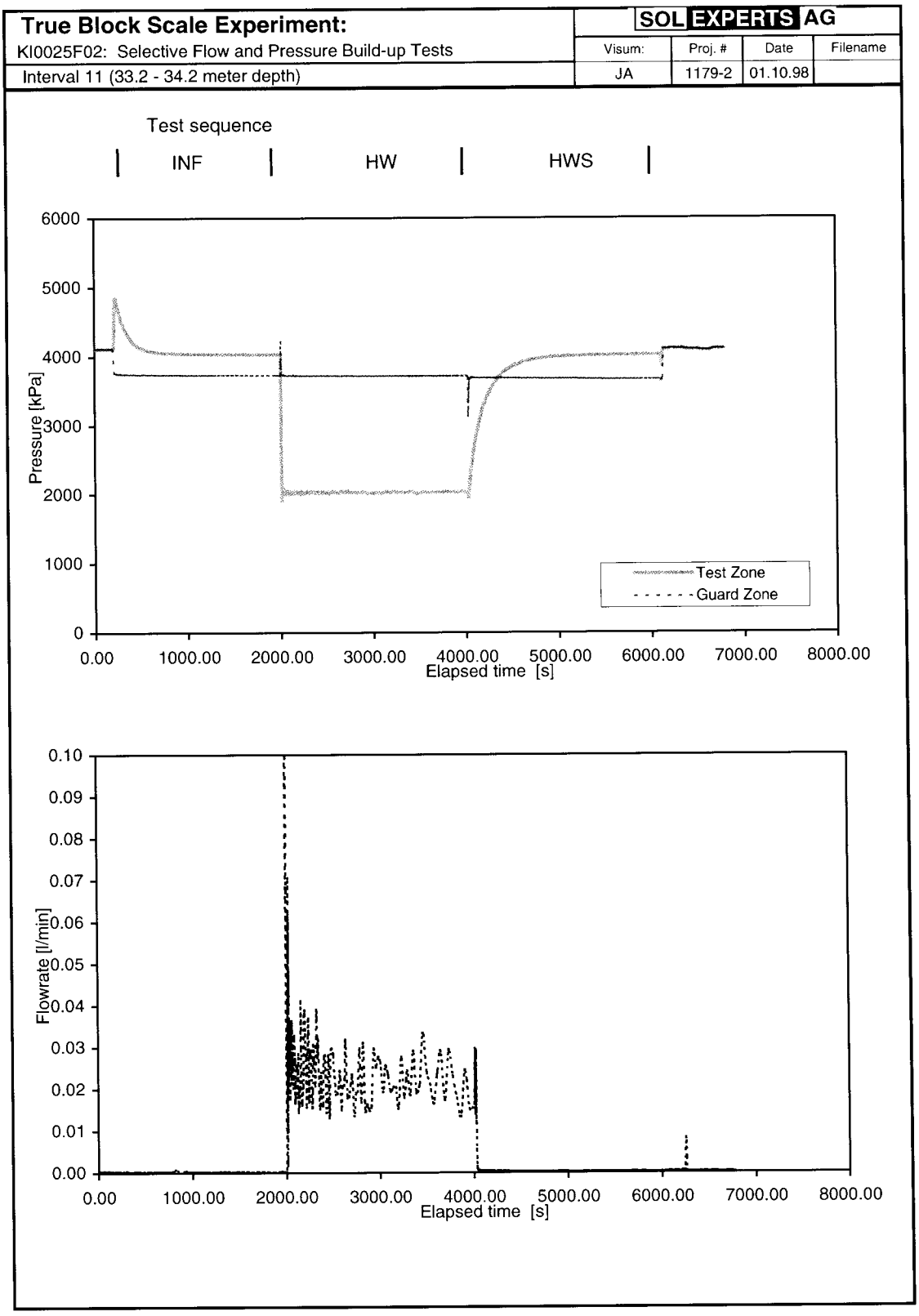

Figure B-1 *Interval 11: Cartesian Plots of Interval Pressure, Guard-zone Pressure and Flow Rate –vs- Time*

True Block Scale Experiment

KI0025F02: Selective Flow and Pressure Build-up Tests

Interval 11 (33.2 - 34.2 meter depth)

SOL EXPERTS AG

Visum:	Proj. #	Date	Filename
JA	1179-2	01.10.98	

HW Phase Semi-log analysis:

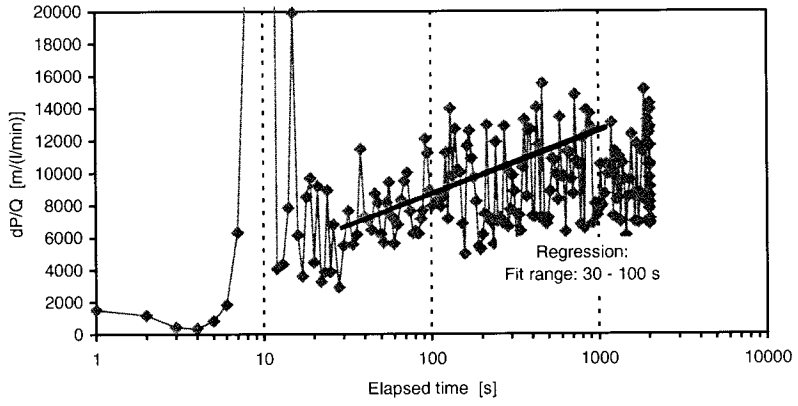

HW Phase

Input Values

dP =	2001 kPa
q =	0.02 l/min
m =	3913.4 /LC
t_o =	6.E-01 Sec
L =	1.00 m
r_w =	0.038 m
S_{est} =	5.0E-07 -

Results

transient

T =	7.8E-10 m^2/s
K =	7.8E-10 m/s
sf =	-0.2

steady state

T =	1.3E-09 m^2/s
K =	1.3E-09 m/s

specific capacity

C_s =	1.8E-09 m^2/s

HWS Phase : Log-Log Diagnostic Plot

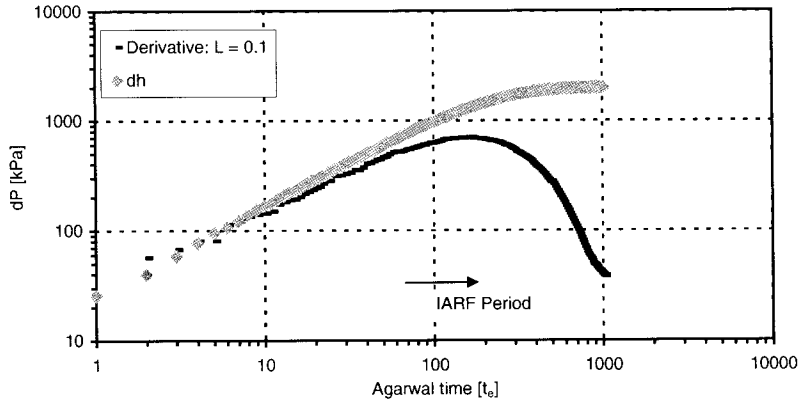

HWS Phase Semi-log analysis:

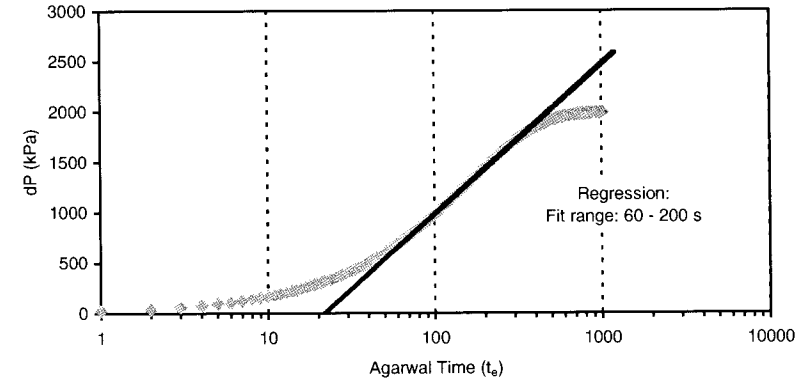

HWS Phase

Input Values

m =	1485.82 kPa/LC
t_o =	2.E+01 Sec
L =	1.00 m
Q_{end} =	0.02 l/min
r_w =	0.038 m
t_p =	2021 Sec
S_{est} =	1.0E-07 -

Results

T =	4.4E-10 m^2/s
K =	4.4E-10 m/s
sf =	-2.5 -
R_i =	4.5 m
u =	1.4E-03 -

Figure B-2 Interval 11: Analysis Plots

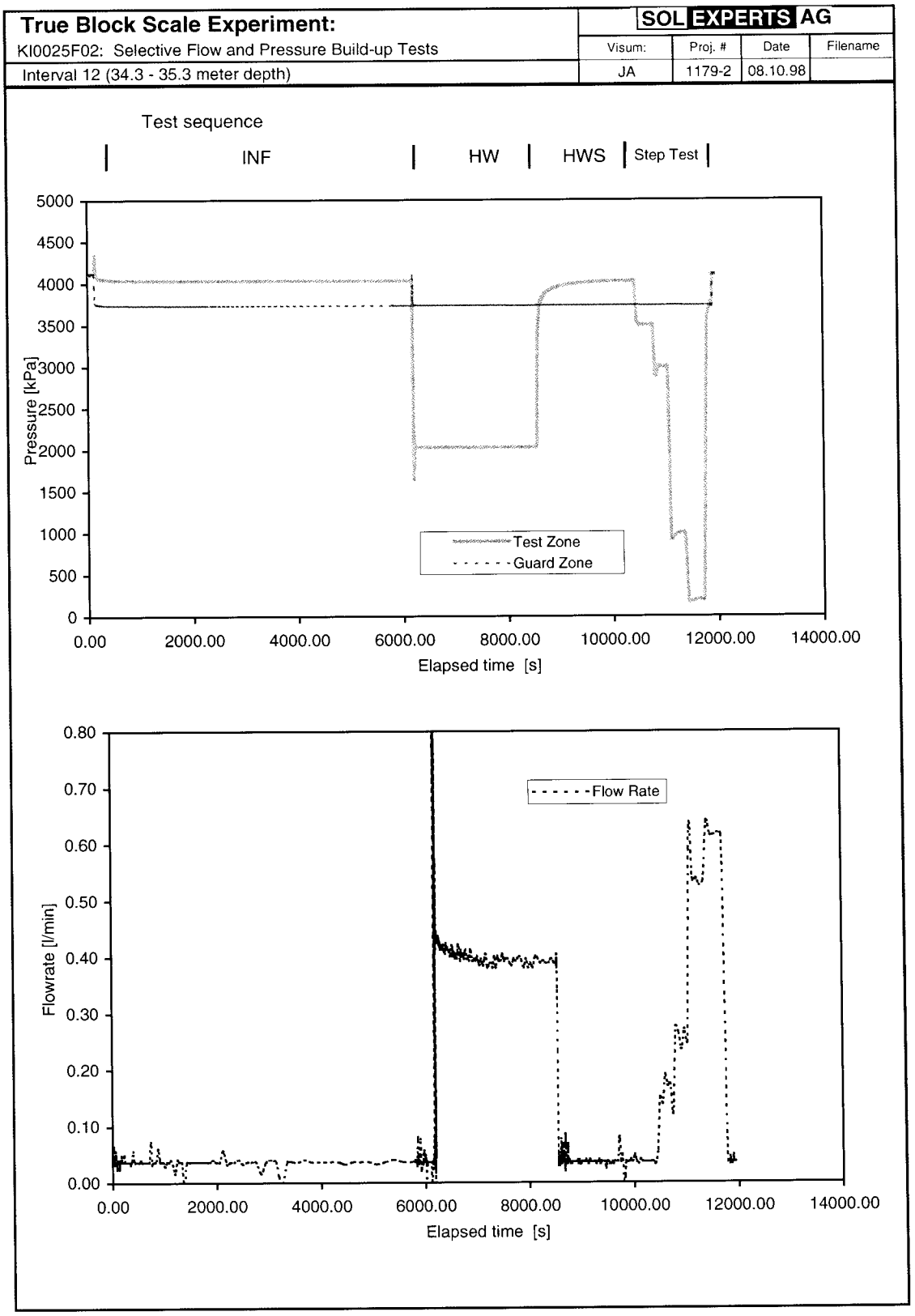

Figure B-3 *Interval 12: Cartesian Plots of Interval Pressure, Guard-zone Pressure and Flow Rate –vs- Time*

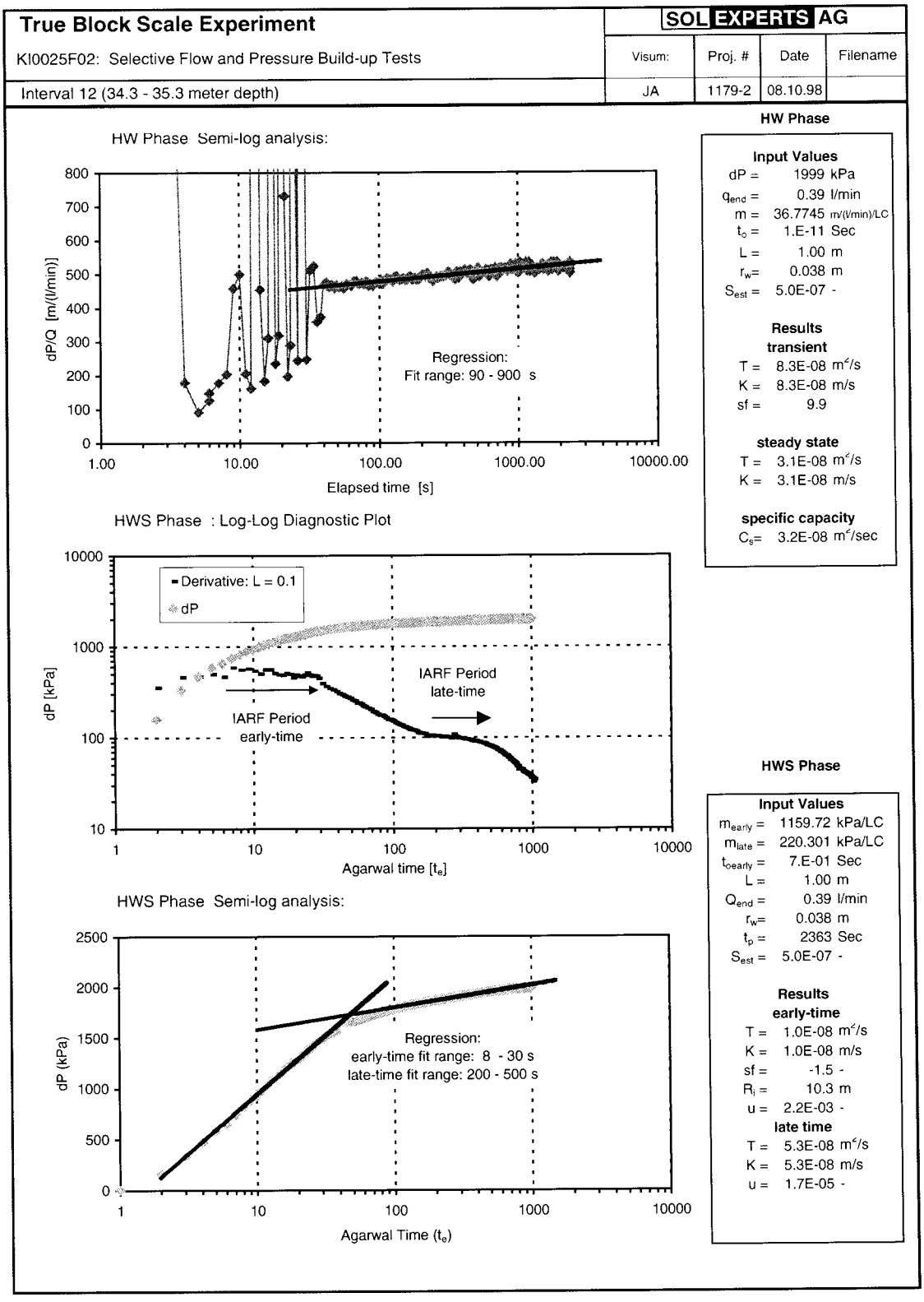

Figure B-4 Interval 12: Analysis Plots

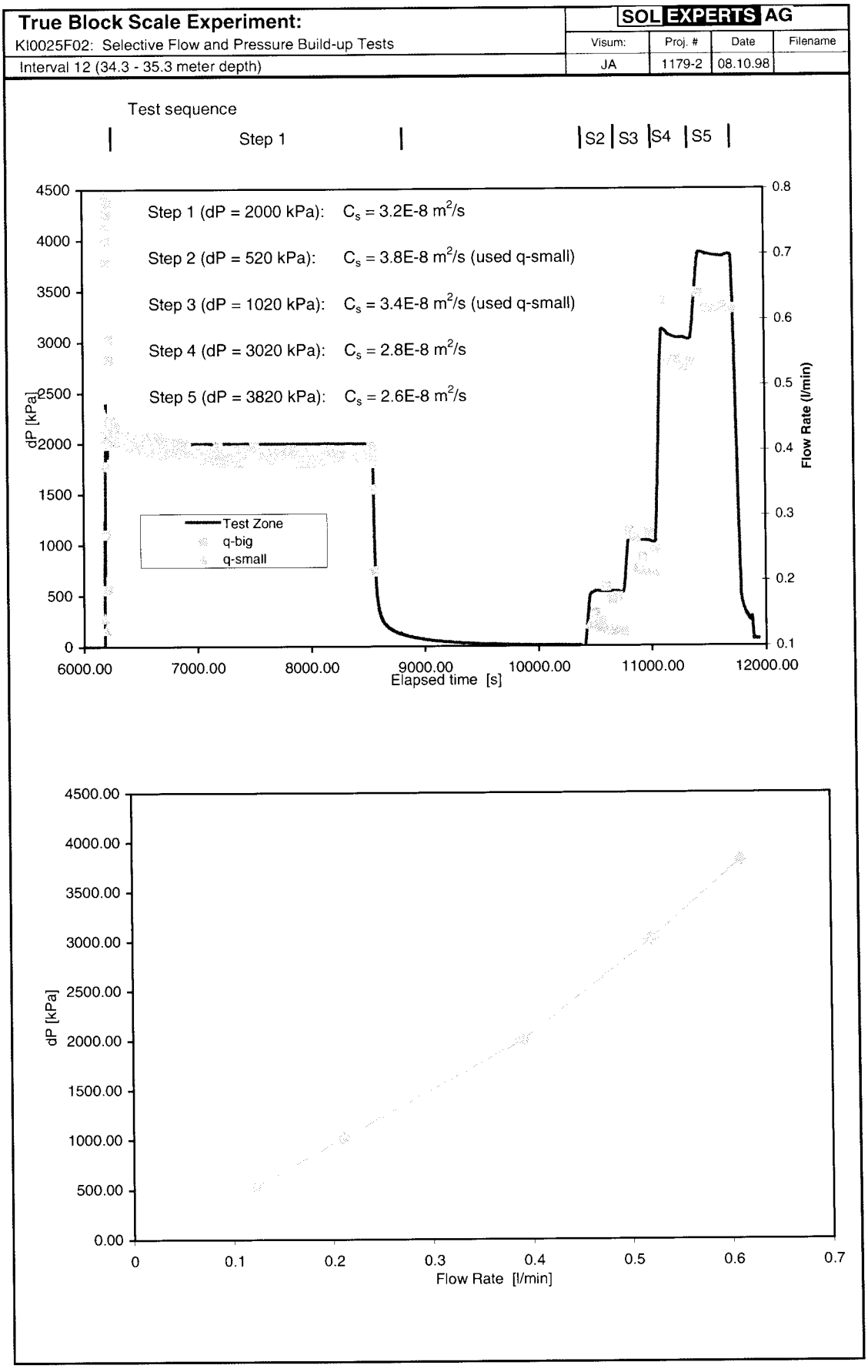

Figure B-5 Interval 12: Step Drawdown Analysis

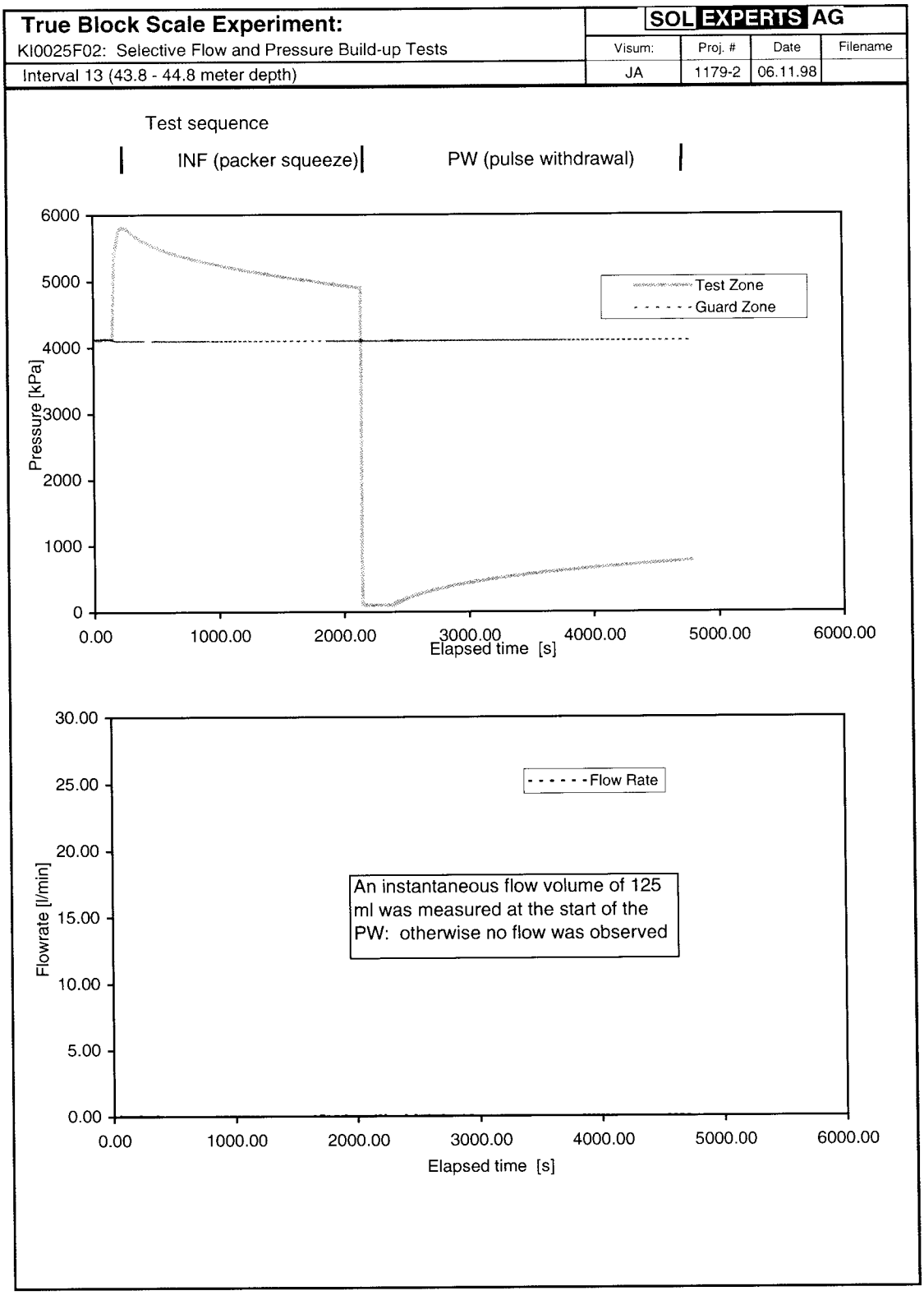

Figure B-6 *Interval 13: Cartesian Plots of Interval Pressure, Guard-zone Pressure and Flow Rate –vs- Time*

True Block Scale Experiment	SOL EXPERTS AG			
KI0025F02: Selective Flow and Build-up Tests	Visum	Contr. #	Date	Data File
Interval 13 (43.8 - 44.8 m depth)	JA	1179-3	9.11.98	-

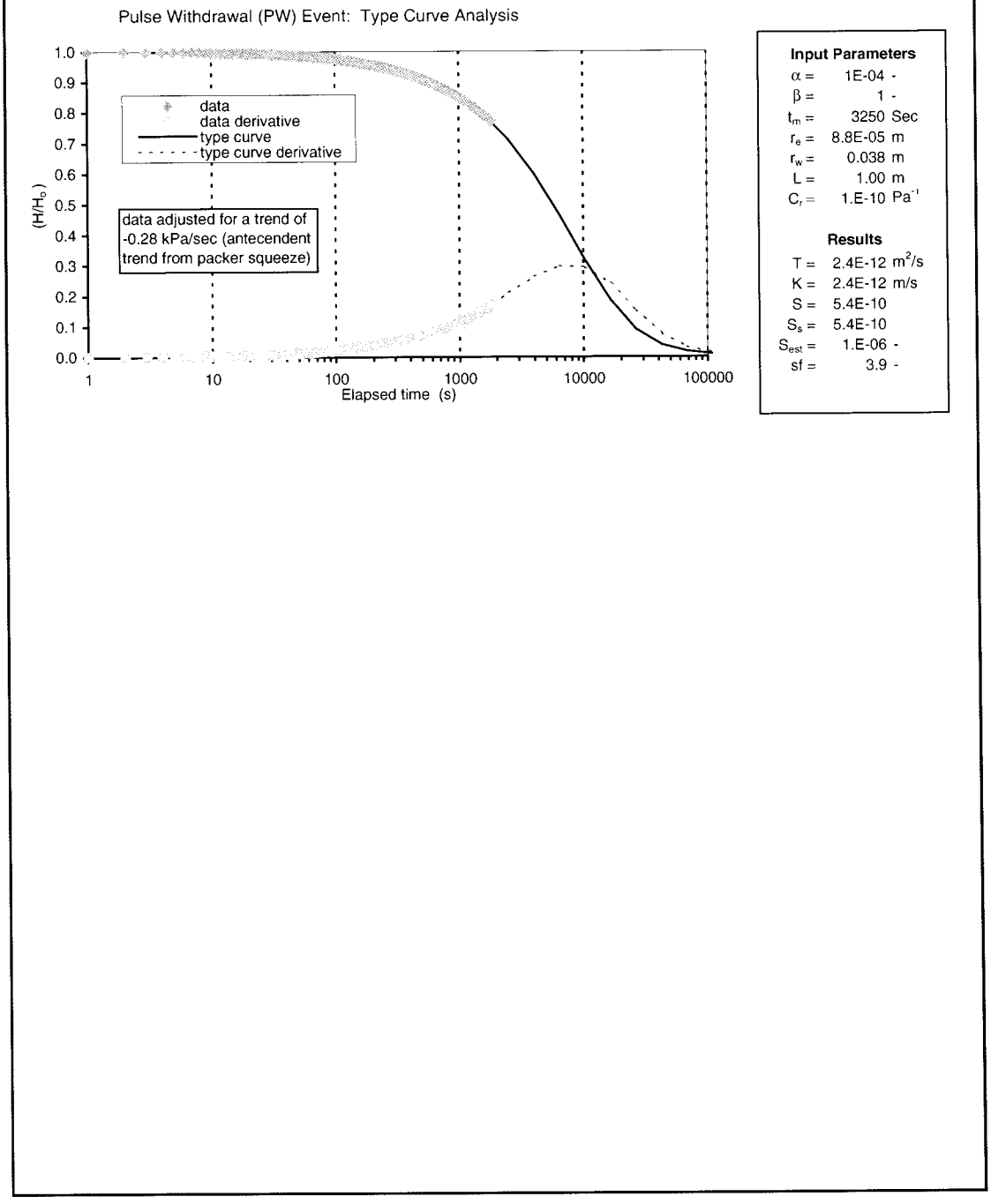

Figure B-7 Interval 13: Analysis Plots

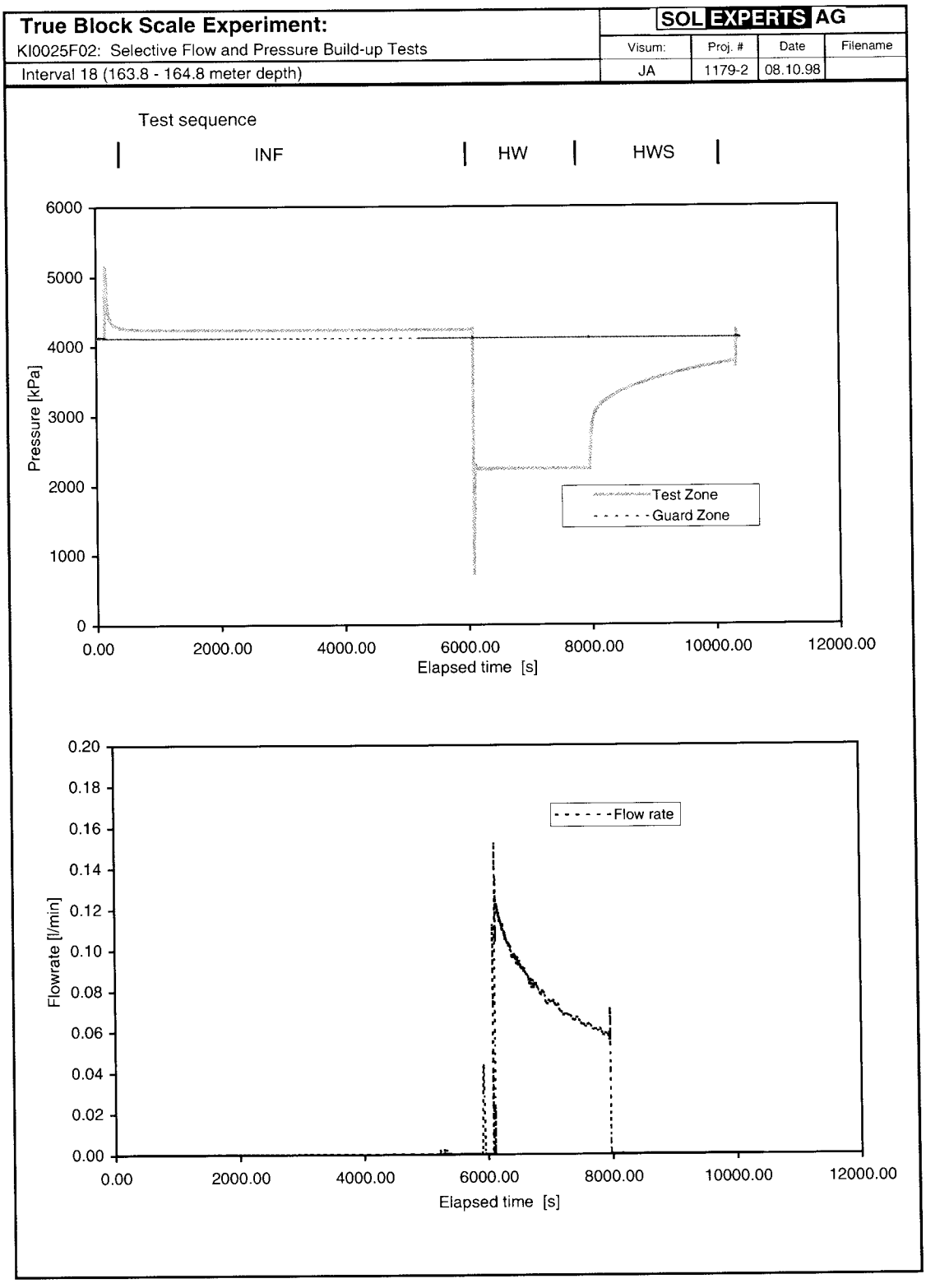

Figure B-8 *Interval 18: Cartesian Plots of Interval Pressure, Guard-zone Pressure and Flow Rate –vs- Time*

True Block Scale Experiment

KI0025F02: Selective Flow and Pressure Build-up Tests

Interval 18 (163.8 - 164.8 meter depth)

SOL EXPERTS AG

Visum:	Proj. #	Date	Filename
JA	1179-2	08.10.98	

HW Phase Semi-log analysis:

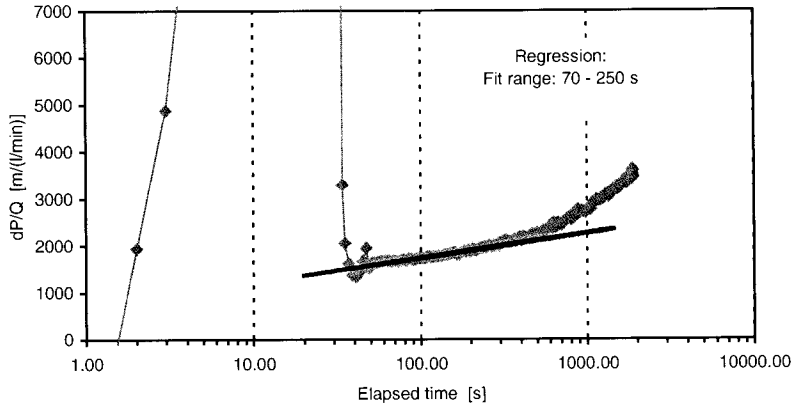

HW Phase

Input Values

dP =	2000	kPa
q_{end} =	0.06	l/min
m =	527.227	m/(l/min)/LC
t_o =	5.E-02	Sec
L =	1.00	m
r_w =	0.038	m
S_{est} =	5.0E-07	-

Results

transient

T =	5.8E-09	m^2/s
K =	5.8E-09	m/s
sf =	0.0	

steady state

T =	3.7E-09	m^2/s
K =	3.7E-09	m/s

specific capacity

C_s= 4.6E-09 m^2/sec

HWS Phase : Log-Log Diagnostic Plot

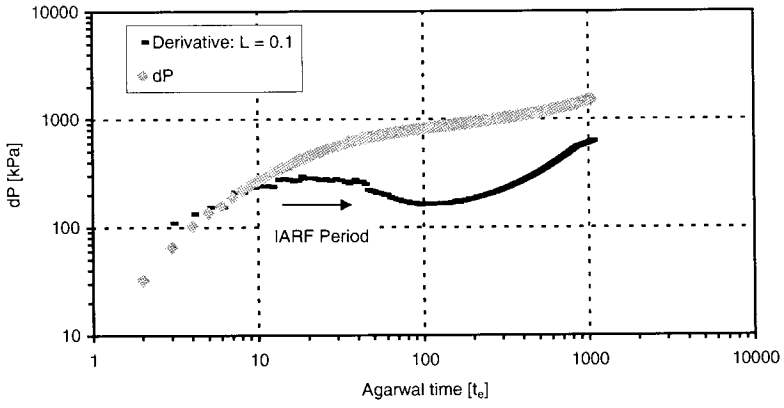

HWS Phase Semi-log analysis:

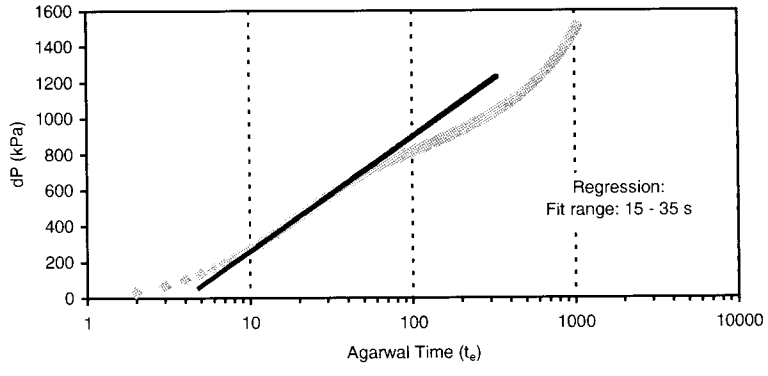

HWS Phase

Input Values

m =	676.074	kPa/LC
t_o =	4.E+00	Sec
L =	1.00	m
Q_{end} =	0.06	l/min
r_w =	0.038	m
t_p =	1880	Sec
S_{est} =	5.0E-07	-

Results

T =	2.5E-09	m^2/s
K =	2.5E-09	m/s
sf =	-1.7	-
R_i =	4.6	m
u =	4.8E-03	-

Figure B-9 Interval 18: Analysis Plots

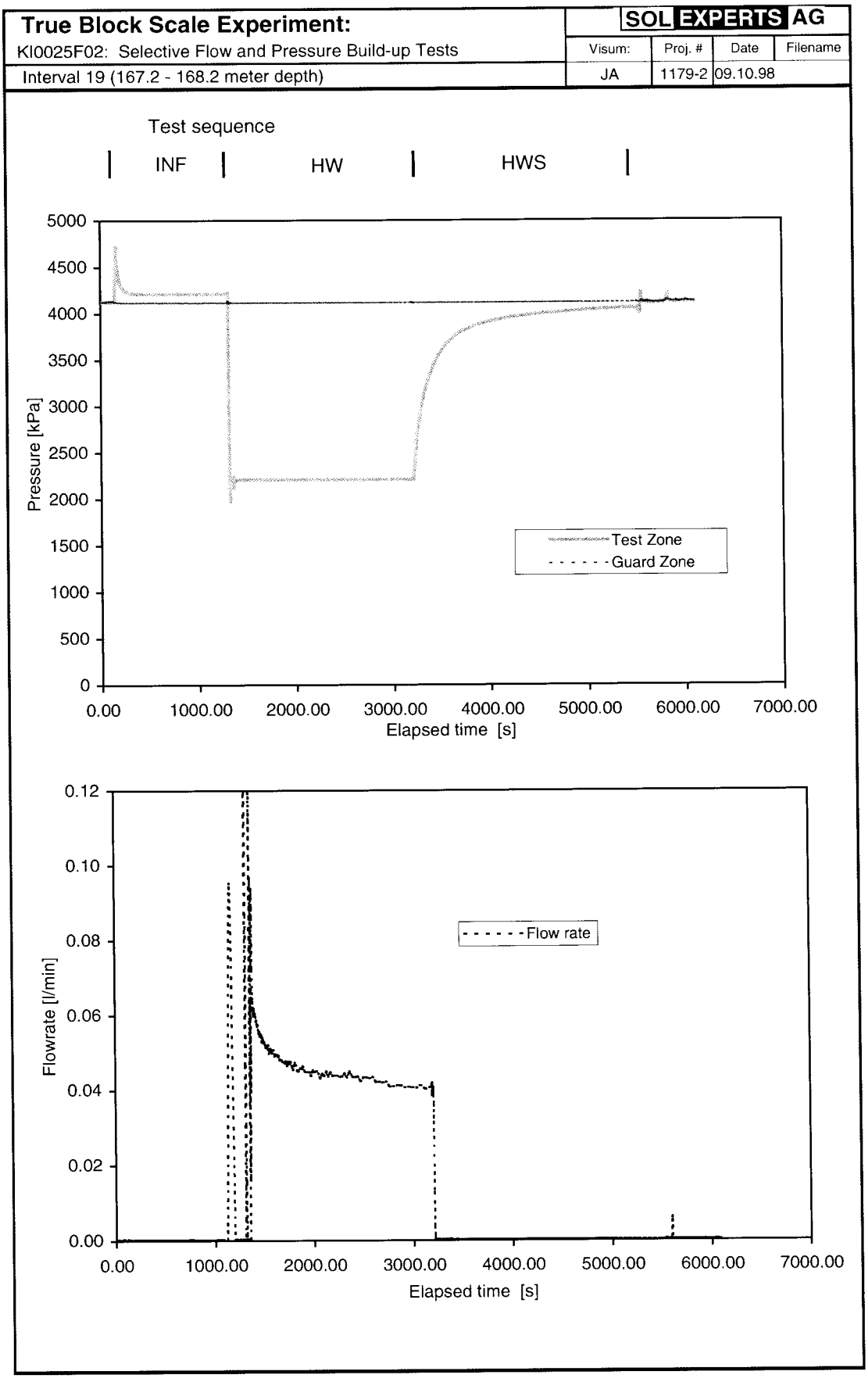

Figure B-10 Interval 19: Cartesian Plots of Interval Pressure, Guard-zone Pressure and Flow Rate –vs- Time

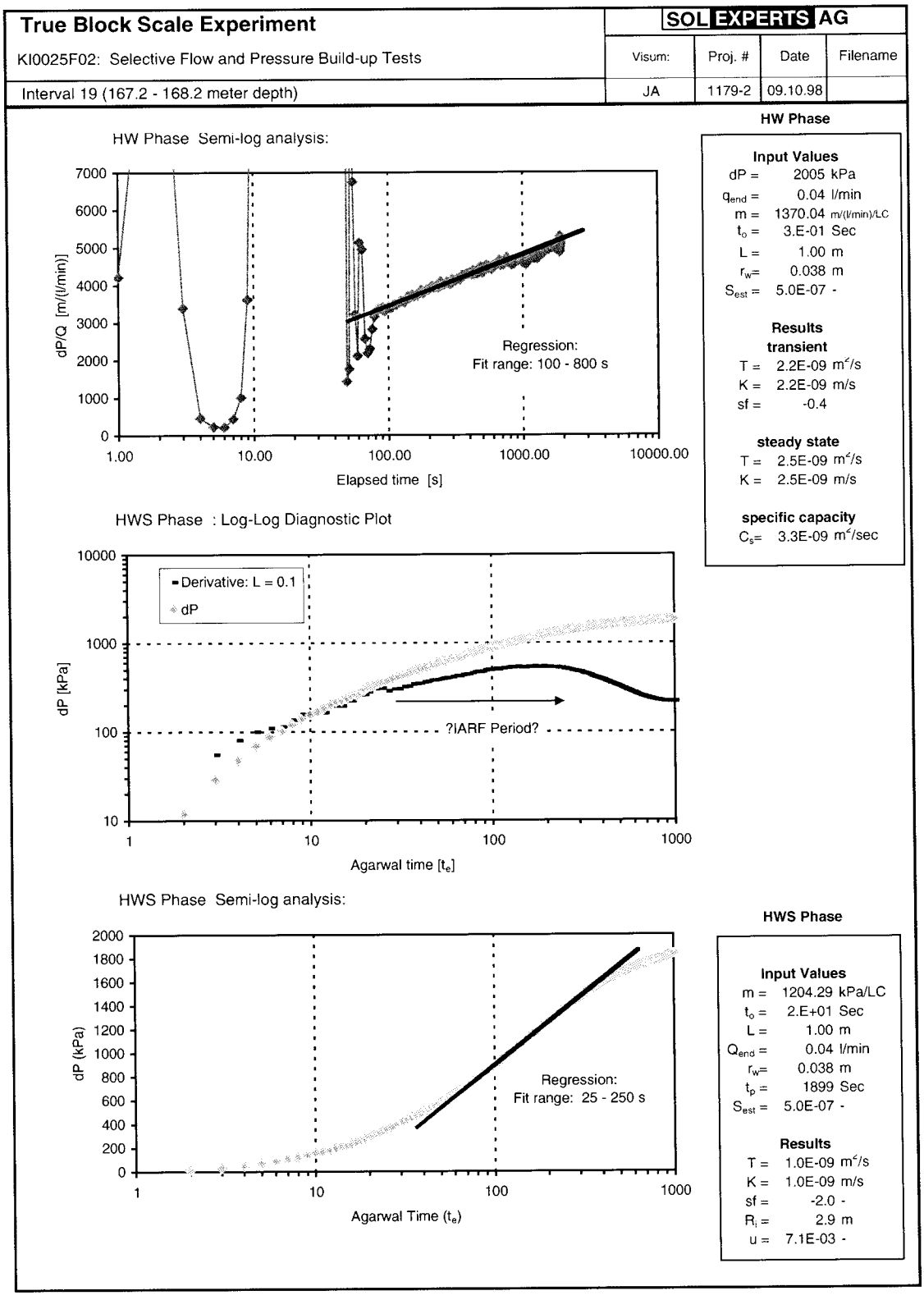

Figure B-11 Interval 19: Analysis Plots

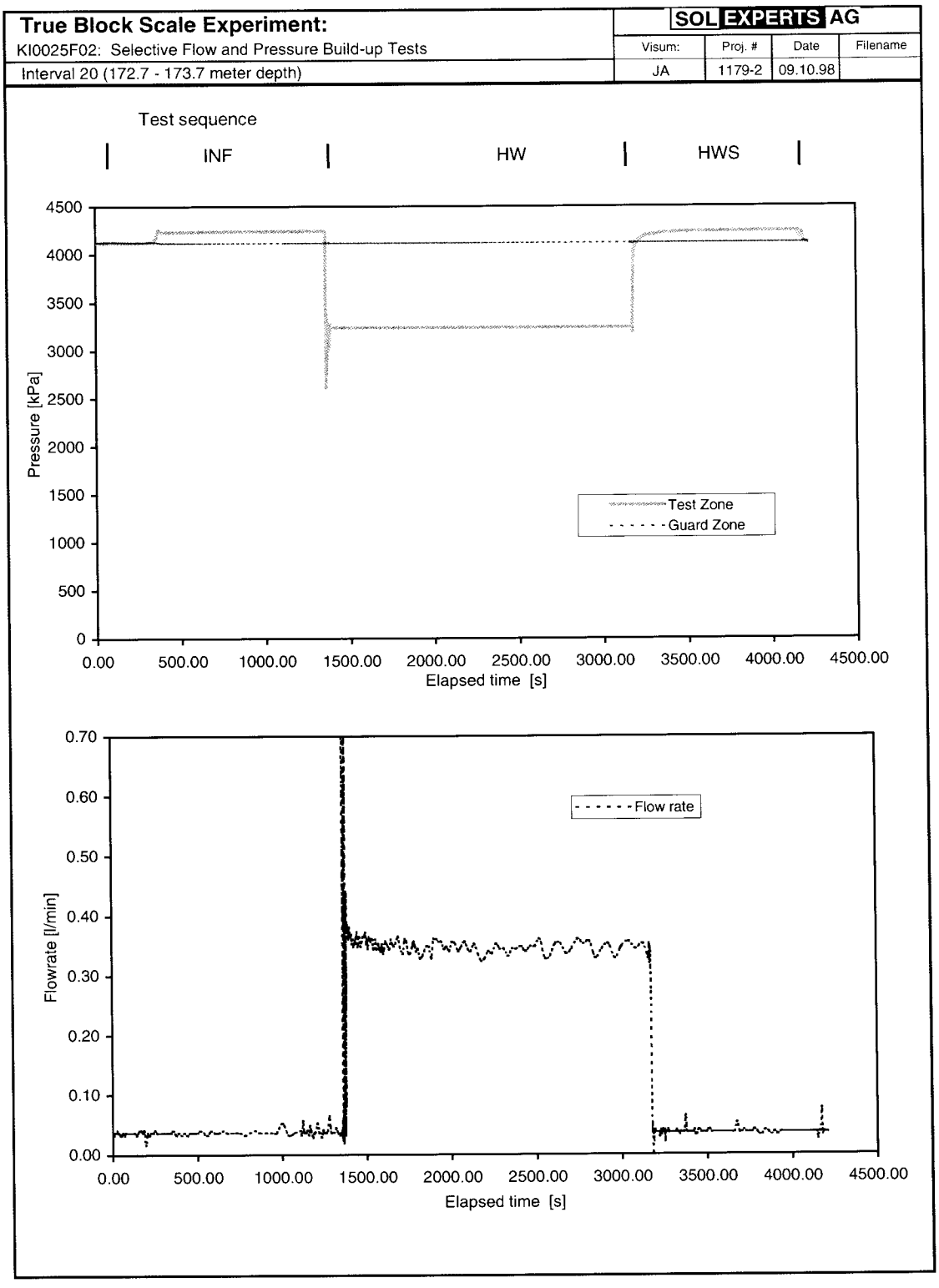

Figure B-12 Interval 20: Cartesian Plots of Interval Pressure, Guard-zone Pressure and Flow Rate –vs- Time

True Block Scale Experiment

KI0025F02: Selective Flow and Pressure Build-up Tests

Interval 20 (172.7 - 173.7 meter depth)

SOL EXPERTS AG

Visum:	Proj. #	Date	Filename
JA	1179-2	09.10.98	

HW Phase Semi-log analysis:

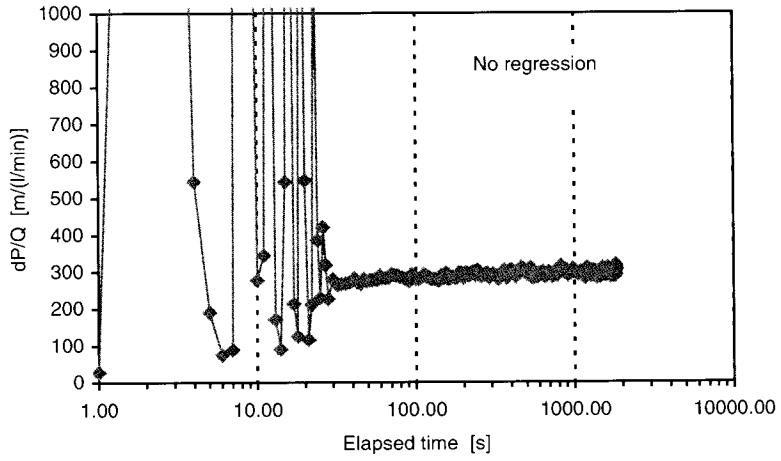

HW Phase

Input Values

dP =	1004	kPa
q_{end} =	0.32	l/min
m =	2319.5	m/(l/min)/LC
t_o =	6.E+01	Sec
L =	1.00	m
r_w =	0.038	m
S_{est} =	5.0E-07	-

Results

transient

T = -	m^2/s
K = -	m/s
sf = -	

steady state

T = 5.3E-08	m^2/s
K = 5.3E-08	m/s

specific capacity

C_s = 5.3E-08 m^2/sec

HWS Phase : Log-Log Diagnostic Plot

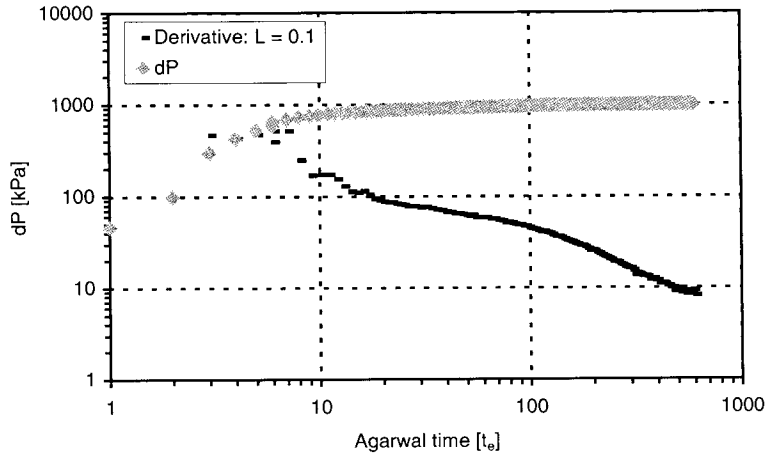

HWS Phase Semi-log analysis:

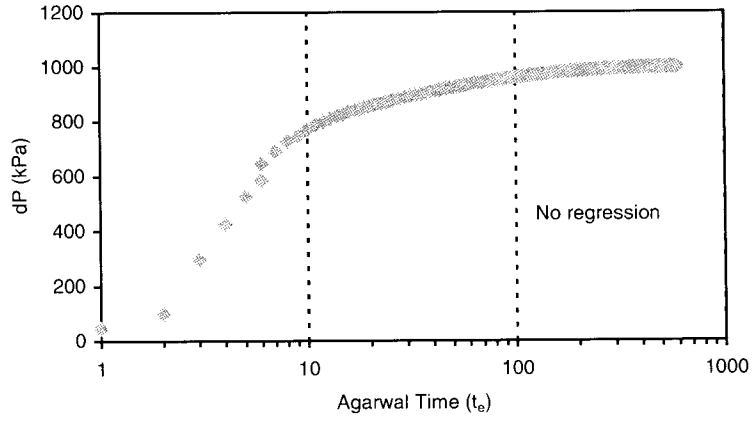

HWS Phase

Input Values

m =	676.07	kPa/LC
t_o =	4.E+00	Sec
L =	1.00	m
Q_{end} =	0.32	l/min
r_w =	0.038	m
t_p =	1816	Sec
S_{est} =	5.0E-07	-

Results

T = -	m^2/s
K = -	m/s
sf = -	-
R_i = -	m
u = -	-

Figure B-13 Interval 20: Analysis Plots

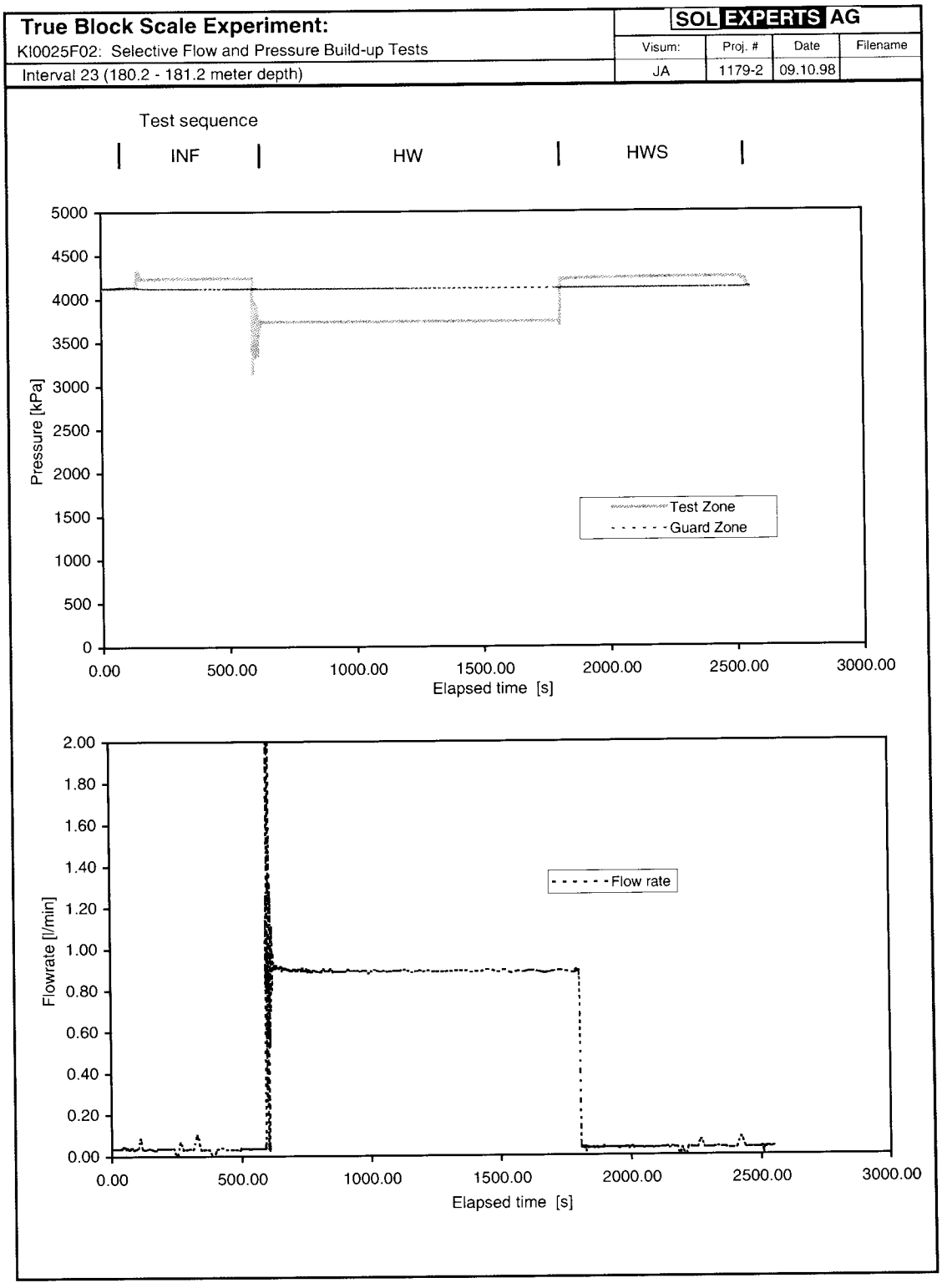

Figure B-14 Interval 23: Cartesian Plots of Interval Pressure, Guard-zone Pressure and Flow Rate –vs- Time

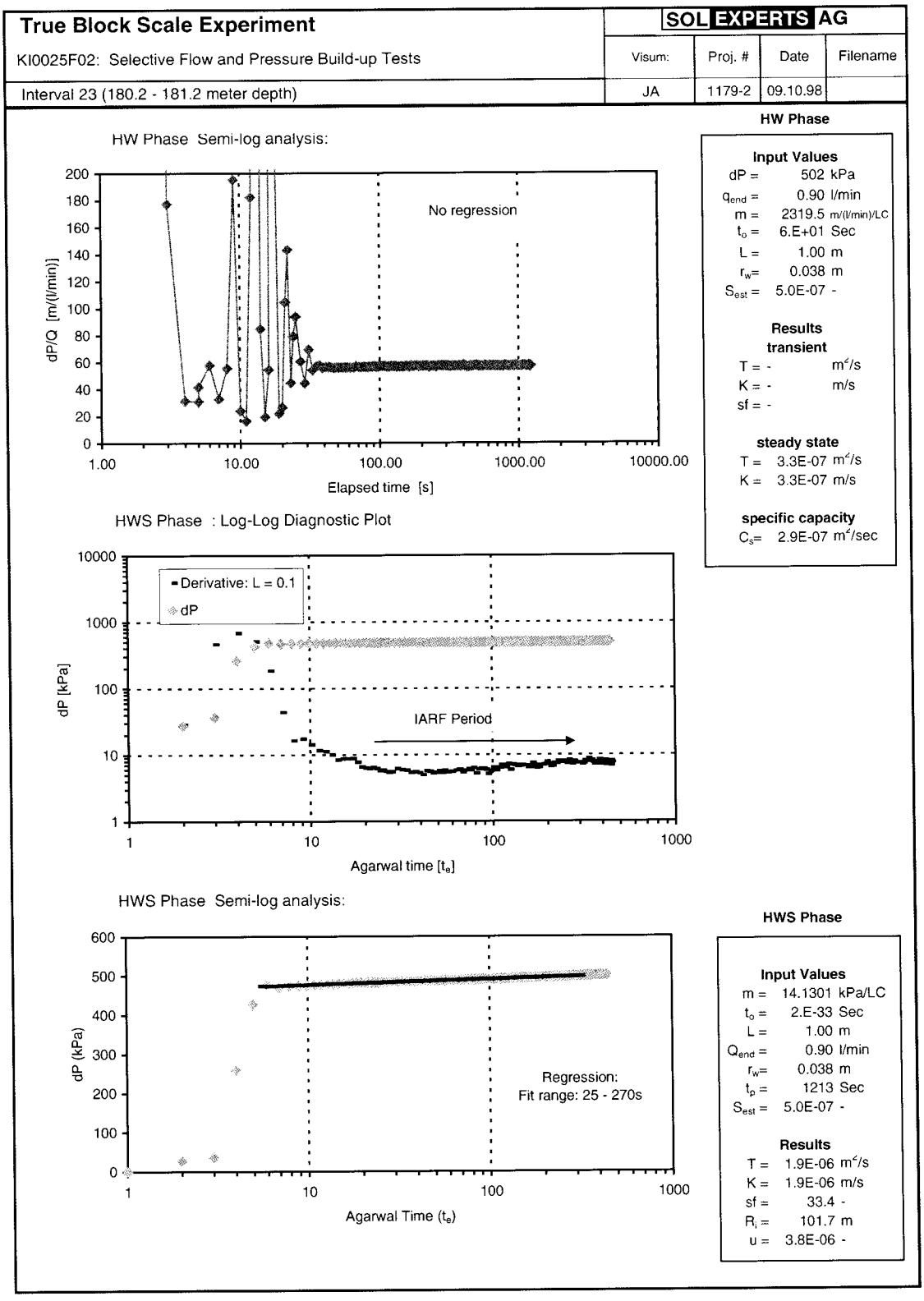

Figure B-15 Interval 23: Analysis Plots

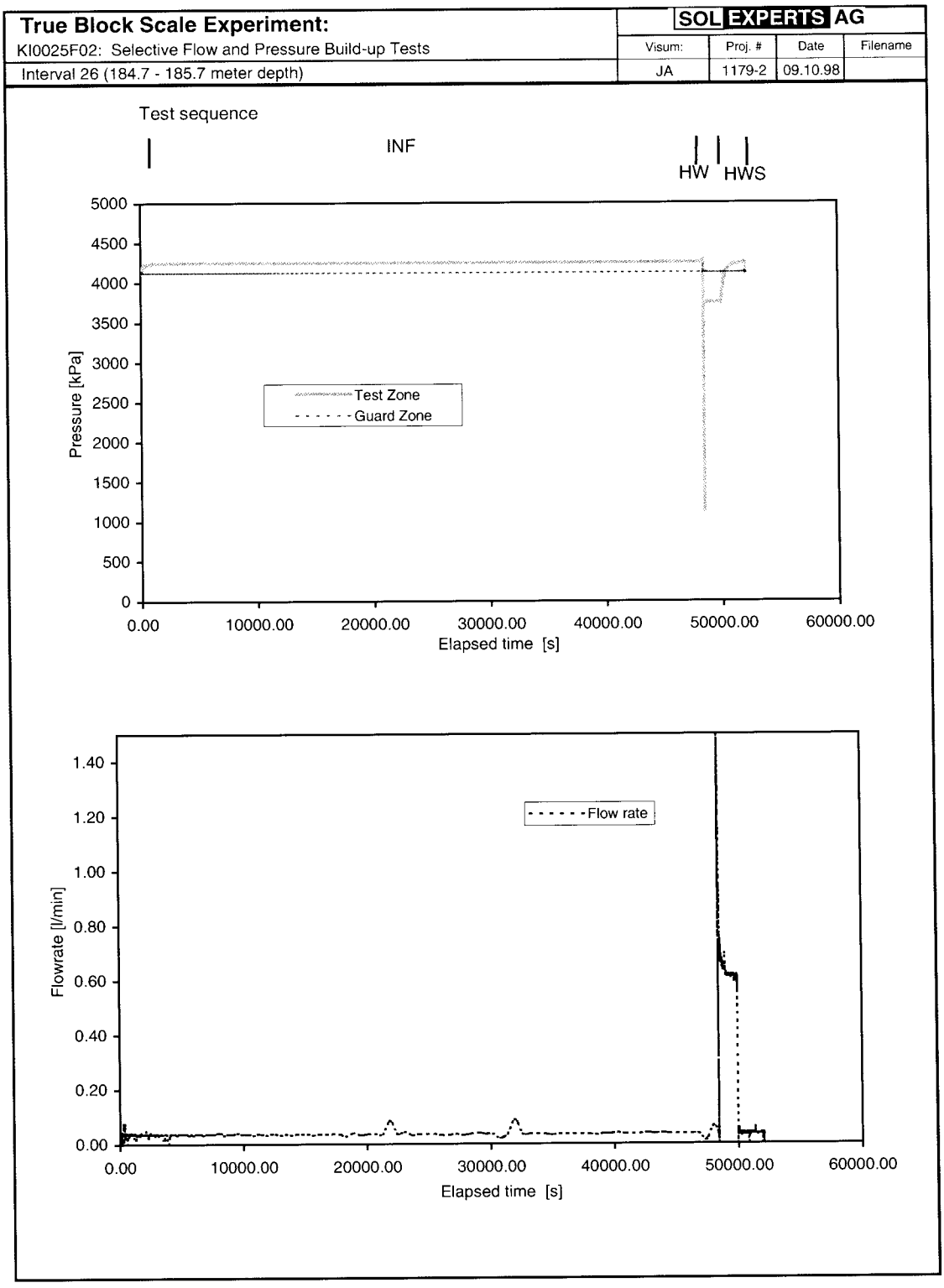

Figure B-16 Interval 26: Cartesian Plots of Interval Pressure, Guard-zone Pressure and Flow Rate –vs- Time

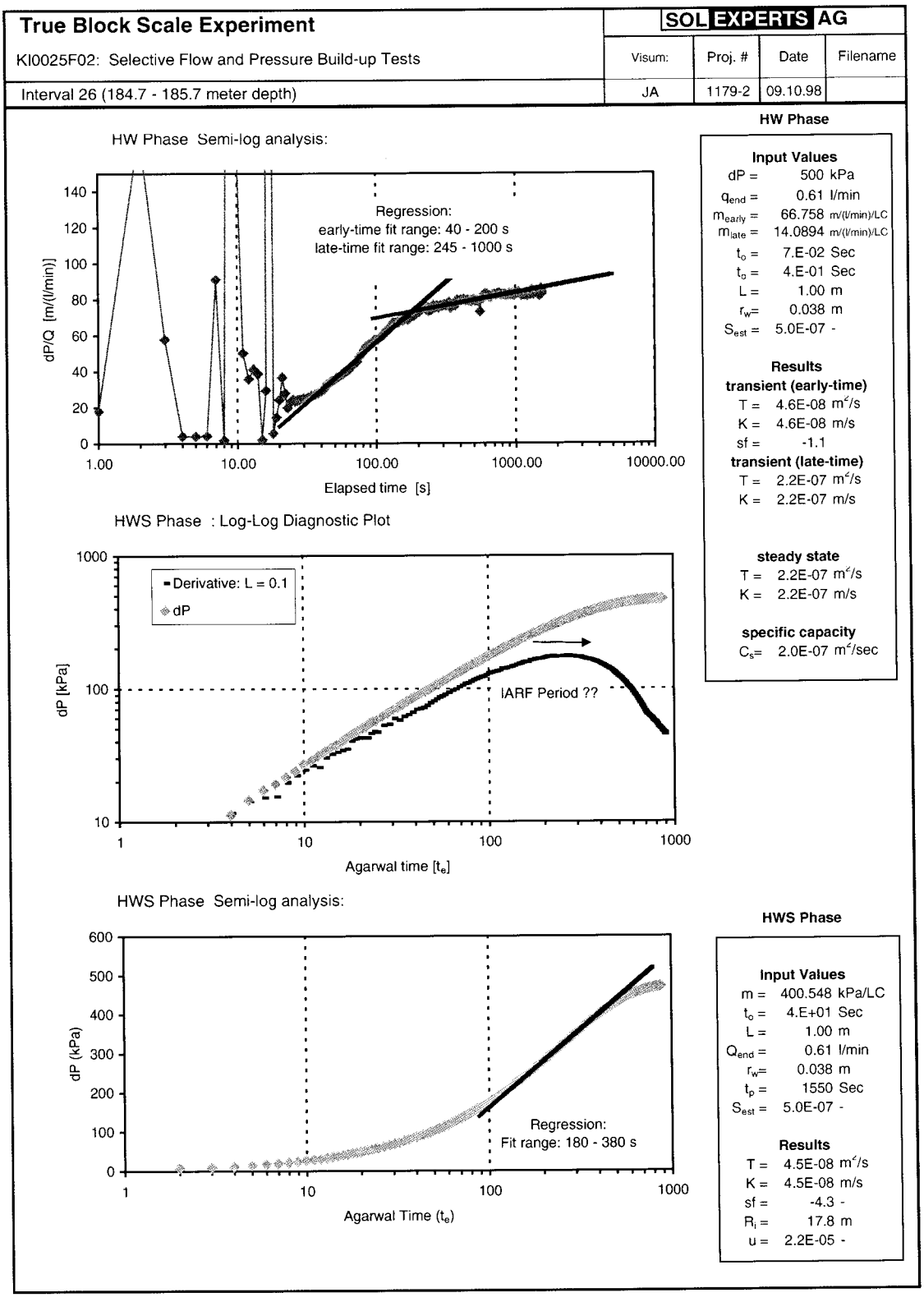

Figure B-17 Interval 26: Analysis Plots

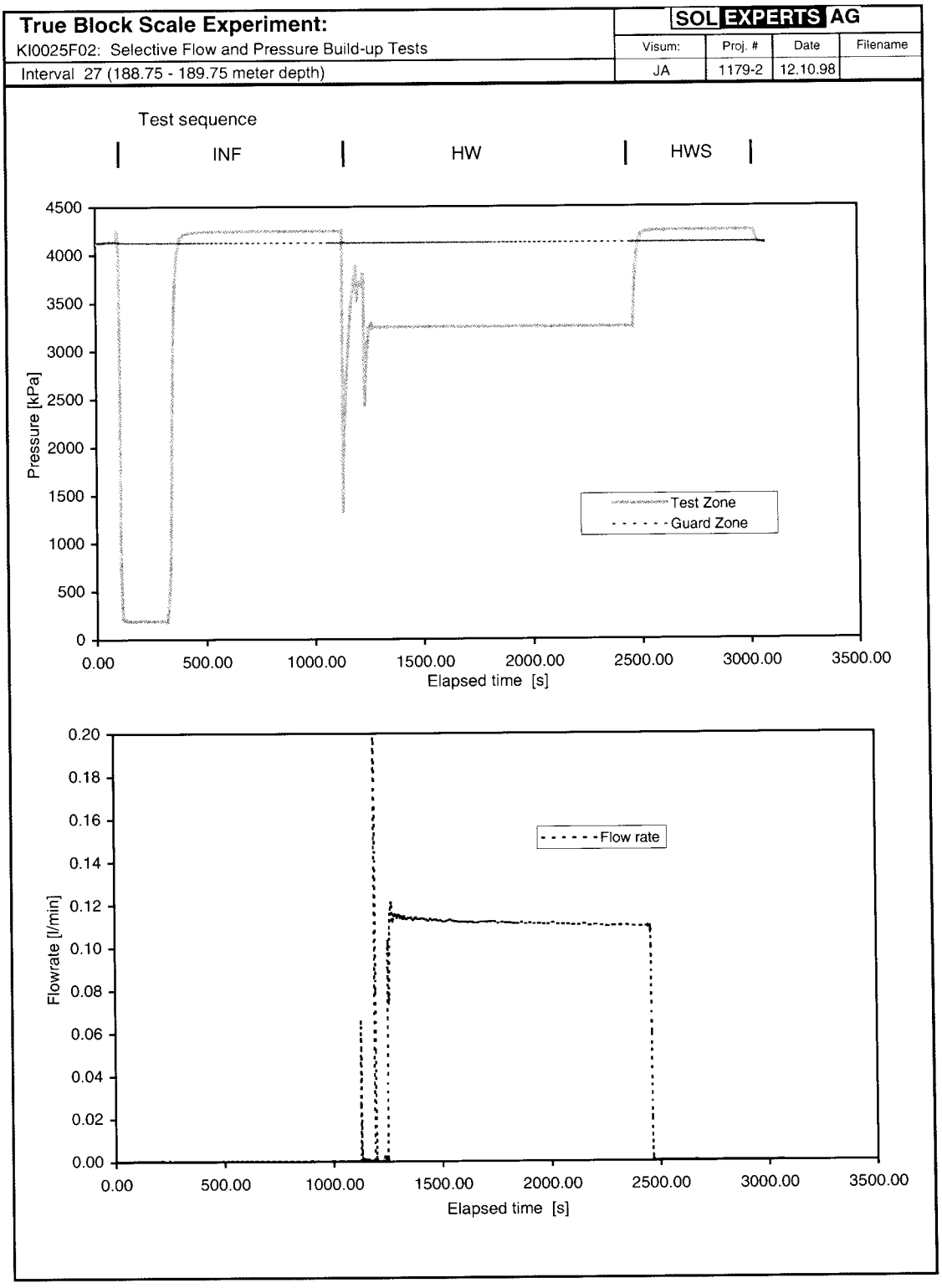

Figure B-18 Interval 27: Cartesian Plots of Interval Pressure, Guard-zone Pressure and Flow Rate –vs- Time

True Block Scale Experiment

KI0025F02: Selective Flow and Pressure Build-up Tests

Interval 27 (188.75 - 189.75 meter depth)

SOL EXPERTS AG

Visum:	Proj. #	Date	Filename
JA	1179-2	12.10.98	

HW Phase Semi-log analysis:

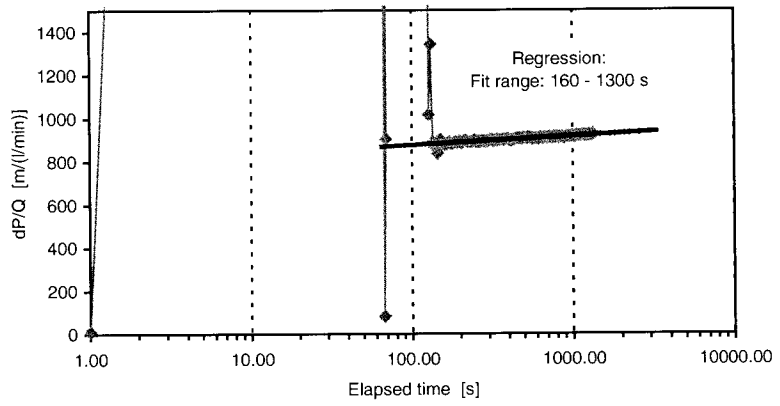

HW Phase

Input Values

dP =	997	kPa
q_{end} =	0.11	l/min
m =	40.3195	m/(l/min)/LC
t_o =	2.E-20	Sec
L =	1.00	m
r_w=	0.038	m
S_{est} =	5.0E-07	-

Results

transient

T =	7.6E-08	m^2/s
K =	7.6E-08	m/s
sf =	20.0	

steady state

T =	1.6E-08	m^2/s
K =	1.6E-08	m/s

specific capacity

C_s=	1.8E-08	m^2/sec

HWS Phase : Log-Log Diagnostic Plot

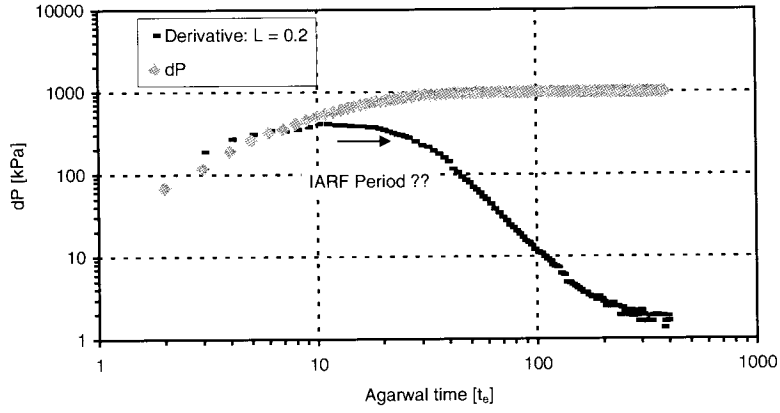

HWS Phase Semi-log analysis:

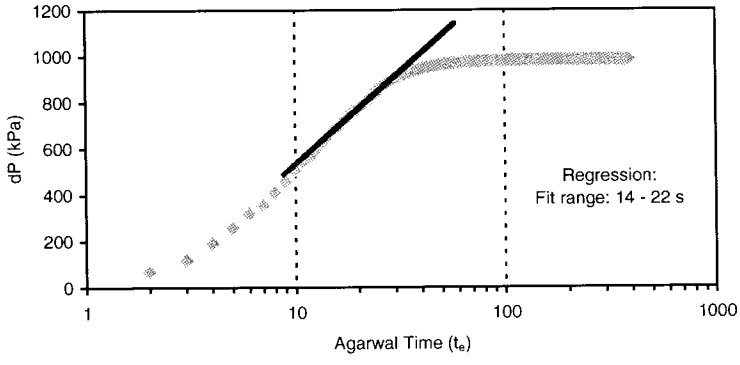

HWS Phase

Input Values

m =	894.557	kPa/LC
t_o =	3.E+00	Sec
L =	1.00	m
Q_{end} =	0.11	l/min
r_w=	0.038	m
t_p =	1334	Sec
S_{est} =	5.0E-07	-

Results

T =	3.7E-09	m^2/s
K =	3.7E-09	m/s
sf =	-1.7	-
R_i =	4.7	m
u =	3.5E-03	-

Figure B-19 Interval 27: Analysis Plots

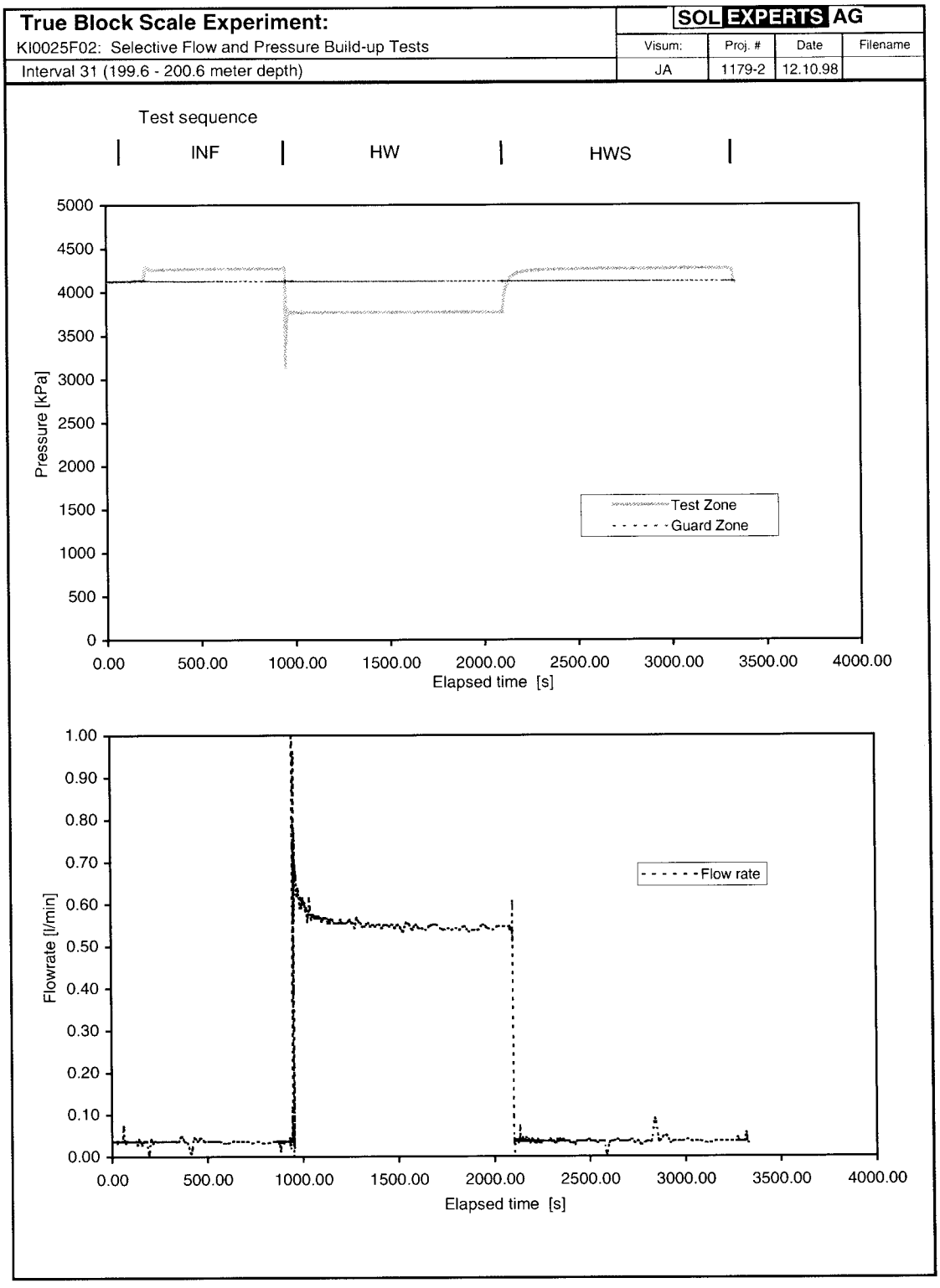

Figure B-20 Interval 31: Cartesian Plots of Interval Pressure, Guard-zone Pressure and Flow Rate –vs- Time

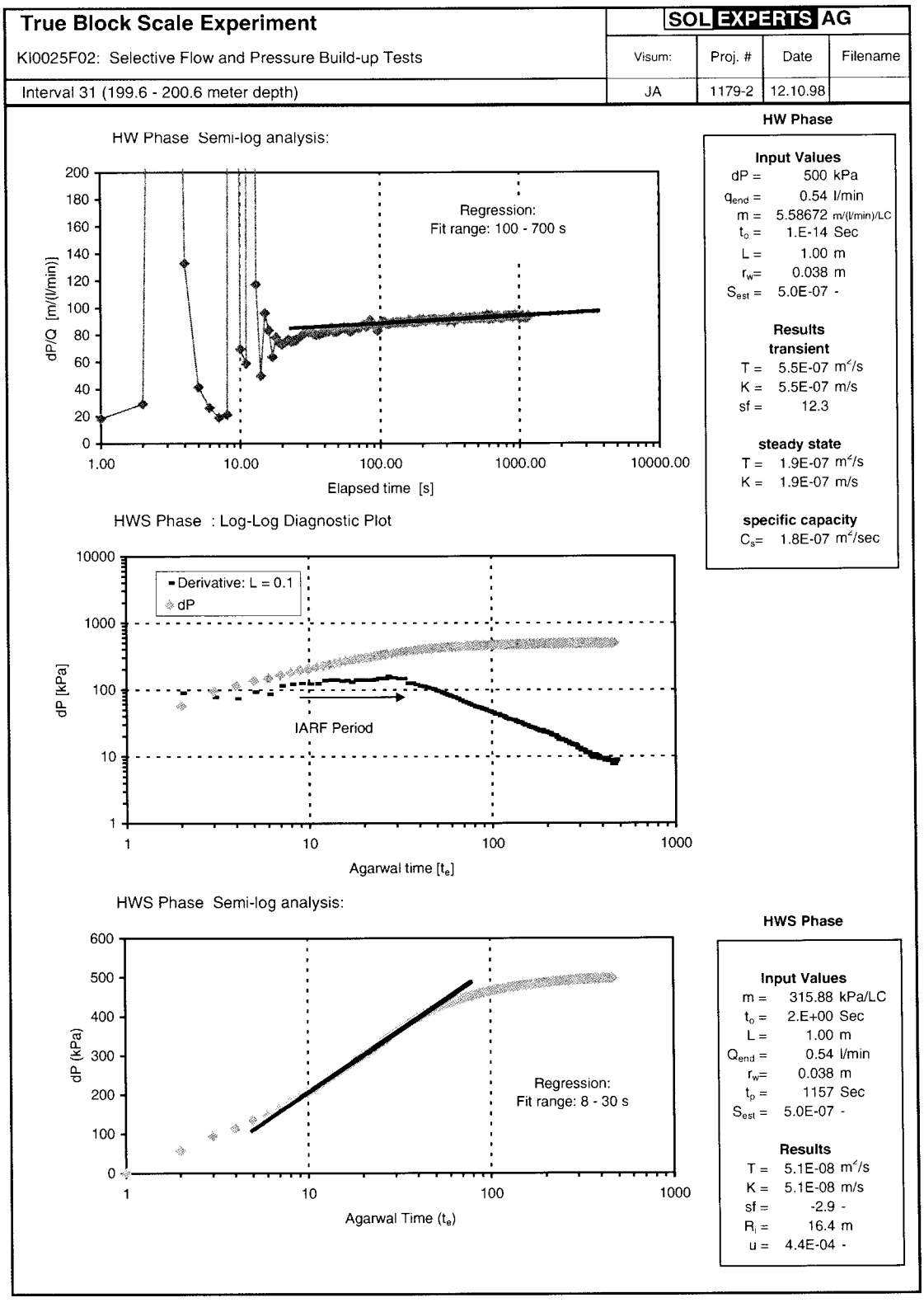

Figure B-21 Interval 31: Analysis Plots

APPENDIX C

Single-hole Analyses

During Tracer-Dilution Tests

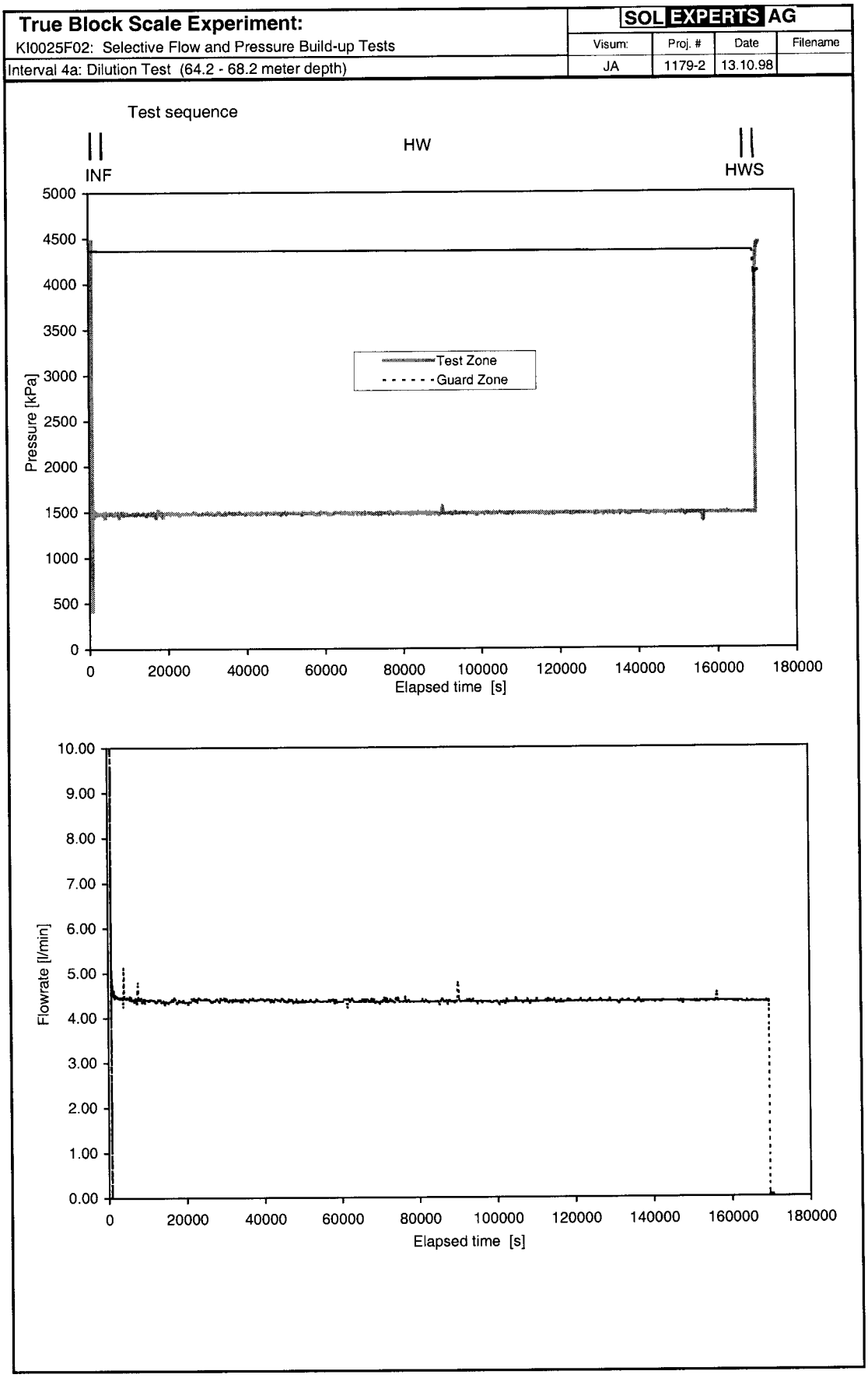

Figure C-1 *Interval 4a: Cartesian Plots of Interval Pressure, Guard-zone Pressure and Flow Rate –vs- Time*

True Block Scale Experiment

KI0025F02: Selective Flow and Pressure Build-up Tests

Interval 4a: Dilution Test (64.2 - 68.2 meter depth)

SOL EXPERTS AG

Visum:	Proj. #	Date	Filename
JA	1179-2	13.10.98	

HW Phase Semi-log analysis:

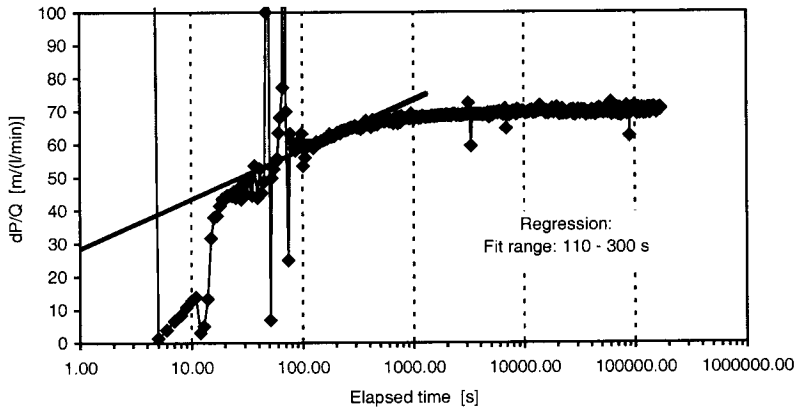

HW Phase

Input Values

dP =	2996	kPa
q_{end} =	4.33	l/min
m =	15.0074	m/(l/min)/LC
t_o =	1.E-02	Sec
L =	4.00	m
r_w =	0.038	m
S_{est} =	5.0E-07	-

Results

transient

T =	2.0E-07	m^2/s
K =	5.1E-08	m/s
sf =	-1.0	

steady state

T =	3.6E-07	m^2/s
K =	9.0E-08	m/s

specific capacity

C_s =	2.4E-07	m^2/sec

HWS Phase : Log-Log Diagnostic Plot

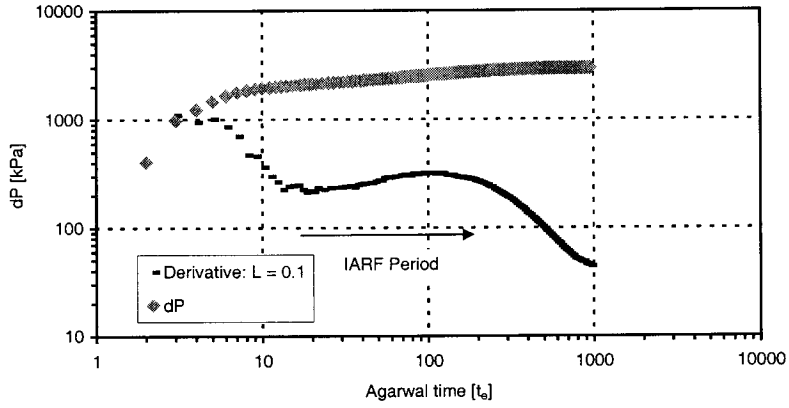

HWS Phase Semi-log analysis:

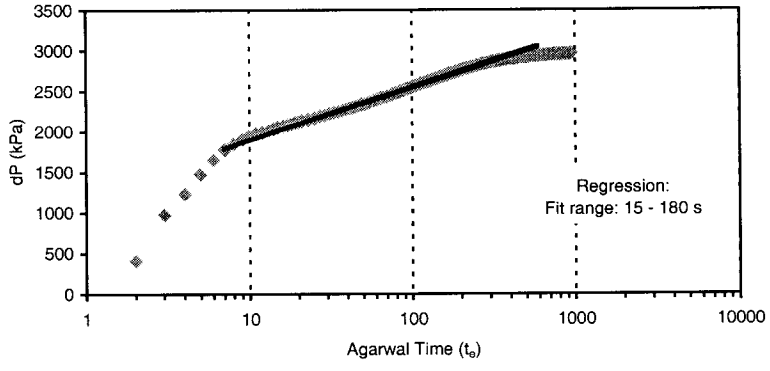

HWS Phase

Input Values

m =	654.436	kPa/LC
t_o =	1.E-02	Sec
L =	4.00	m
Q_{end} =	4.33	l/min
r_w =	0.038	m
t_p =	168849	Sec
S_{est} =	5.0E-07	-

Results

T =	2.0E-07	m^2/s
K =	4.9E-08	m/s
sf =	-1.0	-
R_i =	387.7	m
u =	6.1E-05	-

Figure C-2 Interval 4a: Analysis Plots

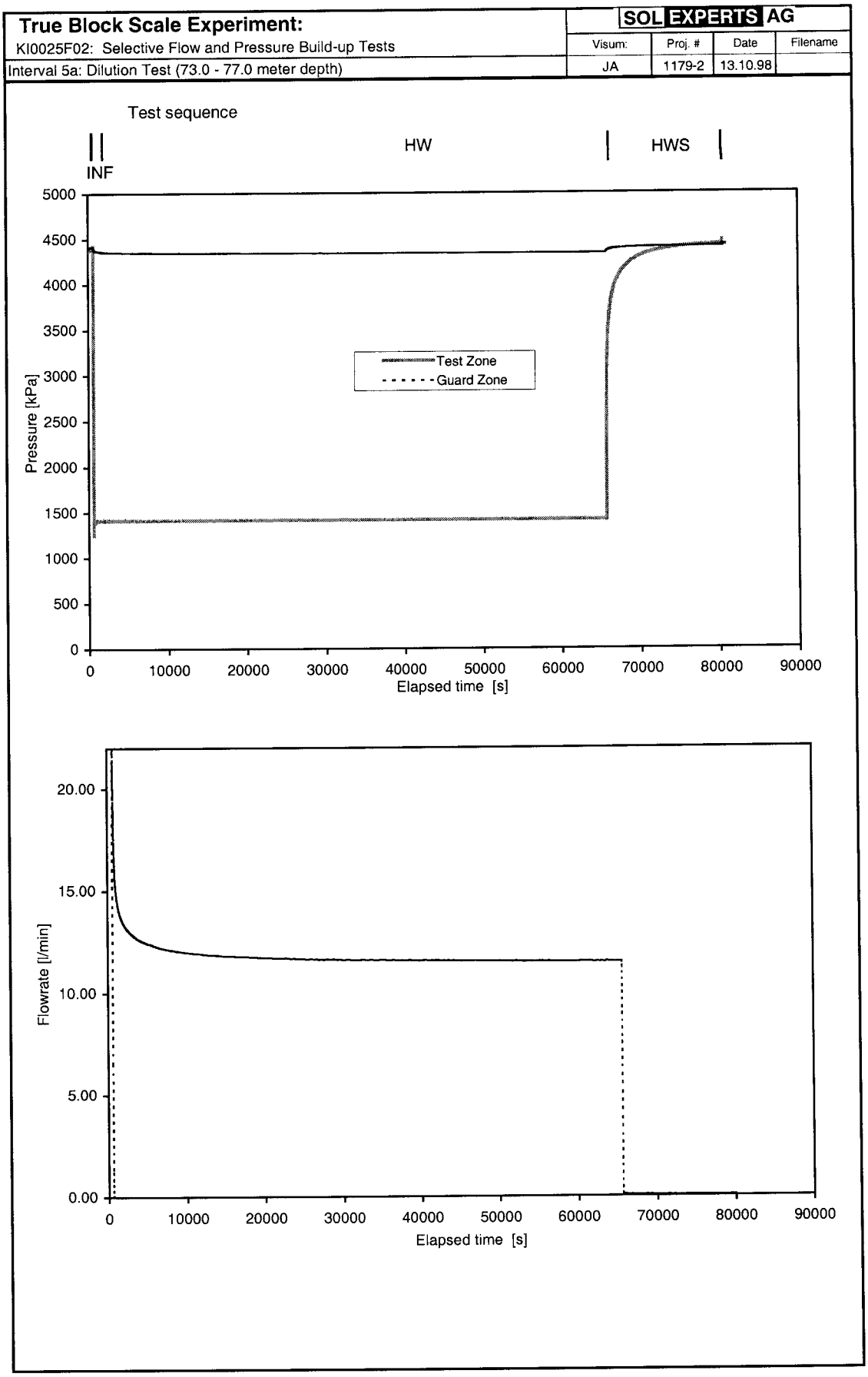

Figure C-3 Interval 5a: Cartesian Plots of Interval Pressure, Guard-zone Pressure and Flow Rate –vs- Time

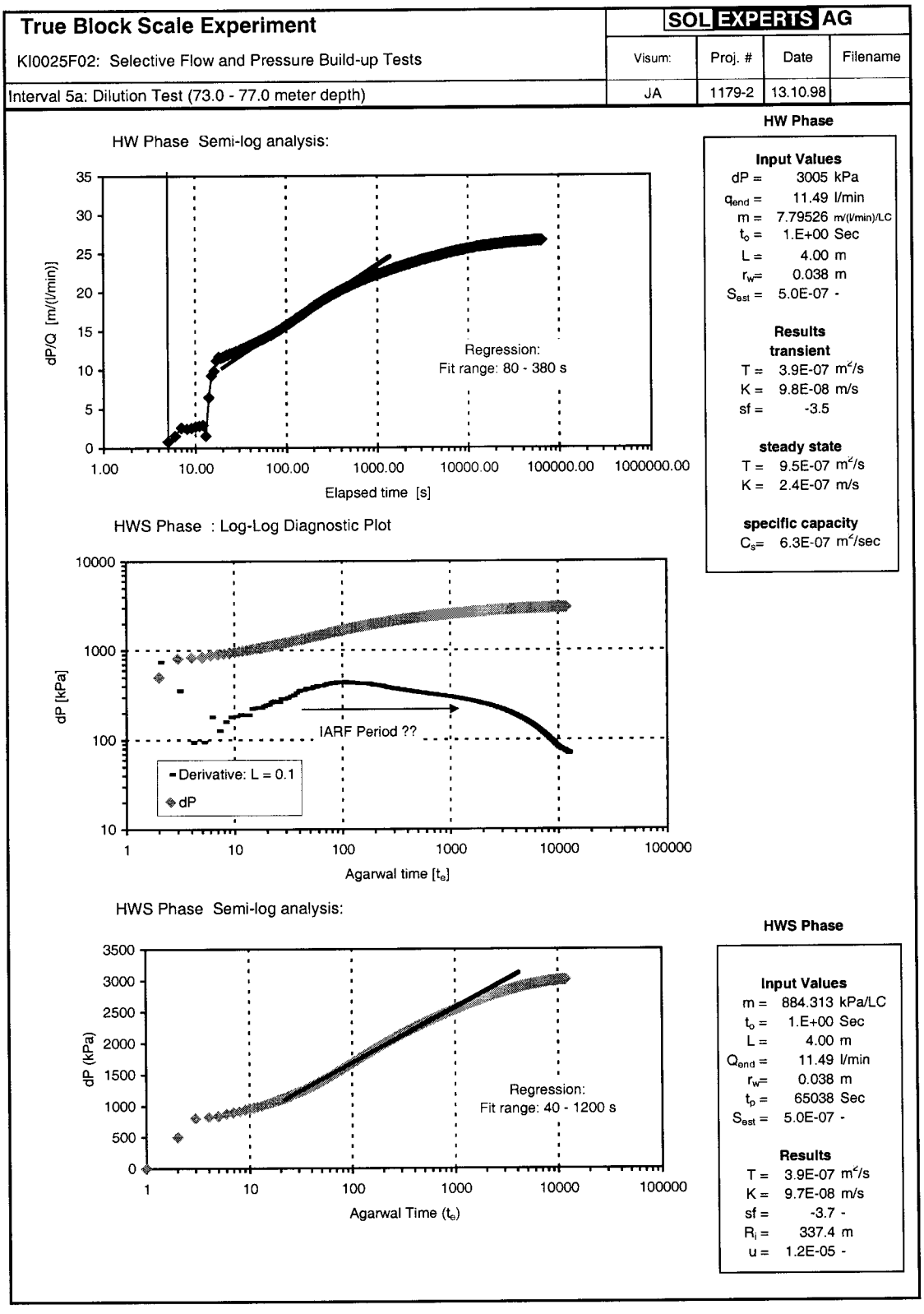

Figure C-4 Interval 5a: Analysis Plots

APPENDIX D

Cross-hole Analyses

During Tracer-Dilution Tests

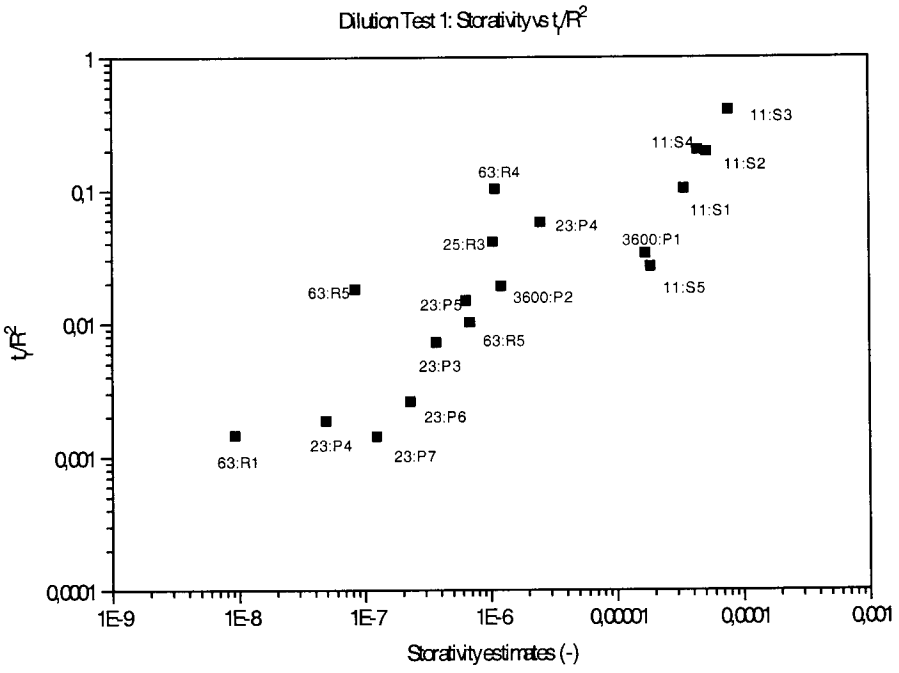

Figure D-1 Dilution test 1/ Connectivity measures: Storativity vs. t_r/R^2 (Note, the fast response of interval 63 :R1 may be due to an equipment related artifact)

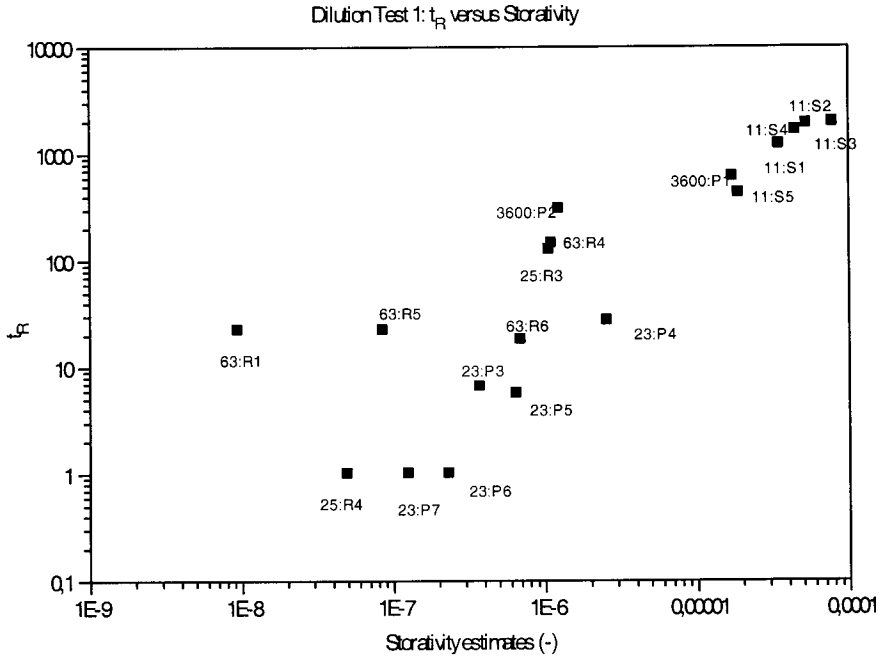

Figure D-2 Dilution test 1/ Connectivity measures: Storativity vs. t_r (Note, the fast response of interval 63 :R1 may be due to an equipment related artifact)

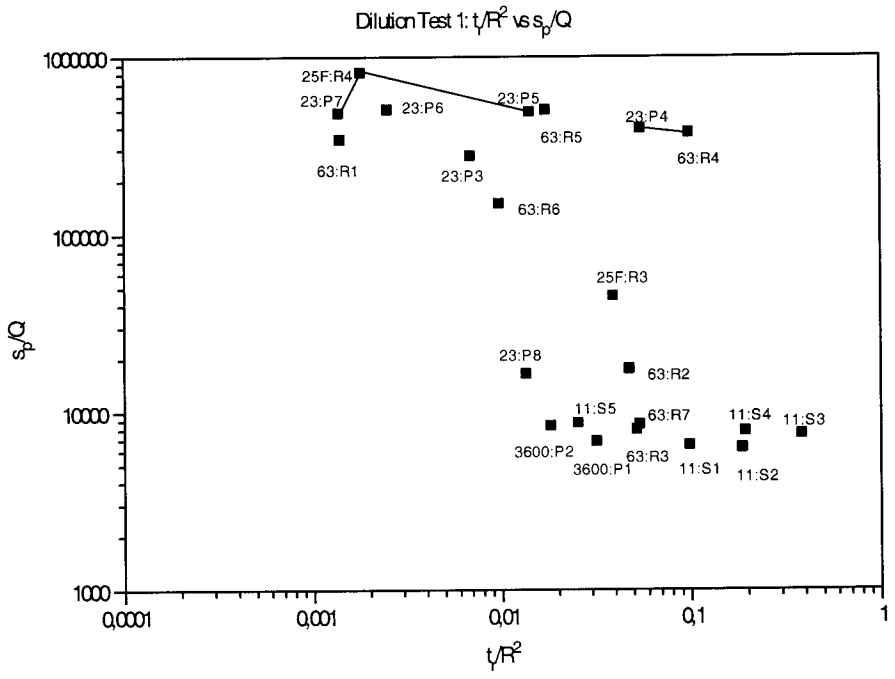

Figure D-3 Dilution test 1/ Connectivity measures: t_r/R^2 vs. s_p/Q; 23 :P7, 25F :R4 and 23 :P5 lie within structure #20 ; 23:P4 and 63:R4 within structure #13. (Note, the fast response of interval 63:R1 may be due to an equipment related artifact)

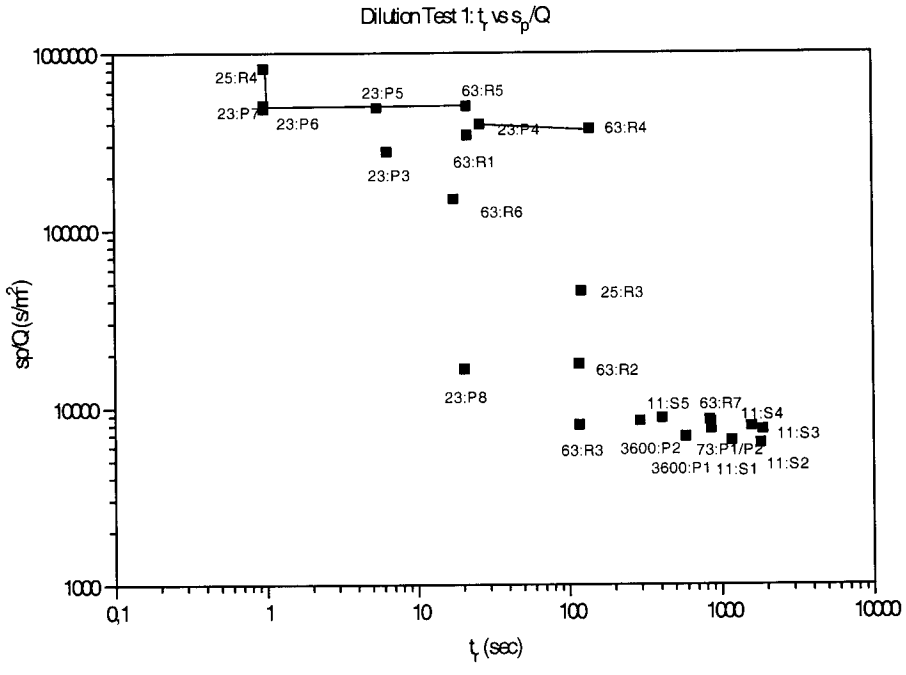

Figure D-4 Dilution test 1/ Connectivity measures: t_r vs. s_p/Q (23 :P7, 25F :R4 and 23 :P5 lie within structure #20 ; 23 :P4 and 63 :R4 within structure #13), (Note, the fast response of interval 63 :R1 may be due to an equipment related artifact)

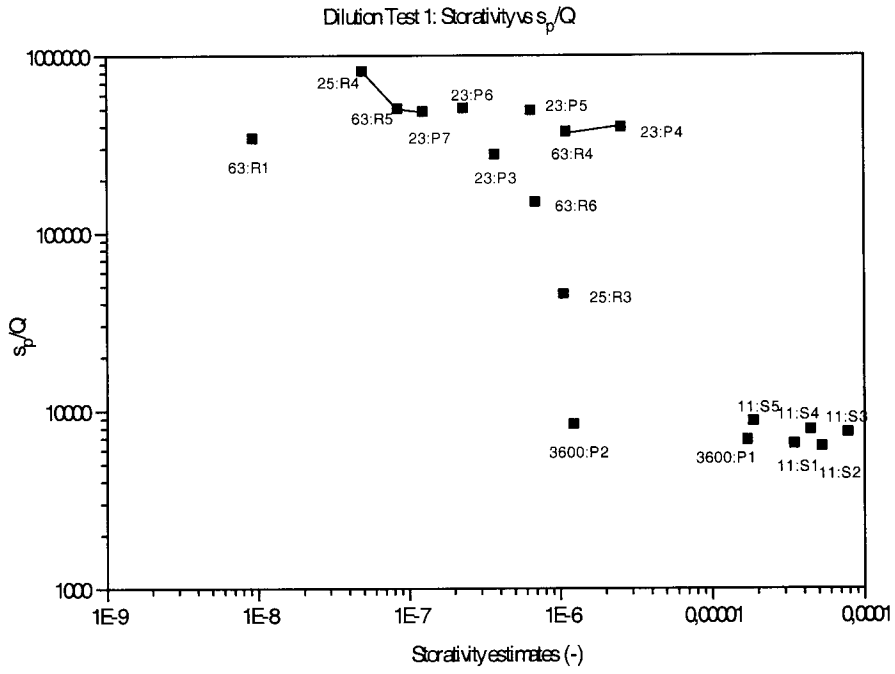

Figure D-5 Dilution test 1/ Connectivity measures: Storativity vs. s_p/Q (23 :P7, 25F :R4 and 23 :P5 lie within structure #20 ; 23 :P4 and 63 :R4 within structure #13); (Note, the fast response of interval 63 :R1 may be due to an equipment related artifact)

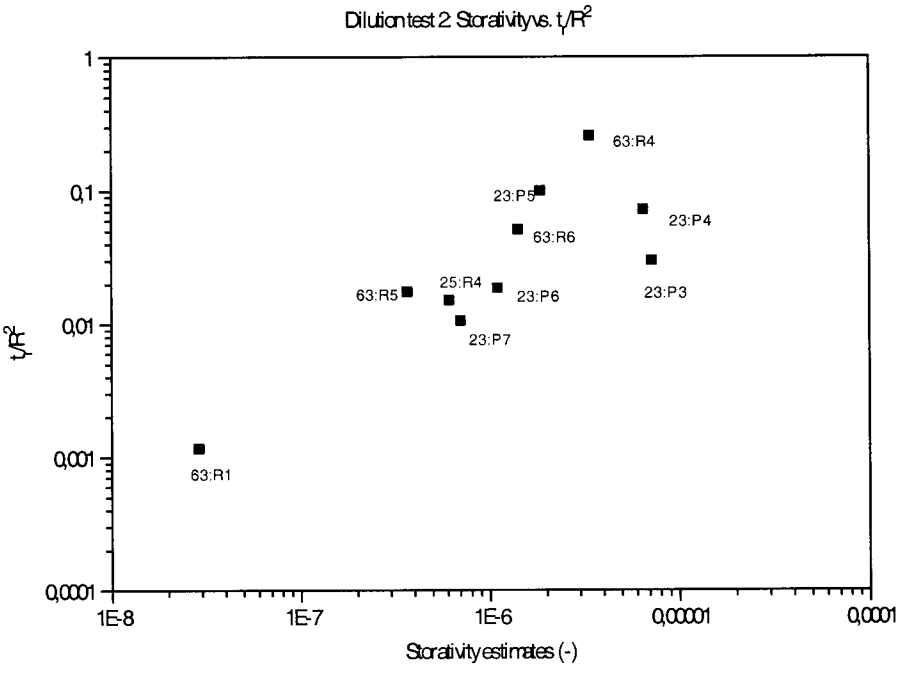

Figure D-6 Dilution test 2/ Connectivity measures: Storativity vs. t_r/R^2 (Note, the fast response of interval 63 :R1 may be due to an equipment related artifact)

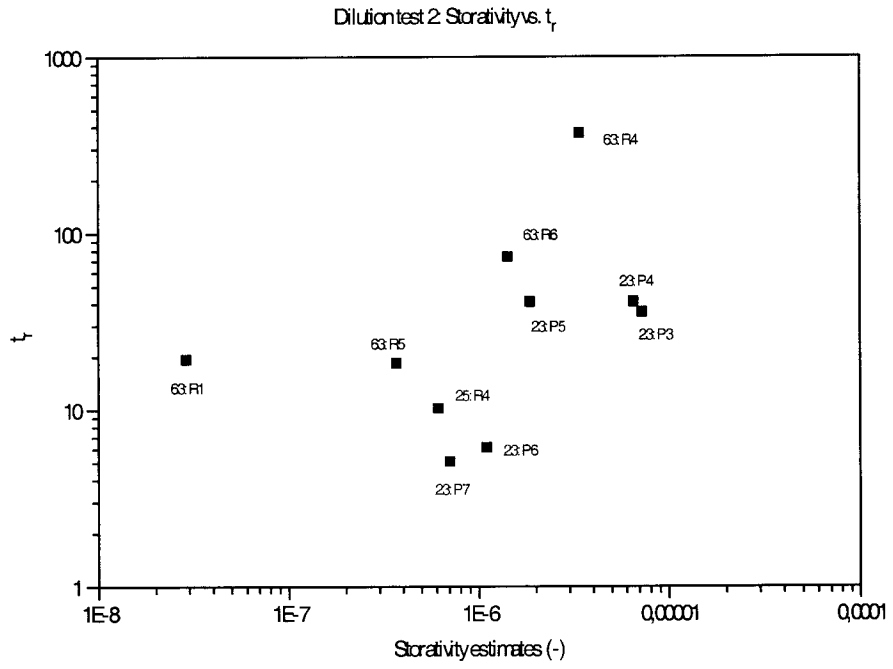

Figure D-7 Dilution test 2/ Connectivity measures: Storativity vs. t_r (Note, the fast response of interval 63 :R1 may be due to an equipment related artifact)

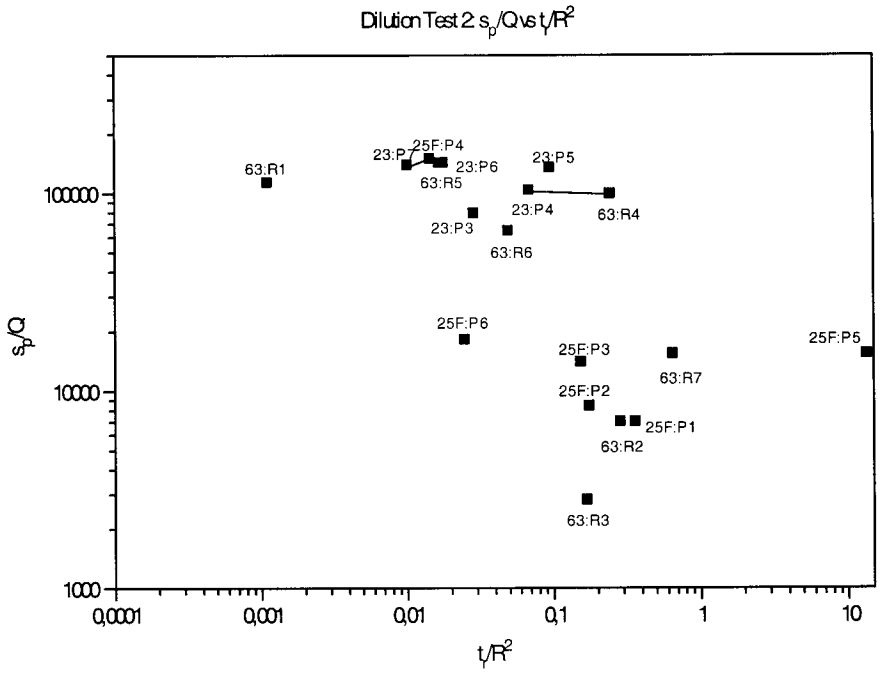

Figure D-8 Dilution test 2/ Connectivity measures: t_r/R^2 vs. s_p/Q (23 :P7, 25F :R4 and 23 :P5 lie within structure #20 ; 23 :P4 and 63 :R4 within structure #13); (Note, the fast response of interval 63 :R1 may be due to an equipment related artifact)

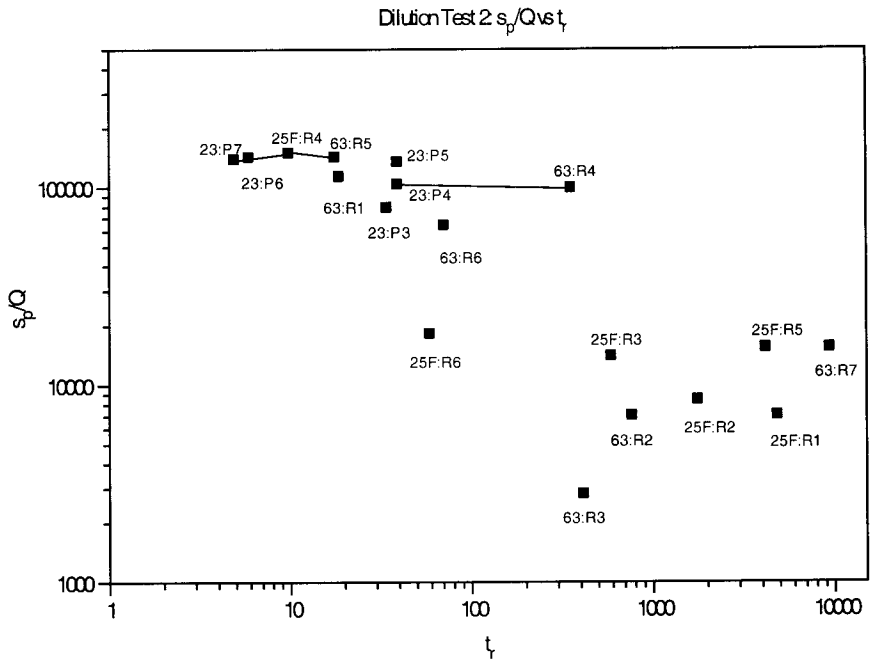

Figure D-9 Dilution test 2/ Connectivity measures: t_r vs. s_p/Q (23 :P7, 25F:R4 and 23:P5 lie within structure #20 ; 23:P4 and 63:R4 within structure #13); (Note, the fast response of interval 63 :R1 may be due to an equipment related artifact)

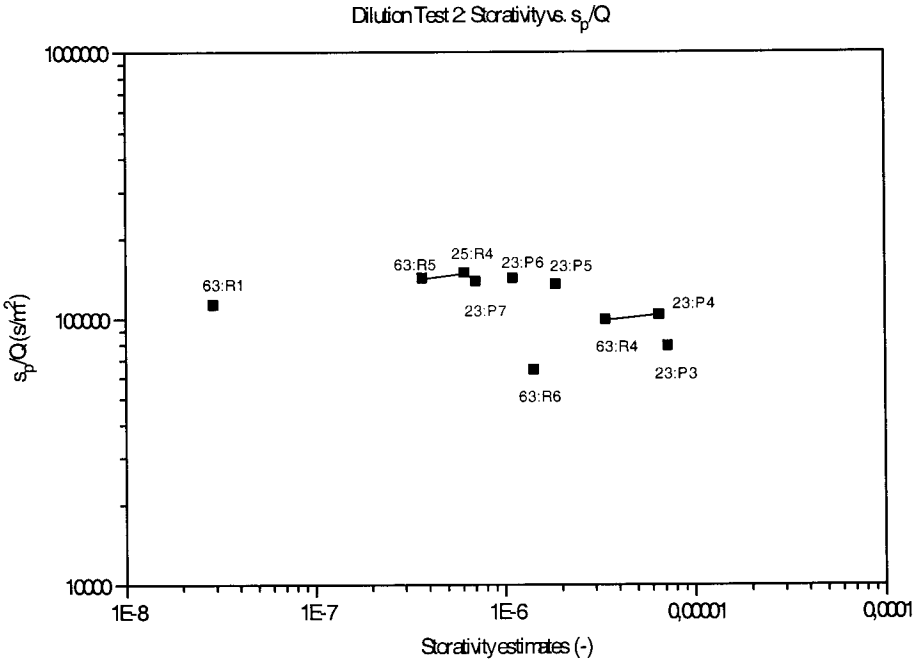

Figure D-10 Dilution test 2/ Connectivity measures: Storativity vs. s_p/Q (23:P7, 25F:R4 and 23:P5 lie within structure #20; 23:P4 and 63:R4 within structure #13); (Note, the fast response of interval 63 :R1 may be due to an equipment related artifact)

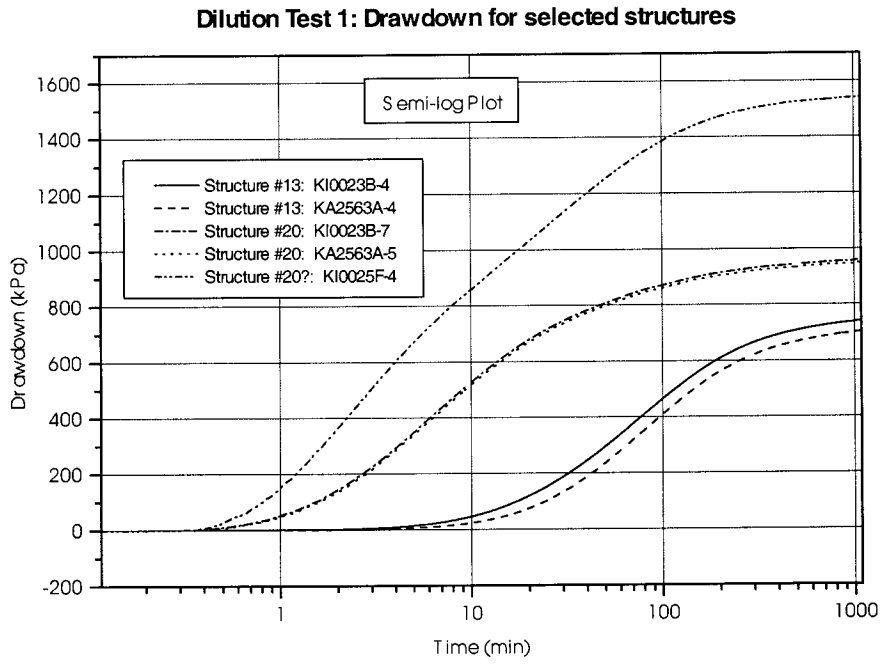

Figure D-11 Dilution test 1 : Drawdown at observation points lying within strutures #20 and #13

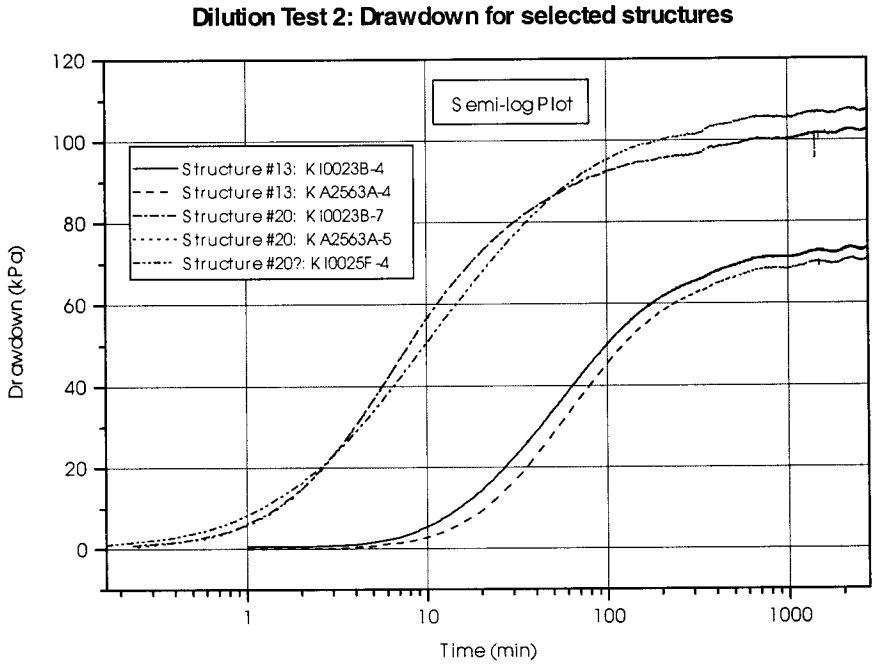

Figure D-12 Dilution test 2 : Drawdown at observation points lying within strutures #20 and #13

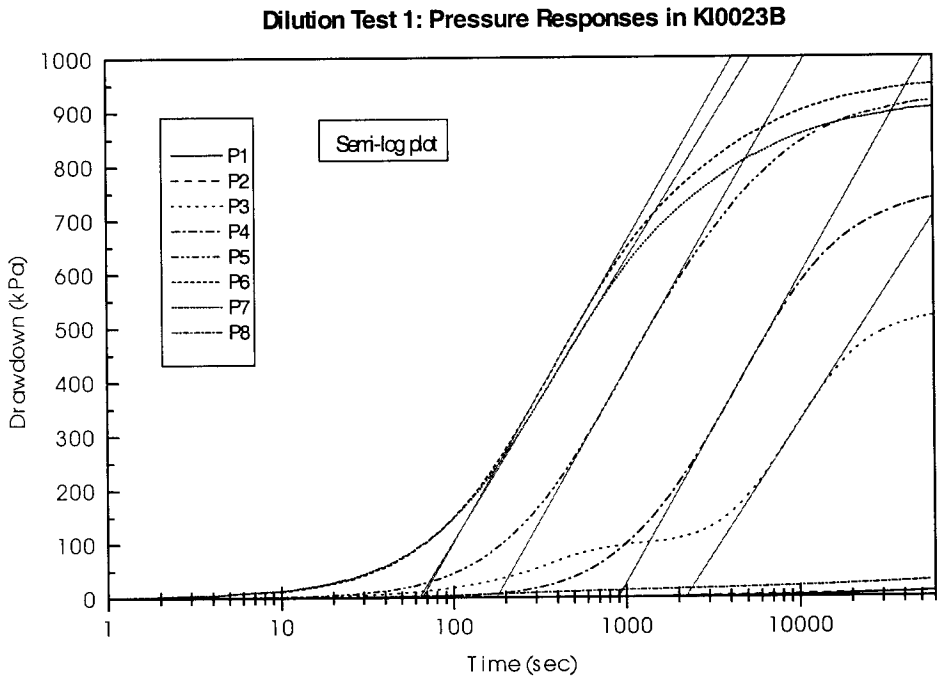

Figure D-13 Dilution test 1: Drawdown curves and semi-log straight line fits for observation borehole KI0023B

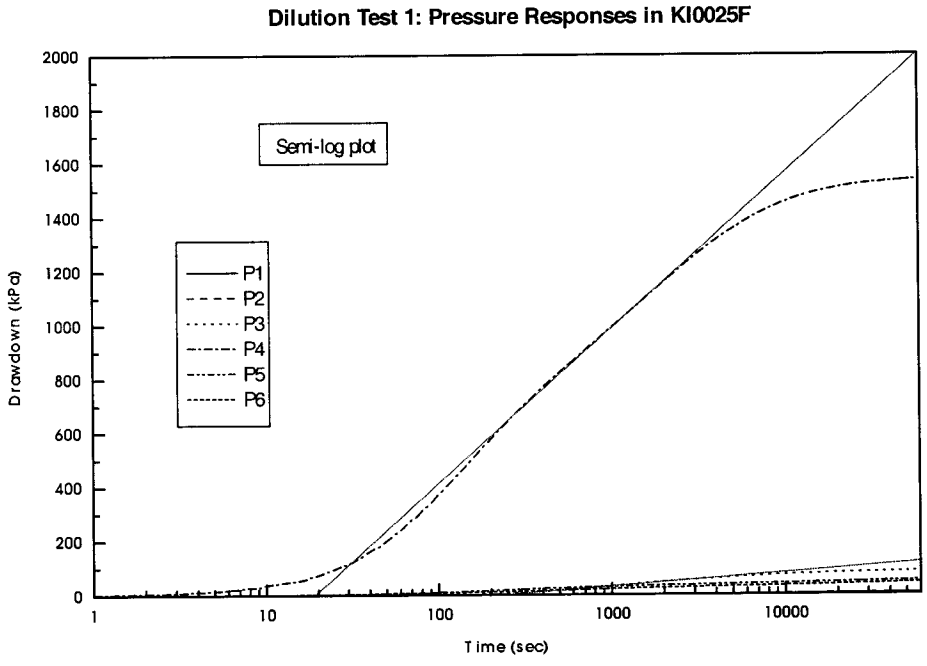

Figure D-14 Dilution test 1: Drawdown curves and semi-log straight line fits for observation borehole KI0025F

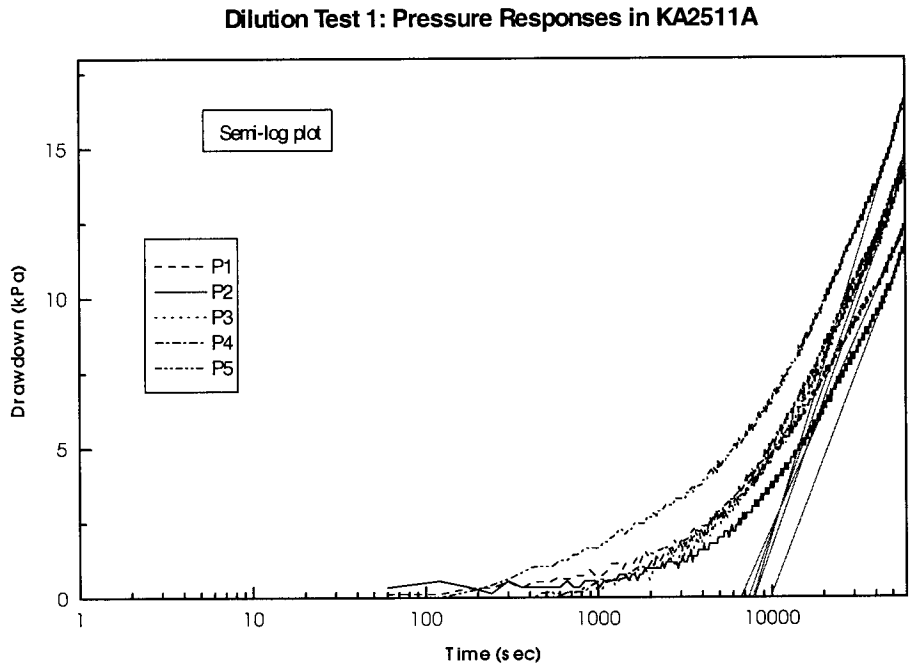

Figure D-15 Dilution test 1: Drawdown curves and semi-log straight line fits for observation borehole KI2511A

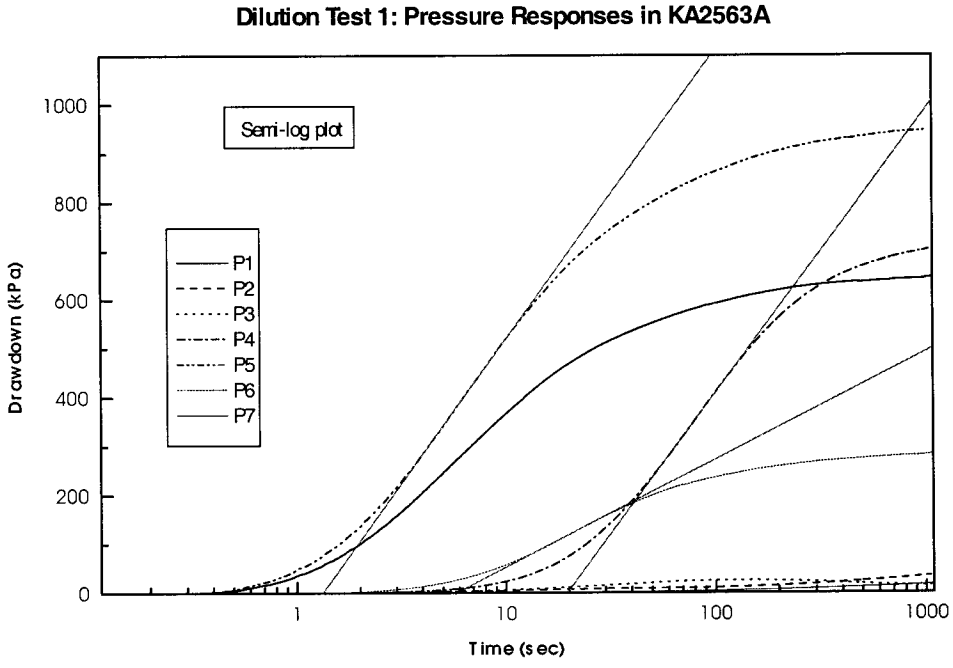

Figure D-16 Dilution test 1: Drawdown curves and semi-log straight line fits for observation borehole KI2563A. (Note, the fast response of interval 63 :R1 may be due to an equipment related artifact)

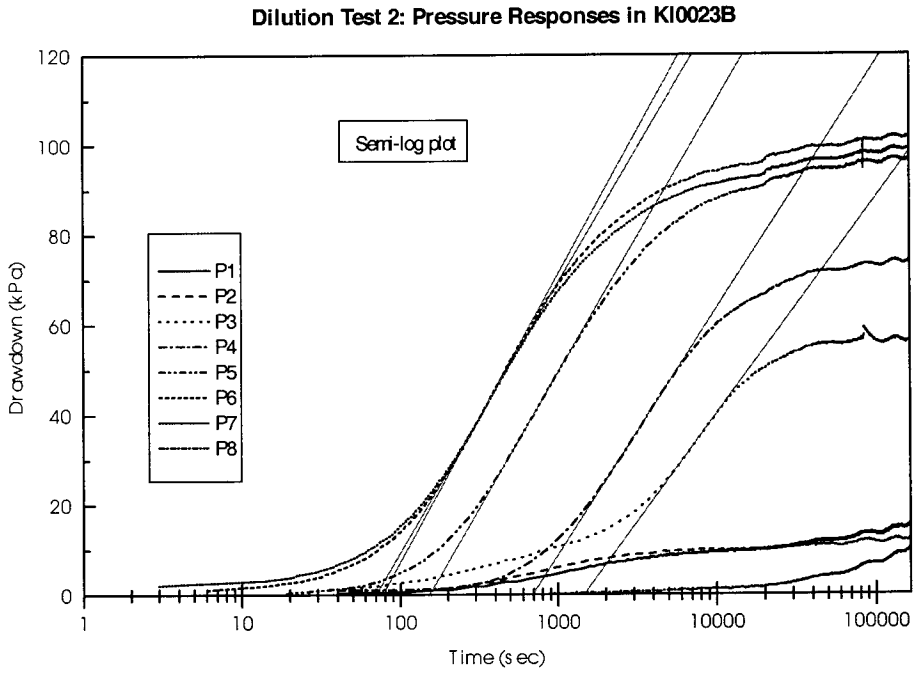

Figure D-17 Dilution test 2: Drawdown curves and semi-log straight line fits for observation borehole KI0023B

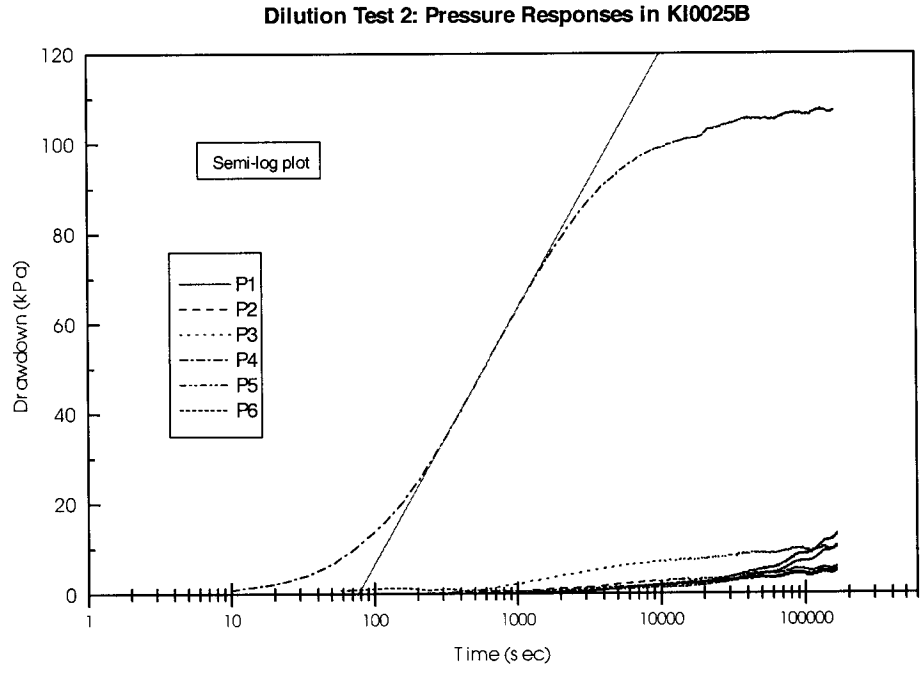

Figure D-18 Dilution test 2: Drawdown curves and semi-log straight line fits for observation borehole KI0025F

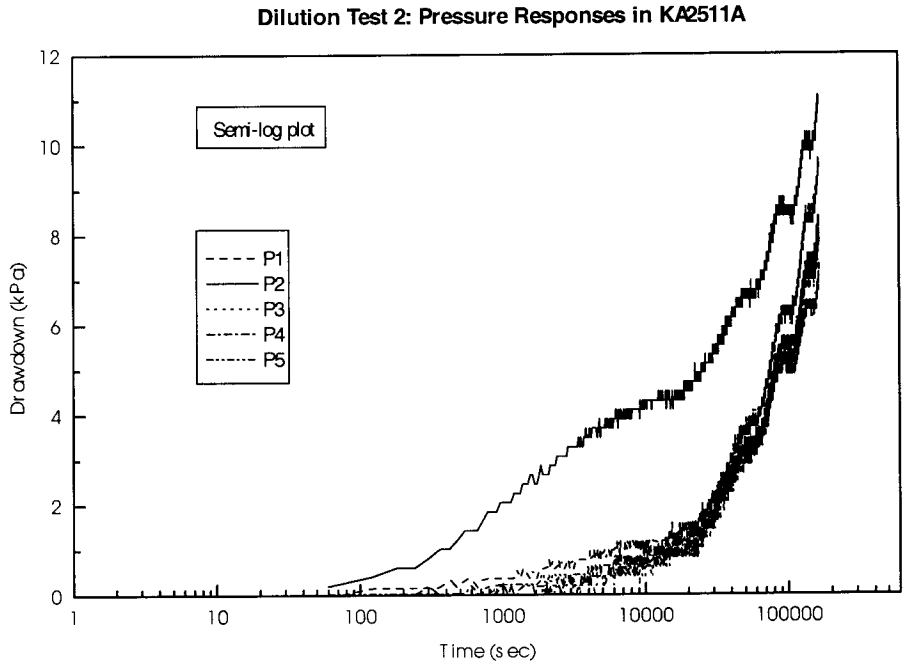

Figure D-19 Dilution test 2: Drawdown curves and semi-log straight line fits for observation borehole KI2511A

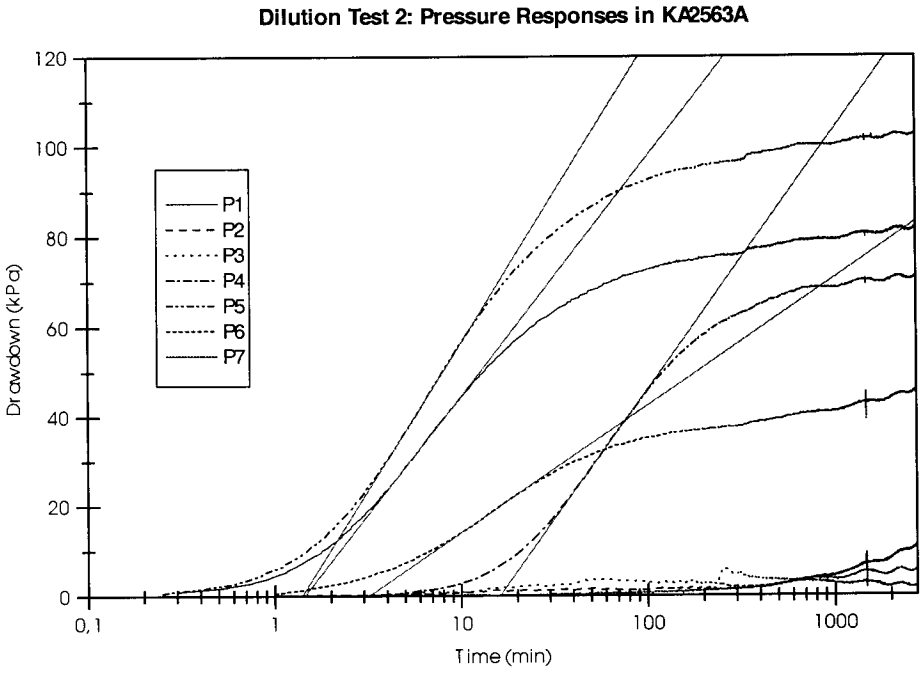

Figure D-20 Dilution test 2: Drawdown curves and semi-log straight line fits for observation borehole KI2563A. (Note, the fast response of interval 63 :R1 may be due to an equipment related artifact).

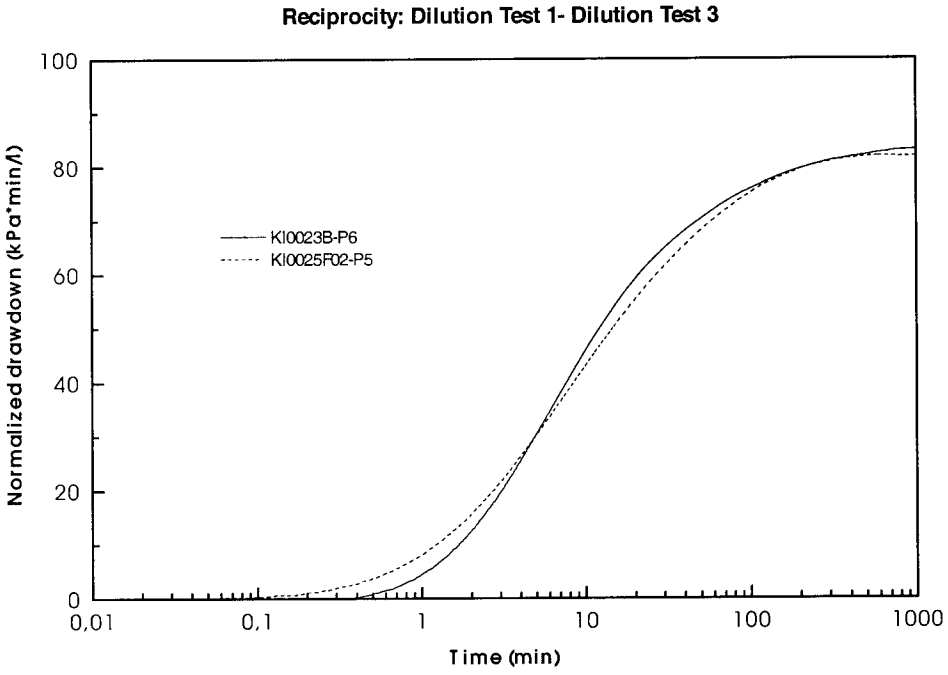

Figure D-21 Check on reciprocity for dilution tests 1 and 3.

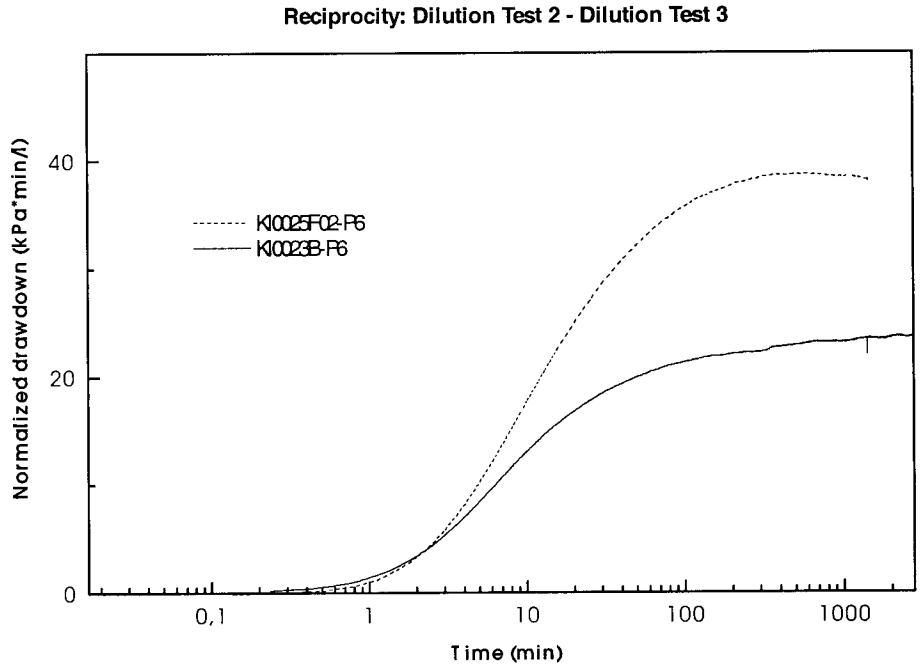

Figure D-22 Check on reciprocity for dilution tests 2 and 3.